A Simple Finite Element For The Dynamic Analysis of Rotating Composite Beams

by

Vikas B. Dhar

Thesis submitted to the Faculty of the

Virginia Polytechnic Institute and State University

in partial fulfillment of the requirements for the degree of

Master of Science

in

Aerospace and Ocean Engineering

APPROVED:

Rakesh K. Kapania, Chairman

Raphael T. Haftka

Eric R. Johnson

William H. Mason

May, 1990

Blacksburg, Virginia

A Simple Finite Element For The Dynamic Analysis of Rotating Composite Beams

by

Vikas B. Dhar

Rakesh K. Kapania, Chairman

Aerospace and Ocean Engineering

(ABSTRACT)

An attempt is made to understand the phenomenon of aeroelasticity as applied to the helicopter rotors, specifically laminated composite rotor blades. Realizing the immense complexity of the problem, a beginning has been made by developing a structural model for a rotating composite beam. Present work has three objectives; 1) To carry out an extensive survey of research related to the aeroelastic analysis of rotor blades, 2) To expand an existing finite element model by introducing new degrees of freedom and validate the changes, 3) and, finally using this model to carry out a linear static and dynamic analysis for a rotating composite beam. It was found that the rotation and fiber orientations have a pronounced effect on the static deflections and the natural frequencies of vibration of the laminated beam.

Acknowledgements

My thanks are due to Dr. Rakesh K. Kapania for his constant help and advice, and Drs. Raphael T. Haftka, Eric R. Johnson, and William H. Mason for serving on my committee. I would also like to thank Dr. J. A. Schetz, Head of the Department, for providing me with timely financial assistance.

Table of Contents

Nomenclature **1**

Introduction **6**

Literature Survey **17**

Introduction 17

Structural Modeling 18

Reviews 18

Isotropic Blades 20

Composite Rotor Blades 26

Aerodynamic modeling 32

Classical Unsteady Aerodynamic Theories. 34

Three Dimensional Vortex Theories 37

Dynamic Inflow Theory 39

Models **41**

Structural Model 41

Incremental Stiffness Matrix 47
Static Deflection and Free Vibration Analysis 50
Aerodynamic Model 51
Solution for Aeroelastic results. 52

Results **54**
Validation 56
Static deflections 56
Free Vibrations 57
Aeroelastic results 59
Results from the rotating beam. 59
Static deflections. 60
Free Vibration. 60

Conclusions and Recommendations for Future Work **62**

References **64**

Figures and Tables **75**

Appendix A. The Incremental Stiffness Matrix **98**

Appendix B. The Data File **101**

Vita **142**

List of Illustrations

Figure 1. a)A typical Helicopter configuration b) defining precone and droop 80

Figure 2. Various hub configurations of rotor blades, Reference [7] 81

Figure 3. Typical Helicopter rotor configuration 82

Figure 4. Block diagram of inflow dynamics 83

Figure 5. Built-up blade model. 84

Figure 6. Element degrees of freedom 85

Figure 7. Strain-Displacement Matrix 86

Figure 8. Configuration of a rotating beam. 87

Figure 9. Distribution of deflections due to bending and shear deformations and twisting angle for a 16 ply $[45_4 / -45_4]_s$ under a tip load 88

Figure 10. Box Beam Geometry Ref. [14] 89

Figure 11. Box Beam Tip Deflection Under a Tip Load 90

Figure 12. Critical Speed of an Unswept Graphite/Epoxy Plate, $(\theta_2 / 0)_s$ 91

Figure 13. Flutter and Divergence Speeds of an Unswept Box Beam 92

Figure 14. Tip deflection vs θ for a rotating $(\theta_2 / 0)_s$ plate. 93

Figure 15. Variation of first natural frequencies of vibration with angular velocity for an isotropic beam, $\bar{R} = 0$. 94

Figure 16. Variation of first natural frequencies of vibration with angular velocity for isotropic beam with different values of $\bar{R}$ 95

Figure 17. Variation of first natural frequencies of vibration with angular velocity for the Graphite/Epoxy plate $\bar{R} = 0$. 96

Figure 18. Variation of first natural frequencies of vibration with angular velocity for the Box-Beam with different values of $\bar{R}$ 97

List of Tables

Table 1. Maximum deflection w_s in $\frac{Plh^2}{4EI}$ due to shear deformation only 76

Table 2. Natural frequencies for the Aluminium plate 77

Table 3. Natural Frequencies of a 30 Degrees Off-Axis Graphite/Epoxy Cantilever Beam . 78

Table 4. Natural frequencies of a $[45_4/0_4]_T$ Boron/Epoxy plate 79

Nomenclature

a	non-dimensional offset between semichord and origin
a_c	nondimensional offset between the aerodynamic center and the mid chord
a_o	section lift curve slope
$[a]$	complex element aerodynamic matrix
A^e	elemental area
A_{ij} , i,j = 1,...,6	extensional stiffness coefficients
A_{44}	transverse shear stiffness
[A]	assembled aerodynamic matrix
b	beam chord
b_r	reference airfoil semichord
B_{ij} , i,j = 1,...,6	bending-extension stiffness coefficients
c	chord of the cross - section
$C(k_n)$	Theodorsen's circulation function

Cl_α	lift curve slope
D_{ij} , i,j = 1,...,6	bending stiffness coefficients
[D]	beam force-strain matrix
[DL]	cover skins force-strain matrix
e	distance between aerodynamic center and the elastic axis of the cross-section
$\hat{i},\hat{j},\hat{k}$	undeformed blade reference axes
$\hat{i}',\hat{j}',\hat{k}'$	deformed blade reference axes
E_i , i = 1,...,8	stringers' moduli
{f}	element nodal load vector
{F}	assembled nodal load vector
$F_{x'}$	centrifugal force at x'
g	damping coefficient
H_i , i = 1,...,5	Gaussian quadrature weights
J	mass polar moment of inertia
J_n	Bessel function of the first kind
k	reference reduced frequency
k_n	reduced frequency
[k]	element stiffness matrix
K	Timoshenko's shear factor
[K]	assembled stiffness matrix
[KG1]	constant part of the incremental stiffness matrix
[KG2]	linear part of the incremental stiffness matrix
[KG3]	quadratic part of the incremental stiffness matrix

l	element length
L	aerodynamic lift
$L_w, L_\tau, L_\theta, L_\tau$	lift components
[m]	element mass matrix
M	aerodynamic moment
$M_w, M_\tau, M_\theta, M_\tau$	aerodynamic moment components
$M_x^n, M_x^v, M_y, M_{xy}$	plate resultant moments
[M]	assembled mass matrix
n	total number of skin layers
N_i , i = 1,...,4	Hermitian interpolation polynomials
N_x, N_y, N_{xy}, N_{xz}	plate resultant forces
$N_w, N_\tau, N_\theta, N_\tau$	aerodynamic displacements interpolation vectors
{N}	resultant force vector
p	number of elements covered
q	total number of elements in the analysis
{q}	nodal displacement vector
$[\overline{Q}]$	reduced transormed local stiffness matrix
r	offset between center of gravity and origin
R	radius of the hub
$\overline{R}$	radius of the hub non - dimensionalized w.r.t. the element length.
$[S]$	transformation matrix from undeformed to deformed state
T	element kinetic energy

u	axial displacement
U	element strain energy
U_{centri}	element strain energy due to the centrifugal force
v	lateral deflection due to bending
V	flow speed over the blade
w	transverse deflection
W	wake spacing function
w_b	transverse deflection due to bending
w_s	transverse deflection due to shear
x-y-z	element dimensional coordinate system
x'	element dimensional coordinate axis along the length of the element.
x_i , i = 1,...,5	Gaussian quadrature abscissas
X-Y-Z	global coordinate system
Y_n	Bessel function of the second kind
YA_i, YB_i, YD , i = 1,...,6	stiffness coefficients pertaining to the lateral deflection
β	in-plane shear angle
γ	beam material density
δ **W**	Aerodynamic forces virtual work
$\varepsilon_x^0, \varepsilon_y^0, \gamma_{xy}^0$	reference surface in-plane strains
$\varepsilon_x, \varepsilon_y, \gamma_{xy}, \gamma_{xz}$	local strains
$\{\varepsilon\}$	active strain vector
$\{\varepsilon^0\}$	reference surface strains and curvatures vector

η	non-dimensional elemental coordinate along the length
ζ	non-dimensional chordwise coordinate
θ_b	transverse bending slope
θ_s	transverse shear slope
$\kappa_x^w, \kappa_x^r, \kappa_y, \kappa_{xy}$	curvatures
ξ	non-dimensional spanwise coordinate
ρ	air density
ρA	element mass per unit length
τ	twist angle
τ_s	twist angle component due to the geometric transformation of the transverse shear slope θ_s
ϕ	torsion variable
ω	beam oscillation frequency
Ω	angular velocity of the rotating beam

Introduction

Aeroelasticity is a branch of science which is concerned with the motion of deformable bodies through fluids. It is often also defined as, a science which studies the mutual interaction between aerodynamic, inertial and elastic forces and its influence on airplane design and performance. One more and a rather graphic way of defining it could be "*as an interface between solid and fluid mechanics, with dynamics serving as the adhesive* " [1]. Regardless of the choice of simile, however, engineers in the field of aircraft and missiles are well aware of its existence and influence on the success of their designs.

Aeroelastic problems would not exist if airplane structures were perfectly rigid. Modern airplane structures are flexible, and this flexibility is fundamentally responsible for various aeroelastic phenomena. On its own structural flexibility may not be objectionable. But when the deformations in a flexible structure

induce additional aerodynamic forces, which in turn lead to higher deformations and so on, they are singled out as the culprit. Problems in the realm of aeroelasticity are diverse and they are a fast multiplying species. Their classification; however, quite ingeniously done by Collar [2] back in 1946, still remains widely accepted. The triangle of forces, with aerodynamic, elastic and inertia forces at the three vertices show how these forces interact to pose a wide variety of problems for an aeroelastician. Duncan [3], in 1968, suggested another way of classifying the aeroelastic problems. They may be classified in the first place as oscillatory or non-oscillatory, further depending on the role flexibility plays in the phenomena.

Group A Phenomena in which structural flexibility plays an important part.

A.1 Non-oscillatory phenomena

A.2 Oscillatory phenomena

Group B Phenomena in which structural flexibility does not play an essential part.

B.1 Non-oscillatory phenomena.

B.2 Oscillatory phenomena.

The phenomena of Group A would not occur if the structure could be made rigid. Those in Group B are significantly influenced by structural flexibility but could still occur in its absence. The content of various categories are as follows;

A.1 Structural divergence of surfaces

Reversal of control.

A.2 Flutter

B.1 Non-oscillatory behaviour of the aircraft as a whole (in relation to stability, control and response)

B.2 Snaking and longitudinal snaking

Oscillatory behavoiur of the aircraft as a whole.

Buffeting.

The growth of aeroelasticity in its early years was not in any way very general or abstract. It had been developed with the immediate aim of application to aeronautics. Hence it grew under the stress imposed by the urgent practical demands and new techniques had to be developed in an *ad hoc* fashion. In fact the problem of aeroelasticity did not attain the prominent role it plays now until the early stages of WW-II. Prior to that time, airplane speeds were relatively low

and the load requirements placed on the aircraft structures by design criteria specifications produced a structure sufficiently rigid to preclude any aeroelastic phenomena. As speeds increased, however, with little or no increase in load requirements, and in absence of a rational stiffness criteria for design, aircraft designers encountered a wide variety of problems in aeroelasticity, the ones classified above.

Although aeroelastic problems have occupied their prominent position for a relatively short period, they have had some influence on airplane design since the beginning of the powered flight. Perhaps the first designer to be effected was Professor Samuel P. Langley of the Smithsonian Institution. It seems likely that the unfortunate wing failure which wrecked Langley's machine on the Potomac river houseboat in 1903, could be described as a wing torsional divergence. Perhaps the success of the Wright biplane and the failure of Langley's monoplane was the original reason for the dominance of the biplanes till the mid-thirties. The most widespread early aeroelastic problem in the days when military aircraft were almost exclusively biplanes was the tail flutter problem. One of the first documented cases of the flutter occured on the horizontal tail of the twin-engined Handley Page 0/400 bomber in the beginning of the WW-I. A second epidemic of tail flutter was experienced by DH-9 airplanes in 1917, and a number of lives were lost before it could be cured. The Fokker D-8 played havoc on the German Air Corps in WW-I. Since the aircraft was high-tech for its time, only the cream of the airforce got to handle it. Unfortunately the aircraft had a number of crashes and many ace pilots were lost. The cause was collapse of wing in torsion

due to very high loads at the tips under the strains of combat manoevers. After the war the D-8 also demonstrated a non-destructive kind of bending-aileron flutter.

The period of developement of the cantilever monoplane seems to have been the period in which serious research in aeroelasticity commenced. Today the subject is quite well developed and boasts of contributions to fields other than aeronautics. *Aerothermoelasticity,* for example, deals with the effect of temperature, *Aeromagnetoelasticity* similarly studies the effect of the strong magnetic field, like that of earth, on the airplane design. Another of the often repeated terms is *Aeroservoelasticity,* which takes into account the effect of dynamics of guidance and control on aeroelasticity.

Although the technological cutting edge of the field of aeroelasticity has centered in the past on the aeronautical applications, applications are found at an increasing rate in Civil Engineering; e.g. flows about bridges and tall buildings; Mechanical Engineering; e.g. flows around turbomachinery blades and fluid flows in flexible pipes; Nuclear Engineering; e.g. flows about fuel elements and the heat exchanger vanes. It may well be that such applications will increase in both absolute and relative number as technology in these areas demands light weight structures under severe flow conditions.

Coming back to the aeronautical applications we have overlooked an important group of flight vehicles influenced rather strongly by the aeroelastic phenomena,

namely those of Rotary-Wing airplanes or Helicopters, as they are popularly called (*Autogyros*, have become history after an unimpressive start). Notwithstanding the developement of the conventional airplane, we have been aware that helicopters are the only means to achieve complete mastery of the air; namely, the ability to stay aloft without maintaining forward speed (what is technically *hovering*) and to ascend and land vertically in restricted areas. A basic introduction to aerodynamics and mechanics of helicopters may be found in References [4] and [5].

It will be in order to mention the V/STOL aircraft configurations which make use of rotors or propellers for the necessary lift or thrust. Even these otherwise conventional aircrafts often have a design criterion based on rotor or propeller stability.

Dynamic stability and response problems associated with rotary-wing aircrafts represent some of the most complex problems in the area of aeroelasticity. There are two basic sources of this complexity. " *One is the unusual flexibility of the prop-rotor blades (even in the case of so-called rigid rotors), and the other is the complexity due to rotation. Flexibility manifests itself both by adding degrees of freedom which can be important and by allowing initial deflections to be large enough to add coupling terms between degrees of freedom. Rotation, of course, leads to 1) much more complicated inertia forces (e.g., centrifugal, Coriolis, gyroscopic) which must always be regarded as potential sources of stiffness or coupling between the degrees of freedom, and 2) an aerodynamic situation of*

exquisite intractability " [6]. The stability problems in helicopters is dealt in two steps, first by considering an isolated blade and a fixed hub, and secondly by carrying out a coupled aeroelastic analysis of rotor and fuselage by assuming a movable hub. Types of motion exhibited by the blade and fuselage of a typical helicopter are shown in Figure 1.

Due to the complicated nature of the aeroelastic problems, rotary- wing aeroelasticity had been considerably less developed than its fixed-wing counterpart. This field has seen intense activity in the last three decades. Still since the classical books in aeroelasticity date back to 50s or 60s, one does not even find a mention of this field of comparable importance.

Over the years a number of configurations of the rotor blades have been developed, each with a specific purpose in mind. The ones in extensive use can be divided into four types , as shown in Figure 2 [7], ; These are (i) semi-articulated or see-saw, (ii) articulated, (iii) hingeless and lastly (iv) bearingless rotors. The see-saw rotor (Bell) is typically a two-bladed rotor with the blades connected together and attached to the shaft by a pin which allows the two-blade assembly to rotate such that tips of the blades may freely move up and down with respect to the plane of rotation (flapping motion). In the fully articulated rotor, each blade is individually attached to the hub through two perpendicular hinges allowing rigid motion of the blade in the two directions, out of the plane of rotation (flapping) and in the plane of rotation (lead-lag) as typified by Sikorsky, Boeing-Vertol and Hughes helicopters.The third type is the

hingeless rotor in which the rotor blade is a cantilever beam. Being a long thin member, elastic deformations of the hingeless blade are significant in the analysis of the dynamics of the vehicle. Both hingeless and bearingless rotors were built with an eye on mechanical simplicity and increased maintainability. A bearingless design eliminates the hinges and the pitch bearing found in an articulated rotor. Some bearingless designs employ lag dampers. The bearingless blade has an elastic flexure consisting of flexbeams and a torque tube to facilitate pitch changes.

Other recent developements in the rotor configuration are the Tilt rotor [8,9], ABC rotor [10,11] and the circulation rotor [12,13].

Present day rotor blades are often made up of composite materials, which have found increasing use in the field of structural design. Composites unlike the metallic counterpart have direction dependent properties. And the fact that they have very high strength to weight or stiffness to weight ratio is of essence. A wise manipulation of these properties can lead to cheaper and much lighter designs. For the laminated composites, the stacking sequence of the plies is of primary importance, which divide them into symmetric and asymmetric categories. The elastic couplings exhibited by both these categories are often used in, what is now popularly termed as *Aeroelastic tailoring*. As the name suggests, fiber composites are *cut* and *pasted* in a particular fashion so as to yield desirable results. This has been possible owing to highly directional behaviour of the these materials. Some of these couplings in the elastic stiffness matrix are,

- Bending-Extension

- Shear-Extension

- Twist-Bending couplings.

The first of these is exhibited only by the unsymmetrically laminated plates/beams, which basically means that the in-plane and the out-of-plane problems are coupled. Much more, in terms of strength, weight and life is expected of today's structures, which has what led to the increasing research in the field of composite structures which provide much more flexibility than their isotropic counterpart.

Castel and Kapania [14] have presented a one dimensional model of a composite laminated beam amenable to linear aeroelastic analysis. They developed a 24 degree of freedom finite element which is capable of analysing a beam/plate of arbitrary cross-section, planform, taper and sweep. The special features of the analysis are the inclusion of shear deformation, warping correction factor, and its capability to study the effect of various elastic stiffness couplings. The element degrees of freedom include transverse, lateral, axial deflections, torsion, and inplane shear. This element was successfully used for aeroelastic analysis of laminated wings. Hence it can be considered quite appropriate for the proposed coupled flap-lag-torsional stability analysis of laminated beams. In the past a major chunk of the literature in composite research has been devoted to the

analysis of symmetrical laminates. But as the requirements get more and more stringent emphasis is fast shifting to the unsymmetrical counterpart which offer many more couplings which mean much more freedom in manipulating elastic properties.

The objective of the present work is three-fold,

1. To understand various aspects of the problem and solution of aeroelastic stability analysis of rotor blades. To this end an extensive literature survey is conducted.

2. To expand the code developed by Castel and Kapania to its maximum potential and validate the changes. The analysis in Reference [14] is carried out using only w_b, w_s, τ and their derivatives. Deformations like u, β and v are not accounted for.

3. and thirdly, to carry out static and free vibration analyses using a simple structural model for the rotating composite beam.

For the aeroelastic analysis in [14], modified strip theory aerodynamics was employed and these results will be used in validating the changes in the code. Rotary-wing aerodynamics, as discussed later, has very different characteristics as compared to the fixed wings. In addition to the modified strip theory or quasi-steady approximations for the unsteady airloads, induced flow through the

rotor disk also needs to be modeled. Present work does not deal with the aeroelastic analysis of rotating blades.

Literature Survey

Introduction

The following survey is towards an effort to appreciate the approach taken by the researchers in the field of rotor blade aeroelasticity as far as structural and aerodynamic modeling of the problem is concerned. Since this study is preliminary in nature, this survey has been restricted to discussion of the formulations. There has been no attempt made to analyse the nature of the results obtained.

Structural Modeling

Reviews

One of the first significant reviews of the rotary-wing V/STOL dynamic and aeroelastic problems was undertaken by Lowey [6] covering a wide range of topics : static and dynamic classical coupled flap-pitch problems, flap-lag flutter, mechanical instability (ground resonance), coupled airframe/rotor instabilities in flight (air resonance), problems associated with forward flight and periodic coefficients like prop-rotor whirl flutter (where both blade and hub motions are involved). With increased flexibility and use of anisotropic materials for the rotor blades flap-lag-torsional problem have gained an increased significance for both vertical (hover) and forward flight. A more restricted survey emphasizing the role of unsteady aerodynamics and vibration problems in the forward flight was presented by Dat [15]. Flight dynamics problems of hingeless rotors including experimental results were treated by Hohenemser [16]. Blade stability was also discussed in [16], since it is considerd to be a part of the broader flight dynamics problem. Another detailed survey by Ormiston [17] discussed the aeroelasticity of hingeless and bearingless rotors in hover, from an experimental and theoretical point of view.

Friedmann presented three comprehensive reviews [18 - 20] between 1977 - 87. In Reference [18] a detailed chronological discussion of flap-lag and coupled

flap-lag-torsion problems in hover and forward flight was presented emphasizing the inherently non-linear nature of the hingeless blade aeroelastic problem. The nonlinearities considered were geometrical due to moderate deflections. In [19] the role of unsteady aerodynamics, including dynamic stall, was examined together with the treatment of nonlinear aeroelastic problem in forward flight. Finite element solutions to the rotary-wing aeroelastic problems were also considered together with the treatment of coupled rotor/fuselage problems. In Reference [20] more than hundred papers published between 1981-86 were reviewed. To simplify the review, papers were classified based on the subjects they dealt with. Categories were (1) structural modelling, (2) aerodynamic modelling, (3) aeroelastic problem formulation using automated or computerized methods, (4) aeroelastic analyses in forward flight, (5) coupled rotor/ fuselage analyses, (6) active control and their application to aeroelastic response and stability, (7) applications of structural optimization to vibration reduction, and (8) aeroelastic analysis and testing of special configurations.

Among the reviews emphasizing aeroelastic stability, two other surveys [21, 22] dealt exclusively with the vibration problem and its active and passive control in rotorcraft. Johnson [23, 24] published a comprehensive review paper which described both the aeroelastic stability and rotor vibration problems in the context of dynamics of advanced rotor system. A review emphasising some practical design aspects capable of alleviating aeromechanical problems was presented by Miao [25]. Recently a very comprehensive research report [26] has been published which contains a detailed review of research carried out by

NASA / Army sponsorship, between 1967 and 1987. Finally recently Friedmann [27] presented a paper providing a detailed discussion of what he called four important current topics in the helicopter rotor dynamics and aeroelasticity, namely, (1) the role of geometric nonlinearities in rotary-wing aeroelasticity, (2) Structural modeling, free vibration and aeroelastic analysis of composite rotor blades, (3) modelling of coupled rotor/fuselage aeromechanical problems and their active control, and (4) use of higher harmonic control (HHC) for vibration reduction in helicopter rotors in forward flight (In this approach the vibratory aerodynamic loads on the blades are modified at their source as against control after their generation, often done in conventional methods).

In the discussion that will follow, we will concentrate on the first two from the above mentioned list of problems. Attempt will be made to understand the basic approaches taken and some significant achievements.

Isotropic Blades

The rotor blade has been traditionally and quite justifiably modeled as a beam, thus reducing a three - dimensional problem to a one - dimensional one along the axis of the beam. A very significant developement in the blade modeling has been recognizing the *inherent non - linearity* of the problem. Thus correct treatment of a wide class of problems in this area need consistent mathematical modelling which will lead to a set of non-linear equations of motion. Nonlinearity due to the

geometry is most dominant amongst the various types. The effect of this nonlinearity seems to be important for the hingeless and bearingless rotor blades [21 - 23], while not so important for the articulated blades (although both articulated and the bearingless configurations fall in the category of cantilever blades) [24]. In the days of articulated rotors, rotor speeds involved were low and blade stability analysis was not of any crucial importance. In fact aeroelasticians went only as far as to carry out a classical bending - torsion, a two degree of freedom flutter analysis assuming linear strain-displacement relations. Often a fixed-wing aerodynamic theory was used and the formulation compared with Reference [28] which was by far the most complete.

From the point of view of geometrical nonlinearities, the beam equations presented in the literature can be put under two categories, (1) ones assuming moderate deflections and rotations and (2) and the other for large deflections and rotations . Assumption of small strains is common to both the theories. Work under the first category was done mainly in the 70s with a lot of effort put in trying to find a consistent ordering scheme used to obtain the equations of motion. It will be in order here to mention the work of Houbolt and Brooks [28] who presented a systematic derivation of the linear partial differential equations of motion for coupled bending and torsion of twisted non - uniform beams which later became a check case, common for all the nonlinear equations derived from different starting points.

References [29 - 31] represent some of the major works in the moderate deflection theory. Reference [29] used Hamilton's principle to derive the non-linear equations of motion, torsion in the blade was totally borne by a root torsional spring. Most of the non-linear terms were present but an inconsistent ordering scheme led to unsymmetric mass and stiffness matrices and the gyroscopic matrix was also not anti-symmetric. A refined version of this work was later presented in [32]. A more complete set of non-linear equations were presented in [30], where bending and torsion and rotations about flap and lead-lag hinges were considered. However, certain non-linear terms present due to elastic deformations were discarded and later found to be important for stability of cantilever blade configurations. Perhaps the most complete of all the moderate deflections work has been due to Hodges and Dowell [31]. Complete and consistent non-linear equations of motion for the elastic bending and torsion of twisted and non-uniform rotor blades were derived using both, the Newtonian method and the Hamilton's principle. On linearizing, the equations reduced to the ones presented in [28]. This paper also describes the various ordering schemes and coordinate transformations between the deformed and undeformed configuration. Attempts have been made to validate the theory of moderate deflections through experiments consisting of static tests [33].

Ordering schemes are basically used to prevent overcomplication of the non-linear equations. Terms are neglected if they are higher than a certain order (which determines the order of non-linearity considered). Grounds of ordering scheme are complicated and quite a few papers may have presented inconsistent

results by discarding wrong terms. "*When neglecting terms in a large system of equations, care must be exercised to ensure that the terms retained constitute self-adjoint structural and inertial operators. These self-adjoint operators lead to a symmetric stiffness and mass matrices and an anti-symmetric gyroscopic matrix in the modal equations* " [31].

The procedure in deriving the non-linear blade equations use transformation matrices relating the deformed with the undeformed configuration. It has been customary to treat the blade as a long slender beam undergoing combined bending and torsion for which the transformation matrix is derived using Euler angles or other parameters. When using the Euler angles, the question of which rotational sequence to use is left to choice. Reference [34] makes a good reading in this respect. Alkire [35] extended the analysis presented in [34] to obtain a better understanding of the role of built-in pretwist and the elastic twist in the derivation of transformation matrices which relate the position vectors of the undeformed and the deformed states of the blade.

As stated earlier, a lot of experience was needed in deriving these non-linear equations using Euler angles and a consistent ordering scheme. To cite an example of such a transformation process, the transformation matrix shown below has been taken from [36]. The theory is second order accurate (governed by the ordering scheme) and uses a typical hingeless rotor blade shown in Figure 3 in the undeformed and the deformed states. Such a tranformation based

on the assumptions of finite deflections and rotations, small strains for a blade undergoing flap, lag and torsional motion has the following mathematical form,

$$\begin{Bmatrix} \hat{i}' \\ \hat{j}' \\ \hat{k}' \end{Bmatrix} = \begin{bmatrix} 1 & v_{,x} & w_{,x} \\ -(v_{,x} + \phi w_{,x}) & 1 & \phi \\ -(w_{,x} - \phi v_{,x}) & -(\phi + v_{,x} w_{,x}) & 1 \end{bmatrix} \begin{Bmatrix} \hat{i} \\ \hat{j} \\ \hat{k} \end{Bmatrix} = [S] \begin{Bmatrix} \hat{i} \\ \hat{j} \\ \hat{k} \end{Bmatrix}$$

and,

$$[S]^{-1} = [S]^{T}$$

where u, v, w are the displacements in the x, y, and z respectively, as shown in the figure. ϕ is the torsional variable about the elastic axis of the beam.

This transformation matrix is of the second order. Orders of magnitude are assigned to the various parameters of the problems in terms of elastic blade slopes which are assumed to be moderate i.e. slopes are of order ε , with $0.1 \leq \varepsilon \leq 0.2$, and using the relation

$$O(1) + O(\varepsilon^2) = O(1)$$

equations of motion are derived.

This technique is used while deriving equations of motion explicitly, i.e. when equation is written explicitly and each expression can be studied independently. Hence this method has an advantage of providing a good physical insight to the problem. Often, and as is particularly true for helicopter blade equations, the procedure for deriving them is varied. Terms of explicitly derived equations can be easily compared, one at a time, thus bringing out the specific differences. Implicit methods like finite element techniques [37], on the other hand, generate each term of the equation numerically. Hence there is a loss of physical understanding of the problem.

In the 80s the trend changed to that of considering the assumption of large deflections and rotations but small strains. This theory dispensed with the ordering schemes and is amenable to explicit (used in conjunction with Euler angles [38]) as well as implicit technniques. References [38 -40] dealt with large rotations using Rodrigue's parameter instead of Euler angles for finite rotations. Rodrigue's parameter is another form of representation of the direction cosine tensor. They are three in number and can totally describe the rotational motion of a vector relative to another. One of their disadvantages is, that they tend to become infinite for certain values of rotation. A good discussion on these parameters can be found in the Reference [41]. Euler angles have been successfully used with an implicit formulation for large deflections of isotropic and composite beams [42]. The only functional code, however, for aeroelastic analysis using this formulation is GRASP (General Rotorcraft Aeromechanical Stability Program) [43].

While discussing implicit formulations, mention should be made of the extensive work that has been devoted to finite element type of discretization in space. Sivaneri and Chopra developed a finite element code for hingeless [44] and bearingless [45] rotor blade configurations. Former work is similar to the one carried out by Friedmann and Straub [46]. GRASP [43] is a FEM (Finite Element Method) code for the bearingless rotor. It utilises higher order elements as compared to the conventional ones used in [44 - 46]. Another,16 d.o.f. finite element model [47] has been used to study the influence of compressible lifting theory on the coupled flap-lag-torsional aeroelastic stability of hingeless blades in hover. More recently Celi and Friedmann [37] presented a FEM model with implicit aerodynamic formulation for rotor blade aeroelasticity.

Composite Rotor Blades

All the structural models discussed above were restricted to isotropic blades. One of the more important recent developements has been the emergence of structural models suitable for the analysis of composite rotor blades, which are widely used in modern helicopters. The reasons for switching over to composite constructions are,

1. Significant improvements in fatigue life and damage tolerance of the blade.

2. Ability to manufacture more refined aerodynamic designs for planform and airfoil geometries.

3. Aeroelastic tailoring.

All the non-linear kinematics involved in the models, discussed so far, were complex since both deformed and undeformed configurations of the beam are three dimensional. With the use of laminated composite materials (anisotropic nature) and this complexity increases many-folds as the non classical effects of beam theory such as transverse shearing deformations, torsion related warpings and various elastic couplings become more pronounced. Cross-sections no longer remain plane after deformation. While dealing with anisotropic materials, the out of plane warping is important to the analysis. Low strain levels, however, still remain valid keeping blade fatigue life in mind.

This field of research is a fairly new one and probably most of the important concepts developed only in the last five years are well covered in References [48,27]. The limited research in this field can be said to have followed one of the two directions namely,

1. Use of one dimensional kinematics amenable for analysing the composite rotor blades.

2. Developing approaches to reduce the general three dimensional constitutive laws of an anisotropic material into a simple one dimensional form of the beam problem.

In the first category, analogous to its isotropic counterpart, two approaches have been taken, one of assuming moderate deflections and the other large deflections, both working with small strains. A comprehensive study using the former was done by Hong and Chopra [49]. The blade was treated a single cell box-beam with arbitrary lay-up of composite plies on all the four walls of the undeformed rectangular cross-section. Strain-displacement relations are taken from [31] and Hamilton's principle is used to derive the equations of motion for the problem of coupled flap-lag-torsion stability. This coupling is shown to be strong and influencing the instability boundaries in hover. The analysis was extended to bearingless rotors in hover [50] and later in forward flight [51]. It was found that ply orientation is effective in reducing both blade response and hub shears.

Bauchau and Hong [52,42,53] presented a large deflection theory accounting for transverse shear deformation, torsional warping effects and elastic couplings. In the final version of this theory naturally curved and twisted beams undergoing large displacements and rotations and small strains were analysed.

Minguet and Dugundji [54,55] used Euler angles in conjunction with large deflection model for static and free vibration analysis. However transverse shear deformation and cross - sectional warping were ignored.

Under the second category, research is focussed on the determination of warp function(s) , shear center location and the cross-sectional stiffness values, in that order. The cross-sectional analysis is usually linear and two dimensional, done once for each cross-section (if the beam is non uniform) and decoupled from the one dimensional non-linear global analysis of the beam. There have been two distinct approaches used in tackling this problem. One is the purely analytical one in which a closed form solution is attempted for the warp functions, shear center location and the stiffness properties. Hegmier and Nair [56] in 1977 developed a technique to analyse heterogenous and transversly isotropic elastic beam with built-in twist. Mansfield and Sobey [57] derived expressions for the coupled torsional, extensional and flexural stiffnesses of a simplified rotor blade modeled as a hollow composite tube. Mansfield [58] extended the theory to two-celled beams. The theory however, did not recieve a follow up. Further it did not account for tranverse shear and warping of the beam cross-section. It did serve the purpose of giving an idea about the control a designer can wield while dealing with composites, basically hinting at aeroelastic tailoring. A similar approach was taken by Rehfield [59] but incorporating the effects of transverse shear and warping (only torsional in nature). The theory was verified by Nixon [60]. He worked with this theory and found a good correlation between coupled beam analysis based on the theory and the results obtained by carrying on a series of axial and torsion tests. Hodges, Nixon, and Rehfield [61], found a good correlation between this theory and a NASTRAN finite element model for a single closed celled beam.

The finite element approach has been very popular approach in contrast to the analytical one owing to its verstality and flexibility. Although it is often argued that one looses physical insight in such numerical techniques. Wörndle [62], probably the first person to work with a finite element model, calculated cross-sectional warping functions using a linear two dimensional model under torsional and transverse shear. The analysis was however restricted to transversly isotropic thus precluding any demonstration of aeroelastic tailoring. Kosmatka [63] revived this theory by applying it to generally orthotropic materials (arbitrary orientation of its material principle axes). The global one dimensional anlysis assumed moderate deflections and small strains.

Giavotto, et al. [64] presented the most general analyses in the sense that it accounts for both inplane and out of plane warping. It talks about an extremity and a central solution to the warping problem. The extremity solutions correspond to warping solutions due to end effect, while the central solution yields warping due to load without the end effect. Work was extended by Borri and Mantegazza [65] and Borri and Merlini [66] to include nonlinear deformation. An anisotropic theory has been developed by Bauchau [67] in which out of plane cross section warping is expanded in terms of eigenwarpings. The cross section is assumed rigid and the analysis is restricted to multi-celled thin walled beams. Initially theory was restricted to only transversly isotropic materials but in [68] it has been expanded to include general orthotropy. The report claimed substantial savings in computational effort as it found that use of

only a few eigenwarpings, that of torsional warping and shear deformation, was sufficient.

All the studies cited till now had a separate linear two dimensional analysis for the cross - sectional properties. A new approach due to Kim,Lee, and Stemple [69 -71] analyses a thin walled beam of arbitrary cross - section, with the provision for arbitrary cross - section warpings and the beam could be of any planform or taper. The cross section warping is coupled with bending, torsion and extension of the beam. Some static and free vibration results have also been presented in [71]. This theory suffers from not so efficient computational characteristics.

Thus we notice a lot of attention being given to the developement of a general anisotropic beam theory. As pointed out in Ref. [27], [49] is the only work which has resulted into aeroelastic stability analysis of composite rotor blades. It is suggested that using the existing moderate deformation theories in conjunction with linear two dimensional analysis like the one presented in [64], might be adequate for the aeroelastic analysis. Moreover, research in this direction might show if a general anisotropic beam theory is worth the extensive attention it has been receiving.

Aerodynamic modeling

The aerodynamic environment of the helicopter rotor is significantly more complex than that of the lifting elements of a fixed wing aircraft because the rotor blade is forced to pass in proximity to its wake on each revolution, and the rotary motion of the blade relative to the fuselage imparts a basic unsteady aspect to the flow. Unlike the fixed wing counterpart , the helicopter rotor is subjected to oscillatory aerodynamic loads even in a steady gustless forward flight since each blade section encounters variation in relative airspeed as the blade travels the azimuth (loosely defined as path along the circumference of the rotor disc). In addition, the local flow encountered by a rotor blade contains, in the relative near field, disturbances from the previous blade passage. Although these disturbances are constant in time for a steady hover or climb, transient blade dynamics can create unsteady flow phenomena that significantly affect the blade dynamics. Also a very flexible rotor blade leads to coupling of aerodynamics with the structural dynamics of the blade. Therefore while attempting to solve the problem of blade dynamics a compatible model for various aspects (lift model, induced wake model, structural model for the blade and the fuselage) of the flow have to be obtained.

Figure 4 provides a schematic diagram [72] of a general dynamic analysis of a helicopter. The forward loop relates the instantaneous blade angle of attack to instantaneous lift and circulation existing on the blade. The time history is

provided to an induced flow theory (such as Biot - Savart law based on a wake geometry) to provide the inflow information that is fed back to the angle of attack to create unsteady aerodynamics. The blade lift is provided to a structural dynamic model of the blade to provide blade motions which, in turn, alter the angle of attack to complete the aeroelastic loop. This double feedback loop shows that the inflow dynamics is strongly coupled with the rotor dynamics to form the dynamic equations of the rotor. For an aerodynamic lift or inflow model to be useful for rotor dynamics, it must be capable of filling the appropriate blocks with defined state variables and must have appropriate coupling capability so that the loops can be closed with computational efficiency.

While in the previous section we encountered some very highly developed structural models of the blade it is interesting to note that the aeroelastic analysis has often involved crude quasi - steady aerodynamics. This situation is a consequence of the lack of an appropriate unsteady aerodynamic theory that can be consistently combined with the periodic equations of motion governing the blade dynamics in forward flight.

As stated before an attempt will be made to give an overall picture of the developemental process in helicopter aerodynamic modeling.

It has been long known that the induced flow associated with a helicopter rotor responds in a dynamic fashion to the changes in blade angle of attack [73 - 75].

It is therefore, the research work in unsteady induced flow that we will be looking into. They can be classified into three main categories;

1. Classical unsteady aerodynamic theories.

2. Rotor vortex theories.

3. Dynamic inflow theories.

Classical Unsteady Aerodynamic Theories.

For many years flutter calculations were restricted to a thin airfoil oscillating in a uniform stream of incompressible fluid [76]. While Glauert [77] partially solved the case of simple harmonic motion, the complete solution was due to Theodorsen [78], where a thin airfoil modeled as a flat plate airfoil with vorticity distribution in a potential flow. Both variation of bound vorticity and its continuously shed vortex wake were considered for unsteady flow. Theodorsen's work resulted in the so - called Theodorsen's lift deficiency function C(k) which accounts for the induced - flow effect on circulatory lift and has the form of,

$$C(k) = \frac{J_1(k) - i\,Y_1(k)}{Y_0(k) - i\,Y_1(K) + (J_1(k) + i\,J_0(k))}$$

where $J_n(k)$ and $Y_n(k)$ are Bessel functions of first and second kind, respectively and $k = \frac{b_r\omega}{V}$ is the reduced frequency. This function relates the net circulatory lift amplitude and phase to the airfoil angle attack as a function of reduced frequency. However, since the helicopter rotor blade is essentially a rotating wing , the shed vorticity no longer remains in the plane of the lifting surface as it travels downstream. Instead it forms a helical pattern below the rotor disk due to the presence of a finite inflow through the rotor disk. Other reasons which prohibit the application of Theodorsen's result in rotary wing analysis is the time varying free-stream and the presence of returning wake. Nevertheless various quasi-steady and unsteady models for the aerodynamic loads based on this theory have been frequently employed in the rotary wing aeroelasticity.

The effect of time variation and the presence of induced flow was taken care of in Greenberg's [79] theory. In applying this theory velocity components, relative to the deformed cross-section of the blade have to be identified and used.

It is worth noting that we are still dealing with fixed wing aerodynamic theories. Loewy's [80] theory is the first significant adaptation of the Theodorsen's theory in approximating the unsteady wake beneath the rotor.In fact Jones [81] and Timmon and van de Vooren [82] also worked on the same lines. All of them considered flow to be incompressible and the main restriction on their theories is that helicopter is operating in a vertical flight or hover condition. Lowey considered the influence of vorticity that is shed and blown below the rotor disk

and which is passed over by successive blades in successive revolutions (basis of the returning wake concept). Based on this inflow assumption,the author was able to formulate a two dimensional wake model for a flat plate airfoil by introducing parallel layers of vorticity. With this wake model, Lowey derived his lift deficiency function (which accounts for the effect of the oscillatory motion on the magnitude and phase of the lift vector), $C'(k)$ for a rotor blade in vertical flight,

$$C'(k) = \frac{J_1(k)(1 + 2W) - iY_1(k)}{Y_0(k) - iY_1(K) + (J_1(k) + iJ_0(k))(1 + 2W)}$$

Here the wake spacing function W accounts for the layers of vorticity beneath the airfoil. Lowey's lift deficiency function looks similar to Theodorsen's function but is different in nature. $C'(k)$ oscillates with the reduced frequency while C (k) does not. Lowey's study concluded that quasi - steady aerodynamic theory is inadequate for rotor dynamic problems such as calculating flutter speeds or damped amplification factor. There are some inherent drawbacks of this theory although it is extensively used for rotor aeroelastic problems.

1. The unsteady wake beneath the rotor in forward flight is a skewed helix while assumed two dimensional flat - layered in the theory.

2. Poor behaviour of the model for low frequency problems.

3. Formulated in the frequency domain (i.e. is based on the assumption of simple harmonic motion) which implies it is strictly valid only at the stability boundary and does not yield meaningful results for off - critical analyses.

Observing that Lowey's theory is for incompressible flows, notable extensions or modifications to his theory to incorporate compressibility has been due to Jones and Rao [83] and Hammond and Pierce [84].

One of the drawbacks of Lowey's method, as discussed above, was its formulation in the frequency domain. Thus it was not compatible with the structural dynamic equations which had periodic coefficients for the forward flight. Friedmann and Venkatesan [85] presented Lowey's theory in the time domain (often referred to as the finite state models), thus solving one of the classical two dimensional unsteady aerodynamic problems (within the approximations) to satisfaction.

Three Dimensional Vortex Theories

Vortex theory has served as a fundamental tool to compute induced velocity field associated with lifting rotors by the Biot - Savart law. This is a more direct approach to the modelling of unsteady rotor wake. The wake is first modelled theoretically / experimentally and the effect of such known patterns are studied.

The theories proposed under this category can be based on wake specification; 1) rigid wake, 2) distorted (or free) wake, and 3) prescribed (experimental) wake.

Among the rigid wake theories important contributions have been due to Drees [86], Heyson [87], and Wang [88]. While Dree's work was essentialy a quasi - steady aerodynamic technique, Heyson described wake as a number of concentric vortex cylinders and studied its induced flow field. Wang presented a very complex model but with some closed form solutions. However with his assumption of infinite number of blades, there is no way of calculating instantaneous values of induced velocities needed for rotor dynamic studies. Miller [89] introduced the concept of 'near wake' and 'far wake' and studied these two vortex distributions using lifting line and lifting surface theories, respectively.

In free wake analysis, segment vortex filaments from each rotor blade is allowed to move freely until a convergent wake is developed. Scully's [90] and Sadler's [91] models are those typically used. Former considered distortion of only tip vortex while the latter considered distortion of bound vorticity too. This theory presents a three dimensional unsteady wake model but there are serious computational problems associated with it.

Gray [92], one of the pioneers in the field of prescribed vortex theory, developed a semi-empirical method for the wake of a single blade rotor based on empirical wake geometry data acquired from smoke-visualization tests.

Dynamic Inflow Theory

Dynamic inflow modelling in rotorcraft flightdynamics is a means of accounting for the low - frequency wake effects under unsteady or transient conditions. Here unsteady aerodynamics is divided into two parts: (i) dynamic inflow that is viewed globally as rotor - disc downwash dynamics under unsteady flight conditions (wake theory or often the steady inflow part) and (ii) the classical unsteady rotor aerodynamics that is viewed locally as airfoil aerodynamics under steady flight conditions (lift model or the perturbation part).

The wake theory (or outer problem) calculates induced velocity associated with the helicopter rotor. In such a formulation, dynamic inflow theory models the wake, leaving a flexible choice for the lift model. Sissingh [74] made the first systematic exploration that established a relation between instantaneous perturbation in thrust, and perturbations in the induced flow. Sissingh's analysis was a quasi - steady approach and was motivated by Amer's observations [73], that a part of the difference between predicted and measured pitch and roll damping is due to dynamic inflow effects. Almost twenty years later Curtiss and Shupe [93,94] revitalized this research by refining Sissingh's quasi-steady

formulation (no time lag) to include induced flow perturbation in pitch and roll moments. Dynamic inflow research is said to have been always driven by the impetus of experimental data. Since 1980s dynamic inflow has been one of the intensly pursued area of research which in good measure, was spurred by Bousman's test data [95] on aeromechanical stability in hover. Present day's research revolves around what is called Pitt and Peter's dynamic inflow model [96,97] and its application to help predict damping and response in forward flight. Although this model has been used extensively due to its practicality, it is worth noting that the model is only a low order approximation of the rotor induced flow field, and can only account for rotor wake dynamics of low frequencies.

References [15,19] and [72] are good treatment and provide a good review of dynamic flow models. References [15,19] also deal extensively with the other two models.

Models

The static and dynamic analysis in the present work uses an extension of the structural model of Castel and Kapania [14]. In this chapter a mere outline of the models will be provided, highlighting their salient features and some important steps. For details of the modeling one is referred to [14].

Structural Model

The blade is modeled as a Timoshenko beam of arbitrary cross section and span. Top and bottom skins are curved and made up of laminated composite material. Four webs and eight stringers run along the span as shown in the Figure 5. The webs are assumed to carry transverse shear stresses τ_{xz} only, while the stringers carry only axial stresses. The properties of any web or stringer can be set to zero, and no membrane type assumption is made concerning the behaviour of the

skins, so that a wide range of structures can be analysed, from beam-plates to monocoque box beams to fully built-up structures.

Transverse shear and the warping correction factor are included in the the formulation. The chord, thickness, and sweep can vary along the span.

The 24 d. o. f. finite element as shown in Figure 6 is used to discretize the one dimensional beam and all the degrees of freedom are assumed to vary cubically along its length. The following equations present them as a function of Hermitian polynomials.

$$
\begin{aligned}
u(x) &= N_1 u_1 + N_2 u'_1 + N_3 u_2 + N_4 u'_2 \\
w_b(x) &= N_1 w_{b1} + N_2 w'_{b1} + N_3 w_{b2} + N_4 w'_{b2} \\
w_s(x) &= N_1 w_{s1} + N_2 w_{s1'} + N_3 w_{s2} + N_4 w'_{s2} \\
\tau(x) &= N_1 \tau_1 + N_2 \tau'_1 + N_3 \tau_2 + N_4 \tau'_2 \\
\beta(x) &= N_1 \beta_1 + N_2 \beta'_1 + N_3 \beta_2 + N_4 \beta'_2 \\
v(x) &= N_1 v_1 + N_2 v'_1 + N_3 v_2 + N_4 v'_2
\end{aligned}
\qquad [1.1]
$$

where the prime stands for $\frac{d}{dx}$. The second order Hermitian polynomials N_i are given as :

$$
\begin{aligned}
N_1(x) &= 1 - 3(\frac{x}{l})^2 + 2(\frac{x}{l})^3 \\
N_2(x) &= x - 2\frac{x^2}{l} + \frac{x^3}{l^2} \\
N_3(x) &= 3(\frac{x}{l})^2 - 2(\frac{x}{l})^3 \\
N_4(x) &= -\frac{x^2}{l} + \frac{x^3}{l^2}
\end{aligned}
\qquad [1.2]
$$

where l is the length of the element.

The strain displacement relations look like,

$$\begin{aligned}
\varepsilon_x^0 &= \frac{du}{dx} = \frac{\partial u}{\partial \xi} \;/\; \frac{\partial x}{\partial \xi} \\
\gamma_{xy}^0 &= \beta \\
\kappa_x^w &= \frac{d^2 w_b}{dx^2} = \frac{\partial^2 w_b}{\partial \xi^2} \;/\; \left(\frac{\partial x}{\partial \xi}\right)^2 \\
\kappa_x^v &= \frac{d^2 v}{dx^2} = \frac{\partial^2 v}{\partial \xi^2} \;/\; \left(\frac{\partial x}{\partial \xi}\right)^2 \\
k_{xy} &= 2\frac{\partial}{\partial x}\left(\frac{\partial w}{\partial y}\right) = 2\frac{d\tau}{dx} = 2\frac{\partial \tau}{\partial \xi} \;/\; \frac{\partial x}{\partial \xi}
\end{aligned} \qquad [1.3]$$

The transverse shear strain is related to the transverse deflection due to shear w_s by :

$$\gamma_{xz} = \frac{dw_s}{dx} = \frac{\partial w_s}{\partial \xi} \;/\; \frac{\partial x}{\partial \xi} \qquad [1.4]$$

Rewriting in the matrix form,

$$\{\varepsilon\} = [B]\{q\} \qquad [1.5]$$

where $\{\varepsilon\} = \{\varepsilon_x^0, \gamma_{xy}^0, \kappa_x^w, \kappa_{xy}, \gamma_{xz}, \kappa_x^v\}^t$ is the strain vector and {q} is the nodal displacement vector. The strain-displacement matrix [B] is shown in Figure 7.

The constitutive equations are obtained as,

$$\begin{Bmatrix} N_x \\ N_{xy} \\ M_x^w \\ M_{xy} \\ M_x^v \end{Bmatrix} = \begin{bmatrix} A_{11} & A_{16} & B_{11} & B_{16} & YA_1 \\ A_{16} & A_{66} & B_{16} & B_{66} & YA_6 \\ B_{11} & B_{16} & D_{11} & D_{16} & YB_1 \\ B_{16} & B_{66} & D_{16} & D_{66} & YB_6 \\ YA_1 & YA_6 & YB_1 & YB_6 & YD \end{bmatrix} \begin{Bmatrix} \varepsilon_x^0 \\ \gamma_{xy}^0 \\ \kappa_x^w \\ \kappa_{xy} \\ \kappa_x^2 \end{Bmatrix} + \begin{bmatrix} A_{12} & B_{12} \\ A_{26} & B_{26} \\ B_{12} & D_{12} \\ B_{26} & D_{26} \\ YA_2 & YB_2 \end{bmatrix} \begin{Bmatrix} \varepsilon_y^0 \\ \kappa_y \end{Bmatrix} \qquad [1.6]$$

The A's, B's and D's are defined by analogy with the Classical Lamination Theory [98] as :

$$A_{ij} = \int_{-\frac{b}{2}}^{\frac{b}{2}} \sum_{k=1}^{n+1} (z_k - z_{k-1}) \overline{Q}_{ij}^k dy$$

$$B_{ij} = \int_{-\frac{b}{2}}^{\frac{b}{2}} \frac{1}{2} \sum_{k=1}^{n+1} (z_\kappa^2 - z_{k-1}^2) \overline{Q}_{ij}^k dy \qquad i,j = 1, \ldots, 6 \qquad [1.7]$$

$$D_{ij} = \int_{-\frac{b}{2}}^{\frac{b}{2}} \frac{1}{3} \sum_{k=1}^{n+1} (z_\kappa^3 - z_{k-1}^3) \overline{Q}_{ij}^k dy$$

and the terms pertaining to the lateral bending deflection are :

$$YA_j = \int_{-\frac{b}{2}}^{\frac{b}{2}} y \sum_{k=1}^{n+1} (z_k - z_{k-1}) \overline{Q}_{1j}^k dy$$

$$YB_j = \int_{-\frac{b}{2}}^{\frac{b}{2}} \frac{y}{2} \sum_{k=1}^{n+1} (z_\kappa^2 - z_{k-1}^2) \overline{Q}_{1j}^k dy \qquad j = 1, \ldots, 6 \qquad [1.8]$$

$$YD = \int_{-\frac{b}{2}}^{\frac{b}{2}} y^2 \sum_{k=1}^{n+1} (z_k - z_{k-1}) \overline{Q}_{11}^k dy$$

where n is the total number of plies and z_k is the coordinate of the top surface of the k-th ply, numbered from the top down.

The transverse shear deformation is included in this formulation by splitting the transverse deflection in two parts :

$$w = w_b + w_s \qquad [1.9]$$

w_s is evaluated following Timoshenko's method in which the transverse shear force-strain relation is :

$$N_{xz} = KA_{44}\gamma_{xz} \qquad [1.10]$$

A_{44} is the transverse shear stiffness :

$$A_{44} = \int_{-\frac{b}{2}}^{\frac{b}{2}} \sum_{k=1}^{n+1} (z_k - z_{k-1}) G_{13}^k dy \qquad [1.11]$$

where G_{13}^k is the transverse shear modulus of the k-th lamina. K is a shear coefficient introduced to account for the discrepancy between the uniform shear strain distribution inherent to the one-dimensional formulation and the true distribution.

Equations [1-6] and [1-11] are combined to obtain the constitutive relations for the laminated cover skins :

$$\{N\} = [DL]\{\varepsilon\} \qquad [1.12]$$

with

$$\{N\} = \begin{Bmatrix} N_x \\ N_{xy} \\ M_x^w \\ M_{xy} \\ N_{xz} \\ M_x^v \end{Bmatrix} \quad , \quad \{\varepsilon\} = \begin{Bmatrix} \varepsilon_x^0 \\ \gamma_{xy}^0 \\ \kappa_x^w \\ \kappa_{xy} \\ \gamma_{xz} \\ \kappa_x^v \end{Bmatrix} \qquad [1.13]$$

Next step is to derive the element stiffness matrix. This is done using the strain energy expression which for a beam element of length l is given as :

$$U = \frac{1}{2}\int_0^l \{\varepsilon\}^t \{N\} dx \qquad [1.14]$$

where [k], the element stiffness matrix, is given by :

$$[k] = \int_0^l [B]^t [D][B] dx \qquad [1.15]$$

Incremental Stiffness Matrix

At this point we add the effect of rotation to the stiffness matrix. Observe that the incremental matrix is derived from a linear analysis, i.e. assumption of small deflections and rotations and, of course, small strains. Assuming a constant force along the chord of the beam at any cross-section, the strain energy contribution due to the centrifugal force acting on the beam is,

$$U_{centri} = \frac{1}{2}\int_0^l \int_{-\frac{b}{2}}^{\frac{b}{2}} f_{x'}(x, y)\left(\frac{\partial w}{\partial x'}\right)^2 dx'\, dy + \frac{1}{2}\int_0^l F_{x'}\left(\frac{\partial v}{\partial x'}\right)^2 dx' \qquad [1.16]$$

where,

$$w(x, y, t) = w_b(x,t) + w_s(x,t) - y\tau(x,t) \qquad [1.17]$$

On substituting [1.17] in [1.16] and assuming f_x to be a function of x only and for a uniform beam,

$$\begin{aligned} U_{centri} = & \frac{1}{2}\int_0^l F_{x'}\left(\frac{\partial w_b}{\partial x'}\right)^2 dx' + \frac{1}{2}\int_0^l F_{x'}\left(\frac{\partial w_s}{\partial x'}\right)^2 dx' \\ & + \frac{1}{2}\,\frac{b^2}{12}\int_0^l F_{x'}\left(\frac{\partial \tau}{\partial x'}\right)^2 dx' + \frac{1}{2}\int_0^l 2\,F_{x'}\left(\frac{\partial w_s}{\partial x'}\right)\left(\frac{\partial w_b}{\partial x'}\right) dx' \\ & + \frac{1}{2}\int_0^l F_{x'}\left(\frac{\partial v}{\partial x'}\right)^2 dx' \end{aligned} \qquad [1.18]$$

The expression for the centrifugal force F_x and the incremental stiffness matrices are given in the Appendix A. Here x' is a dummy variable along the beam axis.

The effective stiffness matrix of the element is obtained on adding the stiffening effect due to rotation to the original stiffness matrix [1.15]

Elemental mass matrix is obtained through the kinetic energy expression. Neglecting rotatory inertia, the kinetic energy of the beam can be written as :

$$T = \frac{1}{2}\int_0^l \rho A\left(\frac{dw}{dt}\right)^2 dx + \frac{1}{2}\int_0^l \rho A\left(\frac{du}{dt}\right)^2 dx + \frac{1}{2}\int_0^l \rho A\left(\frac{dv}{dt}\right)^2 dx \qquad [1.19]$$

Using [1.17] expression for the kinetic energy is obtained as :

$$T = \frac{1}{2}\int_0^l \rho A[\dot{w}_b^2(x) + \dot{w}_s^2(x) + \dot{u}^2(x) + \dot{v}^2(x)]dx$$
$$+ \frac{1}{2}\int_0^l 2\rho A[\dot{w}_b(x)\dot{w}_s(x)]dx + \frac{1}{2}\int_0^l J\dot{\tau}^2 dx \qquad [1.20]$$
$$+ \frac{1}{2}\int_0^l 2r\rho A(\dot{w}_b\dot{\tau} + \dot{w}_s\dot{\tau})dx$$

where ρ is the material density, A(x) is the cross-sectional area of the beam, J(x) is the polar mass moment of inertia of the section and r(x) is the offset between the reference line and the center of gravity position. A more complete expression for the Kinetic Energy leads to terms due to Coriolis and gyroscopic forces. Following expressions for the element mass matrix components obtained in terms of the interpolation polynomials :

for w_b,w_s,u and v :

$$m_{ij} = \int_0^l \rho A(x)N_i(x)N_j(x)dx$$

for τ :

$$m_{ij} = \int_0^l J(x)N_i(x)N_j(x)dx$$

[1.21]

coupling between w_b and w_s: $m_{ij} = \int_0^l \rho A(x)N_i(x)N_j(x)dx$

coupling between τ and w_b,w_s: $m_{ij} = \int_0^l r(x)\rho A(x)N_i(x)N_j(x)dx$

Static Deflection and Free Vibration Analysis

At this stage of analysis we have the total stiffness and the mass matrix. Hence we can go ahead with static analysis or we can find the natural frequencies and mode shapes of the structure depending on the need.

The static deflection equation :

$$[K]\{q\} = \{F\} \qquad [1.22]$$

where [K] is the assembled structure stiffness matrix, {q} the total nodal displacement vector and {F} the total nodal load vector. Eqn. [1.22] is solved by the IMSL subroutine DLSLRG for the nodal displacements given {F}.

The equations of motion of the structure are obtained from Lagrange's equations and for harmonic oscillations are :

$$\left[[K] - \omega^2[M]\right]\{q\} = \{0\} \qquad [1.23]$$

where [M] is the assembled structure mass matrix and ω is the oscillation frequency. This eigenvalue problem is solved with the help of the IMSL subroutine DGVCRG. This code using 24 d.o.f. element for static and free vibration analysis is called AE24.

Aerodynamic Model

The strip theory was developed with the sole aim to analyze a three dimensional wing with a two dimensional approach. Modified strip theory as developed by Yates [99 - 103], is basically Theodorsen's technique (as discussed earlier), taking into account finite span of the wing oscillating (sinusoidally) in compressible flow conditions. Main modifications being,

1. Arbitrary section lift - curve slope $C_{l_\alpha} = C_{l_\alpha}(y)$ used instead of 2π.

2. Arbitrary section aerodynamic center $a_c = a_c(y)$ used instead of quarter - chord.

3. The circulation function of Theodorsen is modified on the basis of 2-D compressible flow theory to account approximately for effects of compressibility on the magnitudes and phase angles of the section lift and moment vectors.

The resulting expressions for the lift and moment are given in [7]. The principle of virtual work is used to derive the aerodynamic matrix,

$$\delta W = \int_0^l \delta w L dx + \int_0^l \delta \tau M dx \qquad [1.24]$$

$$\delta W = \int_0^l [\{\delta q\}^t N_w (L_w N_w^t + L_\theta N_\theta^t + L_\tau N_\tau^t + L_{\tau'} N_{\tau'}^t)\{q\} \qquad [1.25]$$

$$+ \{\delta q\}^t N_\tau (M_w N_w^t + M_\theta N_\theta^t + M_\tau N_\tau^t + M_{\tau'} N_{\tau'}^t)\{q\}]\omega^2 dx$$

$$= \{\delta q\}^t [\int_0^l (L_w N_w N_w^t + L_\theta N_w N_\theta^t + L_\tau N_w N_\tau^t + L_{\tau'} N_w N_{\tau'}^t \qquad [1.26]$$

$$+ M_w N_\tau N_w^t + M_\theta N_\tau N_\theta^t + M_\tau N_\tau N_\tau^t + M_{\tau'} N_\tau N_{\tau'}^t)\omega^2 dx]\{q\}$$

$$= \{\delta q\}^t \omega^2 [a]\{q\} \qquad [1.27]$$

Nodal load vector equivalent to the distributed aerodynamic loading is therefore:

$$\omega^2 [a] \{q\}$$

where [a] is the complex element aerodynamic matrix.

Solution for Aeroelastic results.

The equations of motion of the wing oscillating with frequency ω in unsteady flow are:

$$([K] - [M]\omega^2 - [A]\omega^2)\{q\} = \{0\} \qquad [1.28]$$

where [A], the assembled aerodynamic matrix, is a function of the flow speed V through the reduced frequency $k = \frac{\omega b_r}{V}$. These equations are solved for the flutter speed and frequency, and for divergence speeds using the V - g method. The procedure is explained in [7]. For the flutter boundary it is necessary to find that value of structural damping **g,** which when added to the existing damping, just prevents the structure from going into the instability region. While divergence speed is characterized by the speed at which **g** goes abruptly to zero (from negative), simultaneously with the frequency of oscillation.

Results

Results obtained from the present code for a number of problems found in the literature are presented. One of the objectives of the present work was to make changes in the model developed by Castel & Kapania [14], and validate these changes. AE12 (code using 12 d.o.f. used in Ref. [14]), dealt with six degrees of freedom at each node w_b , w_s , τ and their derivatives. Present code, AE24 , is basically an expansion to use the formulation in its full potential, i.e. addition of u , β , v and their derivatives to render a 24 d.o.f. finite element. Each of these deformations can become significant while dealing with anisotropic materials. To validate this transformation some of the cases dealt with in [14] (and some others) are reconsidered. Having verified the formulation and coding for the stiffness, mass and the aerodynamic matrices through static, free vibration and aeroelastic results respectively, the effects of centrifugal force on the static and dynamic characteristics is studied.

The results are hence divided into two parts, the first dealing with the validation of the new expanded code and the second with the results obtained from the rotating beam analysis.

Validation

Static deflections

In the first case shear deflection for an isotropic beam under tip loading is analysed. Material is aluminum and results are obtained and compared for the case K = 0.667 and 0.867. Comparisons are made with exact solution due to Timoshenko [105], and other references cited in Table 1.

A symmetrically laminated cantilever beam under the end load **P**, is next studied and the distribution of tip deflections, both due to bending and shear deformation, and twist are obtained using one element. The plotted values of the delections are for the non - dimensionalized parameters

$$\frac{4\,\tau}{P\,l^2\,d_{16}} \;,\; \frac{3\,w_b}{P\,l^3\,d_{11}} \;,\; \frac{w_s K\,D_{44}}{Pl}$$

so that they are equal to unity at the tip. d_{16} and d_{11} are the flexural compliances. The properties of the beam $[45_4 / -45_4]_s$ are the same as given in the reference [106]. The results as shown in Figure 9 are in good agreement with ones presented in [106].

Finally in the static analysis, a beam consisting of top and bottom flat laminated skins rigidly connected as shown in Figure 10 with unidirectional layer of orthotropic material oriented at an angle θ from the spanwise axis, is considered. The material properties of the laminae are as follows: $E_1 = 6.9 \times 10^{10}$ N/m^2, $E_2 = 5.0 \times 10^9$ N/m^2, $\nu_{12} = 0.30$, $G_{12} = 1.5 \times 10^{10}$ N/m^2, $\rho = 2.71 \times 10^3$ kg/m^3. Four elements were used to model and the analysis is done for the tip deflection under a vertical tip load **P** = 200 N. The results obtained agreed well with the ones in [14] over the entire range of values of the fibre angle θ as depicted in Figure 11. The variatons are due to the different boundary conditions due to additional degrees of freedom.

Free Vibrations

One example each from isotropic, and composite laminated structures (one each for symmetrical and unsymmetrical laminations) were run.

Aluminum plates of dimension 6″ × 3″ × 0.0416″, is used to perform the analysis. Values for the bending and torsion frequencies, given in Table 2 match well with the ones obtained in [109] confirming that plate analyzing capacity of the code.

Abarcar and Cunniff [110] presented results for the free vibrations of high aspect ratio cantilever beams of unidirectional fiber reinforced composite material. The beam length is l = 7.5 in, its width is b = 0.5 in and its thickness is h = 0.125 in. The material properties are $E_{11} = 18.7 \times 10^6$ psi, $E_{12} = 1.36 \times 10^6$ psi $\nu_{12} = 0.3$, $G_{12} = 0.7479 \times 10^6$ psi, $G_{13} = 0.624 \times 10^6$ psi, $\rho = 0.1449 \times 10^{-3}$ lb $-$ sec^2 /in^4.

The frequencies obtained using 3,4,8 and 9 finite elements to model a 30 ° off-axis beam are shown in Table 3 and are found to agree well with those of Reference [110]. We note a good convergence of results for the first four modes.

For unsymmetrically laminated panels, Thornton [111] evaluated the natural frequencies of unsymmetric cantilevered Boron/Epoxy panels. The panels were square (L = b = 8 in, h = 0.046 in), with the following material properties : $E_1 = 23.3 \times 10^6$ psi, $E_2 = 1.81 \times 10^6$ psi, $\nu_{12} = 0.21$, $G_{12} = 0.98 \times 10^6$ psi, $\rho = 0.174 \times 10^{-3}$ lb-sec^2/ in^4 .

Eight plies constituted each panel, the four bottom plies being oriented at 0 ° while the top four plies were oriented at an off-axis angle to obtain the desired bending-stretching coupling. The $[45_4 / 0_4]_T$ panel was modeled using 4 elements to obtain the results presented in Table 4. The present formulation yields better results for the first four modes than the 12 d.o.f. model from Ref. [14], when compared to the experimental results presented in reference in [111].

Aeroelastic results

Reference [112] presents analytical and experimental results for unswept laminated cantilever plates. Two - dimensional unsteady aerodynamics is used in conjunction with strip theory. Figure 12 shows that values obtained from present study match well with [112], and are quite the same as [14]. Reason for discrepancy can be attributed to one - dimensional nature of modeling of a plate in the AE24 and also since it does not account for camber effect unlike [112].

For the box - beam Figure 10 ,the stability boundaries obtained from AE24 are the same as presented in reference [14], and also match well with those presented in reference [113] as shown in Figure 13.

Results from the rotating beam.

We observe that the analysis using AE24 behaves more or less like the analysis using the code AE12 of Ref. [14]. The incremental matrix introduced in the code from a linear analysis of the rotating composite beam is now verified. The pattern to be followed is the same as that of the first part i.e. static, free vibration and lastly aeroelastic analysis, now with the effect of rotation.

Static deflections.

The effect of rotation on a composite plate under a constant transverse tip load is studied. The plate is a symmetrical Graphite/Epoxy $[\theta_2 / 0]$, considered in reference [112]. The reference work, however, does not deal with static analysis. Plate has the dimensions of $l = 0.305\,m$ $b = 0.076\,m$ and $h = 0.804 \times 10^{-3}\,m$ and the properties are, $E_{11} = 98.0\,x\,10^9\,N/m^2$, $E_{12} = 7.9\,x\,10^9\,N/m^2$, $\nu_{12} = 0.28$, $G_{12} = 5.6\,x\,10^9\,N/m^2$, $G_{13} = 5.6\,x\,10^9 N/m^2$, $\rho = 1.52\,x\,10^3 kgm^{-3}$.

The results obtained are shown in Figure 14. As expected centrifugal forces increase the stiffness of the plate and tip deflections decrease. Higher values of θ mean a lower value of flexural stiffness, a fact clearly represented in the figure. We notice higher values of deflection with increasing θ.

Free Vibration.

Beginning with the isotropic case, the first natural frequency is plotted against the angular velocity of an aluminum rotating beam. The values plotted are non - dimensionalized parameters defined as, $\Omega\,(\frac{\rho A l^4}{EI})$, and $\omega\,(\frac{\rho A l^4}{EI})$, for the angular velocity of rotation and the natural frequency of vibration of the beam respectively. Comparisons are made with several works namely that of Kumar [114], Wang [115], Bhat [116] which used Mykelstad, Galerkin and Raleigh - Ritz methods respectively. Comparison as can be seen in Figure 15 is good.

Effect of the radius of the hub on the vibration characteristics of the blade is also studied. Values are compared with those in reference [104] (which also uses a finite element technique) and the comparison is good. As shown in Figure 16 for $\overline{R}$ values of 2.4 and 6 (which are more true for turbine blades for example), higher hub radius to blade length ratio seem to render a stiffer structure.

A similar study is carried out for a Graphite/Epoxy plate considered in [110]. The plot of angular velocity vs first natural frequency of vibration is presented in Figure 17 for different values of fiber orientation. The behaviour is similar to the isotropic one with plate getting more flexible for higher values of fiber angle as evident from lower values of frequency of vibration.

Figure 18 shows the effect of $\overline{R}$ on the free vibration characteristics of the box beam. The non-dimensionalized parameter used here is of the form, Ω ($\frac{\rho A l^5 h^3}{D_{11} I}$), and ω ($\frac{\rho A l^5 h^3}{D_{11} I}$).

Conclusions and Recommendations for Future Work

The code for 24 degrees of freedom, AE24, was successfully run and validated using several examples. It seemed to perform better than the code AE12 [14], for the unsymmetrical specimen. Linear static and free vibration analysis yielded results consistent with expected ones. Both rotation and fiber orientation are seen to play a prominent role in the determination of the static deflections and the natural frequencies of vibration.

As seen in the literature survey, the state of art structural model used in the aeroelastic analysis of helicopter rotors is much more complex than the one used in the present work.

There is a need for developing a non-linear analysis technique for the structural model. Care should be taken to account for the Coriolis and gyroscopic terms in the mass and the stiffness matrices. Warping, which is very significant in anisotropic materials has to be accounted for in a more efficient way. Stemple and Lee [70] have suggested a coupled analysis for the cross-section warping and the bending, torsion, and extension of the beam. This could be introduced in the present FEM model. Also features like pretwist, droop and precone have been found to be important for the helicopter rotor analysis.

A preliminary aeroelastic analysis for helicopter rotors could be carried out using either a modified-strip theory approximation for unsteady airloads (this model already exists in AE24) or a quasi-steady approximation in conjunction with a simple induced flow model [44]. The state of art classical unsteady aerodynamic approach is the State-Space or Finite-State representation (i.e. in the time domain) of the equations of motion [85, 118].

References

1. Bisplinghoff, R.L., and Ashley, H., *Principles of Aeroelasticity,* John Wiley and Sons, Inc., NY, 1962.

2. Collar, A. R., "The Expanding Domain of Aeroelasticity," *Journal of Royal Aeronautical Society,* Vol. 50, August 1946, pp. 613 - 636.

3. Duncan, W.J., "Inroductory Survey," *AGARD, Manual of Aeroelasticity,* August 1959, pp. 1 - 51.

4. Gessow, A., and Myers, G., C., Jr., *Aerodynamics of Helicopters,* The Macmillan Co., NY, 1952.

5. Bramwell, A.R.S., *Helicopter Dynamics,* John Wiley & Sons, NY, 1976.

6. Loewy, R.G., "Review of Rotary-Wing V/STOL Dynamic and Aeroelastic Problems," *Journal of American Helicopter Society,* Vol. 14, 1969, pp. 3 - 23.

7. Dowell, E., H., "*A Modern Course in Aeroelasticity,*" Sijthoff & Noordhoff, Alphen aan den Rijn, The Netherlands, 1978.

8. Marr, R., L., Blackmann, S., Weiberg, J., A., and Schroer, L., G., "Wind Tunnel and Flight Test for XV-15 Tilt Rotor Research Aircraft," Paper No. 79-54, *Proceedings of the 35th Annual National Forum of the American Helicopter Society,* Washington, D.C., 1979.

9. Bilger, J., Marr, R., L., and Zahedi, A., "Results of Structural Dynamic Testing of the XV-15 Tilt Rotor Research Aircraft," *Journal of the American Helicopter Society,* Vol. 27, No. 2, April 1982, pp. 58 - 65.

10. Jenny, D., S., "ABC Aircraft Developement Status," Paper No. 8, *Proceedings of the 6th European Rotorcraft Forum,* Bristol, England, September 1980, pp. 8.1 - 8.6.

11. Linden, A., and Ruddell, A., "An ABC Status Report," *Proceedings of the 37th Annual National Forum of the American Helicopter Society,*New Orleans, May 1981, pp. 72 - 87.

12. Williams, R., M., "Application of Circulation Control Rotor Technology to a Stopped Rotor Aircraft Design," *Vertica,* Vol. 1, No. 1, 1976, pp. 3 - 16.

13. Potthast, A., J., "X-Wing Stability and Control Developement and Wind Tunnel Demonstration Tests - Helicopter Conversion and Fixed Wing flight," Paper No. 80-27, *Proceedings of the 36th Annual National Forum of the American Helicopter Society,* Washington, D.C., May 1980.

14. Castel, F., and Kapania, R.,K., "A Beam Element for Aeroelastic Analysis of Damaged and Undamaged Wings.", A Report for CCMS (Virginia Tech) CCMS 88-13.

15. Dat, R., "Aeroelasticity of Rotary-Wing Aircraft," *Helicopter Aerodynamics and Dynamics, AGARD Lecture Series,* No. 63, Chapter 4, 1973.

16. Hohenemser, K., H., "Hingeless Rotorcraft Flight Dynamics," *Agardograph,* No. 197, 1974.

17. Ormiston, R., A., "Investigation of Hingeless Rotor Stability," *Vertica,* Vol. 7, pp. 143 - 181.

18. Friedmann, P., P., "Recent Developements in Rotary-Wing Aeroelasticity," *Journal of Aircraft,* Vol. 14, 1977, pp. 1027 - 1041.

19. Friedmann, P., P., "Formulation and Solution of Rotary-Wing Aeroelastic Stability and Response Problems," *Vertica,* Vol. 7, No. 2, 1983, pp. 101 - 141.

20. Friedmann, P., P., "Recent Trends in Rotary-Wing Aeroelasticity," *Vertica,* Vol. 11, No. 1, 1987, pp. 139 - 170.

21. Reichert, G., " Helicopter Vibration Control - A survey, " *Vertica,* Vol. 5, 1981, pp. 1 - 20.

22. Loewy, R., G., "Helicopter Vibrations: A Technological Perspective," *Journal of American Helicopter Society,* Vol. 29, 1984, pp. 4 - 30.

23. Johnson, W., " Recent Developements in the Dynamics of Advanced Rotor Systems - Part I," *Vertica,* Vol. 10, 1986, pp. 73 - 107.

24. Johnson, W., "Recent Developements in the Dynamics of Advanced Rotor Systems - Part II," *Vertica,* Vol. 10, 1986, pp. 109 - 150.

25. Miao, W., "Influence of Pitch - Axis Location and Orientation on Rotor Aeroelastic Stability," *Vertica,* Vol. 11, No. 1/2, 1987, pp. 171 - 185.

26. Ormiston, R.,A., Warmbrodt, W., G., Hodges, D.,H., and Peters, D., A., "Survey of Army / NASA Rotorcraft Aeroelastic Stability Research," NASA TM - 101026, October, 1988.

27. Friedmann, P., P., " Helicopter Rotor Dynamics and Aeroelasticity - Some Key Ideas and Insights, " *Third Workshop on Aeroelastic Stability Modelling of Rotorcraft Rotor Systems,* March 12 - 14, Durham, NC, 1990.

28. Houbolt, J., C., and Brooks, G., W., "Differential Equations of Motion for Combined Flapwise Bending, Chordwise Bending and Torsion of Twisted Non - uniform Rotor Blades," NACA Report 1346, 1958.

29. Friedmann, P., P., and Tong, P., "Dynamic Nonlinear Elastic Stability of Helicopter Rotor Blades in Hover and in Forward Flight," NASA CR - 114485, May 1972.

30. Arcidiacono, P., J., "Steady Flight Differential Equations of Motion for a Flexible Helicopter Blades with Chordwise Mass Unbalance," USAAVLABS TR68 - 18A, Vol. I, February 1969.

31. Hodges, D., H., and Dowell, E., H., "Nonlinear Equations of Motion for Elastic Bending and Torsion of Twisted Non - uniform Blades," NASA TN D - 7818, 1974.

32. Friedmann, P., P., "Influence of Modeling and Blade Parameters on the Aeroelastic Stability of a Cantilevered Rotor," *AIAA Journal,* Vol. 15, February 1977, pp. 149 - 158.

33. Dowell, E., H., Traybar, J., and Hodges, D., H., "An Experimental Theoretical Correlation Study of Nonlinear Bending and Torsion Deformations of a Cantilever Beam," *Journal of Sound and Vibration,* Vol. 50, 1977, pp. 533 - 544.

34. Hodges, D., H., Ormiston, R., A., and Peters, D., A., "On the Nonlinear Deformation Geometry of Euler Bernoulli Beams," NASA TP - 1566, 1980.

35. Alkire, K., "An Analysis of Rotor Blade Twist Variables Associated with Different Euler Sequences and Pretwist Treatment," NASA TM - 84394, 1984.

36. Shamie, J., and Friedmann, P., "Effect of Moderate Deflections on the Aeroelastic Stability of a Rotor Blade in Forward Flight," *Proc. Third European Rotorcraft and Powered Lift Aircraft Forum,* Aix - en - Provence, pp. 24.1 - 24.37, 1977.

37. Celi, R., and Friedmann, P.,P., "Rotor Blade Aeroelasticity in Forward Flight with an Implicit Aerodynamic Formulation," *AIAA Journal*, Vol. 26, No. 12, 1988, pp. 1425 - 1433.

38. Hodges, D., H., "Nonlinear Equations for the Dynamics of Pretwisted Beams Undergoing Small Strains and Large Rotations," NASA TP - 2470, 1985.

39. Hodges, D., H., "Nonlinear Beam Kinematics for Small Strains and Finite Rotations," *Vertica,* Vol. 11, No. 3, 1987, pp. 573 - 589.

40. Danielson, D., A., and Hodges, D., H., "A Beam Theory for Large Global Rotation, Moderate Local Rotation and Small Strain," *Journal of Applied Mechanics,* Vol. 55, pp. 179 - 184.

41. Kane, T., R., Likins, P., W., and Levinson, D., A., "Spacecraft Dynamics," McGraw-Hill, 1983.

42. Bauchau, O., A., and Hong, C., H., "Large Displacement Analysis of Naturally Curved and Twisted Composite Beams," *AIAA Journal,* Vol. 25, No. 11, 1987, pp. 1469 - 1475.

43. Hodges, D., H., Hopkins, A., K., Kunz, D., L., and Hinnant, H., E., "Introduction to GRASP - General Rotorcraft Aeromechanical Stability Program - A Modern Approach to Rotorcraft Modeling," *Proc. 42nd Annual Forum of American Helicopter Society,* Washington D. C., 1986, pp. 739 - 756.

44. Sivaneri, N. T., and Chopra, I., "Dynamic Stability of Rotor Blade Using Finite Element Analysis," *AIAA Journal,* Vol. 20, 1980, pp. 716 - 723.

45. Sivaneri, N. T., and Chopra, I., "Finite Element Analysis of Bearingless Rotor Aeroelasticity," *Journal of American Helicopter Society,* Vol. 29, 1984, pp. 42 - 51.

46. Friedmann, P. P., and Straub, F., "Application of the Finite Element Method to Rotary - Wing Aeroelasticity," *Journal of American Helicopter Society,* Vol. 25, 1980, pp. 36 - 44.

47. Fu, C., and Wang, S., "Aeroelastic Stability of a Rotor by Lifting Surface Theory and Finite Element Method," *Proc. 11th. European Rotorcraft Forum,* London, Paper No. 68, 1986.

48. Hodges, D., H.," Review of Composite Rotor Blade Modeling," AIAA Paper 88 - 2249, Proc. AIAA / ASME / ASCE / AHS 29th Structures, Structural Dynamics, and Materials Conference, Williamsburg, Va, April 18 - 20, 1988, pp. 305 - 312.

49. Hong, C. H., and Chopra, I., "Aeroelastic Stability Analysis of a Composite Rotor Blade," *Journal of American Helicopter Society,* Vol. 30, No. 2, 1985, pp. 57 - 67.

50. Hong, C. H., and Chopra, I., "Aeroelastic Stability Analysis of a Composite Bearingless Rotor Blade," *Journal of American Helicopter Society,* Vol. 31, No. 4, 1986, pp. 29 - 35.

51. Panda, B., and Chopra, I., "Dynamics of Composite Rotor Blades in Forward Flight," *Vertica,* Vol. 11, No. 1/2, 1987, pp. 187 - 209.

52. Bauchau, O., A., and Hong, C., H., "Finite Element Approoach to Rotor Blade Modeling," *Journal of American Helicopter Society,* Vol. 32, No. 1, January 1987, pp. 60 - 67.

53. Bauchau, O., A., and Hong, C., H., "Nonlinear Composite Beam Theory," *Journal of Applied Mechanics,* Vol. 55, March 1988, pp. 156 - 163.

54. Minguet, P., and Dugundji, J., "Experiments and Analysis for Structurally Coupled Composite Blades Under Large Deflections : Part I - Static Behaviour," AIAA Paper No. 89 - 1365 - CP, 1989.

55. Minguet, P., and Dugundji, J., "Experiments and Analysis for Structurally Coupled Composite Blades Under Large Deflections : Part II - Dynamic Behaviour," AIAA Paper No. 89 - 1366 - CP, 1989.

56. Hegemier, G., A., and Nair, S., "A Nonlinear Dynamical Theory for Heterogenous, Anisotropic, Elastic Rods," *AIAA Journal,* Vol. 15, No. 1, 1977, pp. 8 - 15.

57. Mansfield, E. H., and Sobey, A. J., "The Fibre Composite Helicopter Blade , Part I : Stiffness Properties (by E. H. Mansfield) ; Part II :

Prospects for Aeroelastic Tailoring (by A. J. Sobey)," *Aeronautical Quarterly,* May, 1979, pp. 413 - 449.

58. Mansfield, E., H., " The Stiffness of a Two - Cell Anisotropic Tube," *Aeronautical Quarterly,* Vol. 32, 1981, pp. 338 - 353.

59. Rehfield, L., W., "Design Analysis Methodology for Composite Rotor Blades," AFWAL - TR - 85 - 3094, 1985.

60. Nixon, M., W., "Extension - Twist Coupling of Composite Circular Tubes with Applications to Tilt - Rotor Blade Design," AIAA Paper No. 87 - 0772, 1987.

61. Hodges, R., V., Nixon, M., W., and Rehfield, L., W., "Comparison of Composite Rotor Blade Models : a Coupled Beam Analysis and an MSC / NASTRAN Finite Element Model," NASA TM 89024, 1987.

62. Worndle, R., "Calculation of the Cross - Sectional Properties and the Shear Stresses of Composite Rotor Blades," *Vertica,* Vol. 6, 1982, pp. 111 - 129.

63. Kosmatka, J., B., "Structural Dynamic Modeling of Advanced Composite Propellers by the Finite Element Method," Ph.D. Dissertation, University of California, Los Angeles, 1986.

64. Giavotto, V., Borri, M., Mantegazza, P., Ghiringhelli, G., Carmaschi, V., Maffloli, G., C., and Mussi, F., "Anisotropic Beam Theory and Applications," *Computers and Structures,* Vol. 16, 1983, pp. 403 - 413.

65. Borri, M., and Mantegazza, P., "Some Contributions on Structural and Dynamic Modelling of Helicopter Rotor Blades," Presented at U. S. Army Research Office Workshop on Dynamics and Aeroelastic Stability Modeling, Georgia Institute of Technology, Atlanta, Georgia, December 4 - 5, 1985.

66. Borri, M., and Merlini, T., "A Large Displacement Formulation for Anisotropic Beam Analysis," *Meccanica,* Vol. 21, 1986, pp. 30 -37.

67. Bauchau, O., A., "A Beam Theory for Anisotropic Materials," *Journal of Applied Mechanics,* Vol. 52, 1985, pp. 416 - 422.

68. Bauchau, O., A., Coffenberry, B., S., and Rehfield, L., W., "Composite box -beam analysis : Theory and Experiments," *Journal of American Helicopter Society,* Vol. 6, 1987, pp. 25 - 35.

69. Lee, S., W., and Kim, Y., H., "A New Approach to Finite Element Modeling of Beams," *International Journal for Numerical Methods for Engineers,* Vol. 24, 1987, pp. 2327 - 2341.

70. Stemple, A. D., and Lee, S., W., "Finite Element Model for Composite Beams with Arbitrary Cross - Sectional Warping," *AIAA Journal,* Vol. 26, No. 12, December 1988, pp. 1512 - 1520.

71. Stemple, A., D., and Lee, S., W., "Large Deflection Static and Dynamic Finite Element Analysis of Composite Beams with Arbitrary Cross - Sectional Warping," AIAA Paper 89 - 1363 - CP, 1989.

72. Gaonkar, G., H., and Peters, D., A., "Review of Dynamic Inflow Modeling for Rotorcraft Flight Dynamics," AIAA - 86 - 0845, 1986.

73. Amer, K., B., " Theory of Helicopter Damping in Pitch and Roll and Comparison with Flight Measurement," NACA TN 2136, October 1948.

74. Sissingh, G., J., " The Effect of Induced Velocity Variation on Helicopter Rotor Damping in Pitch and Roll, "Aeronautical Research Council (Great Britain), A. R. C. Technical Report C. P. No. 101 (14, 757), 1952.

75. Carpenter, P., J., and Fridovich, B., "Effect of a Rapid Blade Pitch Increase on the Thrust and Induced Velocity Response of a Full Scale Helicopter Rotor," NACA TN 3044, Nov, 1953.

76. Bisplinghoff, R., L., Ashley, H., and Halfman, R., L., *Aeroelasticity,* Addison - Wesley Publishing Company, 1955, pp. 251 - 281.

77. Glauert, H., "The Force and Moment on an Oscillating Airfoil, " Br. A. R. C., R. and M. 1242, 1929.

78. Theodorsen, T., "General Theory of Aerodynamic Instability and the Mechanism of Flutter," NACA R 496, 1985.

79. Greenberg, J., M., "Airfoil in Sinusoidal Motion in Pulsating Stream," NACA TN 1326, 1947.

80. Loewy, R., G., " A Two Dimensional Approach to the Unsteady Aerodynamics of Rotary Wings, " *Journal of Aerospace Science,* Vol. 24, 1957, pp. 81 -98.

81. Jones, W., P., "The Oscillating Airfoil in Subsonic Flow," British Aeronautical Research Council, R & M 2921, 1956.

82. Timman, R., and van de Vooren, A., I., " Flutter of a Helicopter Rotor Rotating in its Own Wake," *Journal of the Aerospace Sciences,* Vol. 24, No. 9, September 1957, pp. 694 - 702.

83. Jones, W., P., and Rao, B., M., "Compressibility Effects on Oscillating Rotor Blades in Hovering Flight," Presented at the AIAA Structural Dynamics and Aeroelasticity Specialist Conference, New Orleans, Louisiana, April 16 - 17, 1969.

84. Hammond, C., E., and Pierce, G., A., "A Compressible Unsteady Aerodynamic Theory for Helicopter Rotors," Presented at the AGARD Specialist's Meeting on "The Aerodynamics of Rotary Wings," Marseille, France, September 13 - 15, 1972.

85. Friedmann, P., P., and Venkatesan, C., "Finite State Modeling of Unsteady Aerodynamics and its Application to a Rotor Dynamic Problem," Presented at Eleventh European Rotorcraft Forum, Paper No. 72, London, England, September 10 - 13, 1985.

86. Drees, J., M., "A Theory of Airflow Through Rotor and its Application to Some Helicopter in Forward Flight," *Journal of the Helicopter Society of Great Britain,* Vol. 3, No. 2, 1949.

87. Heyson, H., H., and Kotzoff, S., "Induced Velocities Near a Lifting Rotor with Non - uniform Disk Loading," NASA TR 1319, 1957.

88. Wang, Shi - Cun, " Generalized Rotor Vortex Theory, Problems of Helicopter Rotor Aerodynamics," NASA TT F - 494, September 1967.

89. Miller, R., H., "Rotor Blade Harmonic Air Loading," *AIAA Journal,* Vol. 2, No. 7, July 1964, pp. 1254 - 1269.

90. Scully, M., P., "A Method of Computing Helicopter Vortex Wake Distortion," MIT, ASRL TR138 - 1, June 1967.

91. Sadler, S., G., "Developement and Application of a Method for Predicting Rotor Free Wake Positions and Resulting Rotor Blade Airloads," NASA CR - 1911, Vol. I : Model and Results, NASA CR - 1912 Program Listing, 1971.

92. Gray, R., B., " On the Motion Helical Vortex Shed from a Single - Bladed Hovering Helicopter Rotor and its Application to the Calculation of the Spanwise Aerodynamic Loading, "Princeton University, Aero. Engineering Dept., Report No. 313, September 1955.

93. Shupe, N., K., " A Study of the Dynamic Motions of Hingeless Rotored Helicopters," Ph.D. Thesis, Princeton University, 1970.

94. Curtiss, H., C., Jr., and Shupe, N., K., "A Stability and Control Theory for Hingeless Rotors," Annual National Forum of the American Helicopter Society, Washington, D.C., May 1971.

95. Bousman, W., G., "An Experimental Investigation of the Effects on Aeromechanical Stability of a Hingeless Rotor Helicopter," *Journal of American Helicopter Society,* Vol. 26, No. 1, January 1981, pp. 46 - 54.

96. Pitt, D., M., and Peters, D., A., " Theoretical Prediction of Dynamic Inflow Derivatives," *Vertica* Vol. 5, No. 1, March 1981, pp. 21 - 34.

97. Peters, D., A., and Ninh HaQuang, "Dynamic Inflow for Practical Application," *Journal of the American Helicopter Society,* Vol. 33, No. 4, October 1988.

98. Jones, R., M., *Mechanics of Composite Materials,* McGraw - Hill, 1975.

99. Yates, E., C., Jr., "Calculation of Flutter Characteristics for Finite - Span Swept or Unswept Wings at Subsonic and Supersonic Speeds by a Modified Strip Analysis," NACA RM L57L10, 1958.

100. Yates, E., C., Jr., "Use of Experimental Steady - Flow Aerodynamic Parameters in the Calculation of Flutter Characteristics for Finite Span Swept or Unswept Wings at Subsonic, Transonic, and Supersonic Speeds," NASA TM X - 183, 1960.

101. Yates, E., C., Jr., "Subsonic and Supersonic Flutter Analysis of a Highly Tapered Swept Wing Planform Including Effects of Density Variation and Finite Wing Thickness and Comparison with Experiments," NASA TN D - 4230, 1967. (Supercedes NASA TM X - 764, 1983)

102. Yates, E., C., Jr., "Modified - Strip Analysis Method for Predicting Wing Flutter at Subsonic to Hypersonic Speeds," *Journal of Aircraft,* Vol. 3, No. 1, January - February 1966, pp. 25 - 29.

103. Yates, E., C., Jr., "Flutter Prediction at Low Mass - Density Ratios with Application to the Finite - Span Noncavitating Hydrofoil," AIAA Paper No. 68 - 472, April - May, 1968.

104. Hoa, S., V., "Vibration of a Rotating Beam With a Tip Mass," *Journal of Sound and Vibration,* Vol. 67, No. 3, 1979, pp. 369 - 381.

105. Timoshenko, S., P., Goodier, J., N., *Theory of Elasticity,* 3rd Edition, McGraw - Hill Book Company, New York, 1970.

106. Chen, A., T., and Yang, T., Y., "Static and Dynamic Formulation of a Symmetrically Laminated Beam Finite Element for a Microcomputer," *Journal of Composite Materials,* Vol. 19, September, 1985.

107. Archer, J., S., "Consistent Matrix Formulations for Structural Analysis Using Finite Element Techniques," *AIAA Journal,* Vol. 3, 1965, pp. 1910 - 1918.

108. Popov, E., P., "*Introduction to Mechanics of Solids,*" Prentice-Hall, Inc. Englewood Cliffs, N.J., 1968, pp. 482 - 487.

109. Crawley, E., F., "The Natural Modes of Graphite/Epoxy Cantilever Plates and Shells," *Journal of Composite Materials,* Vol. 13, July 1979, pp. 195 - 205.

110. Abarcar, R., B., and Cunniff, P., F., "The Vibration of Cantilever Beams of Fiber Reinforced Material," *Journal of Composite Material,* Vol. 6, 1972, pp. 504 - 517.

111. Thornton, E., A., " Free Vibrations of Unsymmetrically Cantilevered Composite Panels," *Shock and Vibration Bulletin,* Part 2, 1976, pp. 79 - 84.

112. Hollowell, S., J., and Dugundji, J., "Aeroelastic Flutter and Divergence of Stiffness Coupled, Graphite/Epoxy, Cantilevered Plates," AIAA Paper 82 - 0722, May 1982.

113. Bergen, F., D., "Shape Sensitivity Analysis of Wing Dynamic Aeroelastic Response," M. S. Thesis, Virginia Polytechnic Institute and State University, July, 1988.

114. Kumar, R., "Vibrations of Space Booms Under Centrifugal Force Field," *Transactions of the C.A.S.I.,* No. 7, 1974, pp. 1 - 5.

115. Wang, J., T., H., Mahrenholtz, O., and Bohm, J., "Extended Galerkin's Method for Rotating Beam Vibrations Using Legendre Polynomials," *Solid Mechanics Reviews,* 1976, pp. 341 - 365.

116. Bhat, R., B., "Transverse Vibrations of a Rotating Uniform Cantilever Beam with Tip Mass as Predicted by Using Beam Characteristic Orthogonal Polynomials in Raleigh-Ritz Method," *Journal of Sound and Vibrations,* Vol. 105, No. 2, 1986, pp. 199 - 210.

117. Weisshaar, T., A., "Divergence of Forward Swept Composite Wings," *Journal of Aircraft,* Vol. 17, No. 6, 1980, pp. 442 - 448.

118. Leishman, J., G., Nguyen, K., Q., "State-Space Representation of Unsteady Airfoil Behavior," *AIAA Journal,* Vol. 28, No. 5, May 1990, pp. 836 - 844.

Figures and Tables

Table 1. Maximum deflection w, in $\frac{Plh^2}{4EI}$ due to shear deformation only

	K = 0.667	K = 0.867
Exact Soln. [105]	1.33	-
Ref. [106]	1.33	1.0
Ref. [107]	1.34	1.17
Strain Energy [108]	1.33	1.04
24 d. o. f.	1.33	1.023

Table 2. Natural frequencies for the Aluminium plate

Mode	Ref. [109] f Hz.	24 d.o.f. f Hz
I Bending	37.6	37.5
I Torsion	158.3	143.9
II Bending	234.9	235.5
II Torsion	518.8	431.83
III Bending	658.1	663.7

Table 3. Natural Frequencies of a 30 Degrees Off-Axis Graphite/Epoxy Cantilever Beam

	Present Work				Prediction Ref. [110]	Experiment Ref. [110]
Mode No.	3 elements f Hz.	4 elements f Hz.	8 elements f Hz.	9 elements f Hz.	f Hz.	f Hz.
1	52.6	52.6	52.6	52.6	52.7	52.7
2	329.3	328.3	327.9	327.9	329.3	331.8
3	922.1	918.8	910.3	910.1	915.9	924.7
4	2290.9	1800.4	1777.2	1775.6	1896.5	1827.4

Table 4. Natural frequencies of a $[\,45_4\,/0_4\,]_T$ Boron/Epoxy plate

	24 d.o.f.	Ref. [14]	Experiment Ref.[111]
Mode No.	f, Hz	f, Hz	f, Hz
1	23.0	25.0	24.4
2	47.6	41.7	55.1
3	131.6	117.0	141.0
4	156.4	143.5	157.0

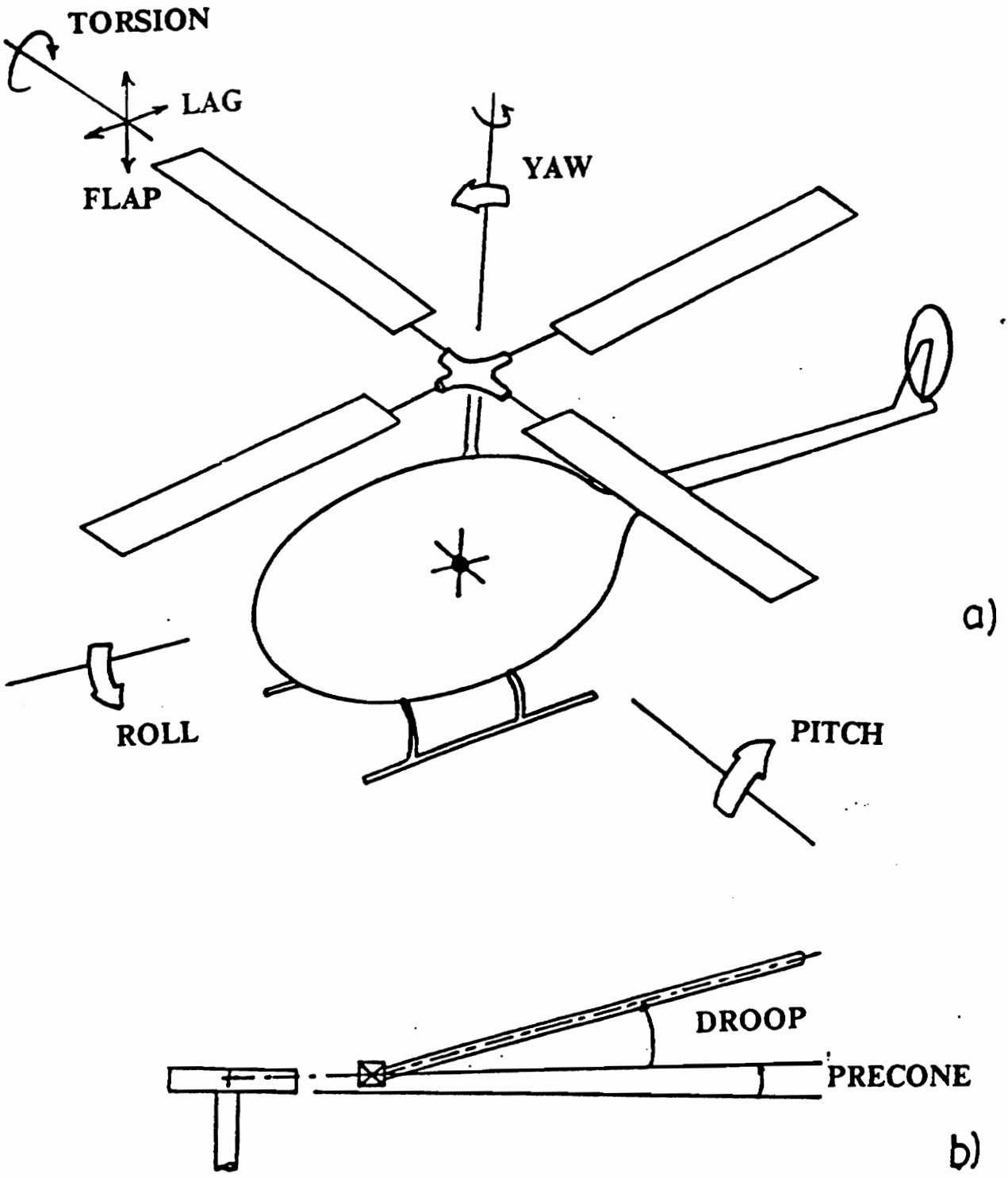

Figure 1. a)A typical Helicopter configuration b) defining precone and droop

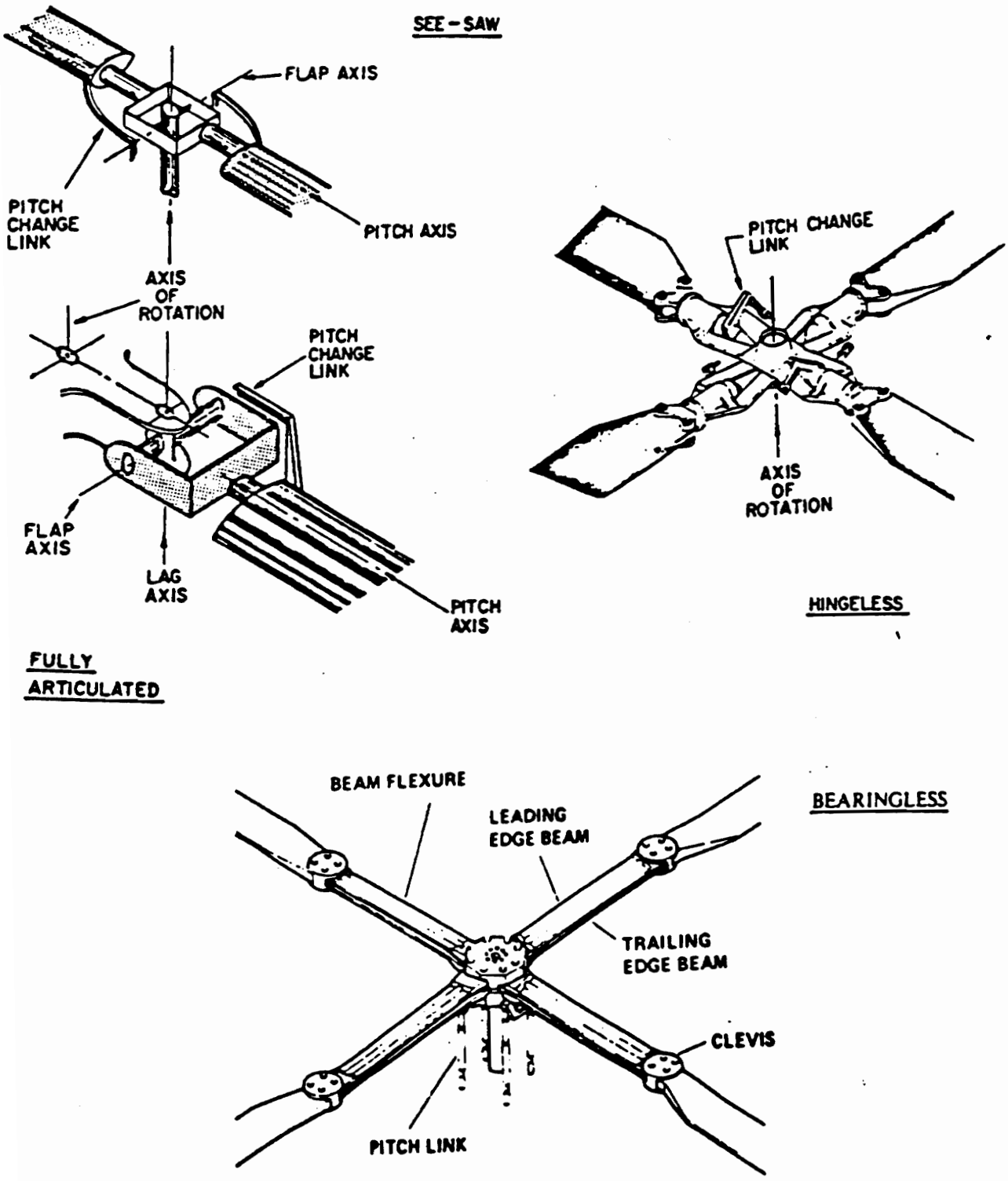

Figure 2. Various hub configurations of rotor blades, Reference [7]

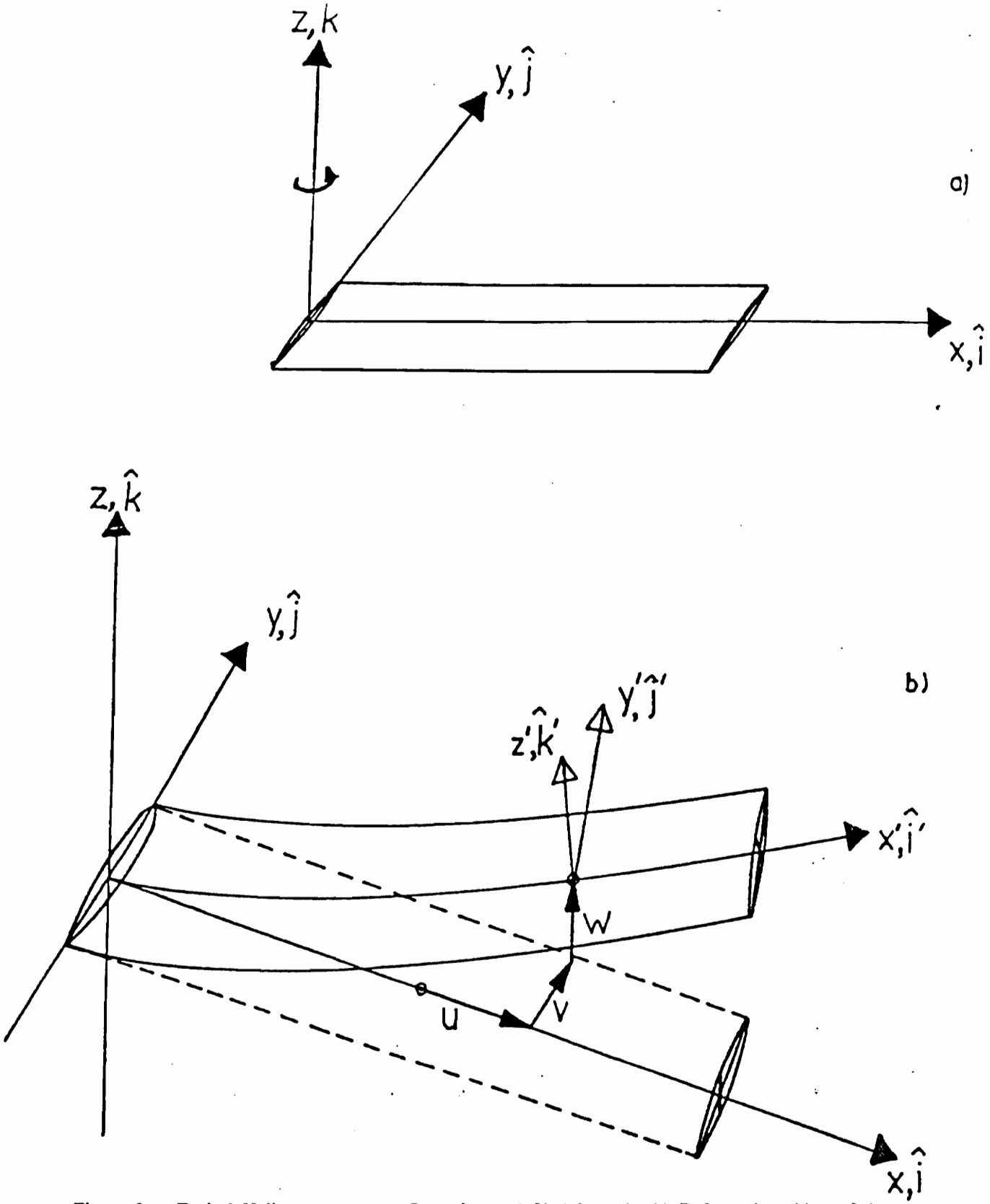

Figure 3. Typical Helicopter rotor configuration: a) Undeformed , b) Deformed position of the elastic axis

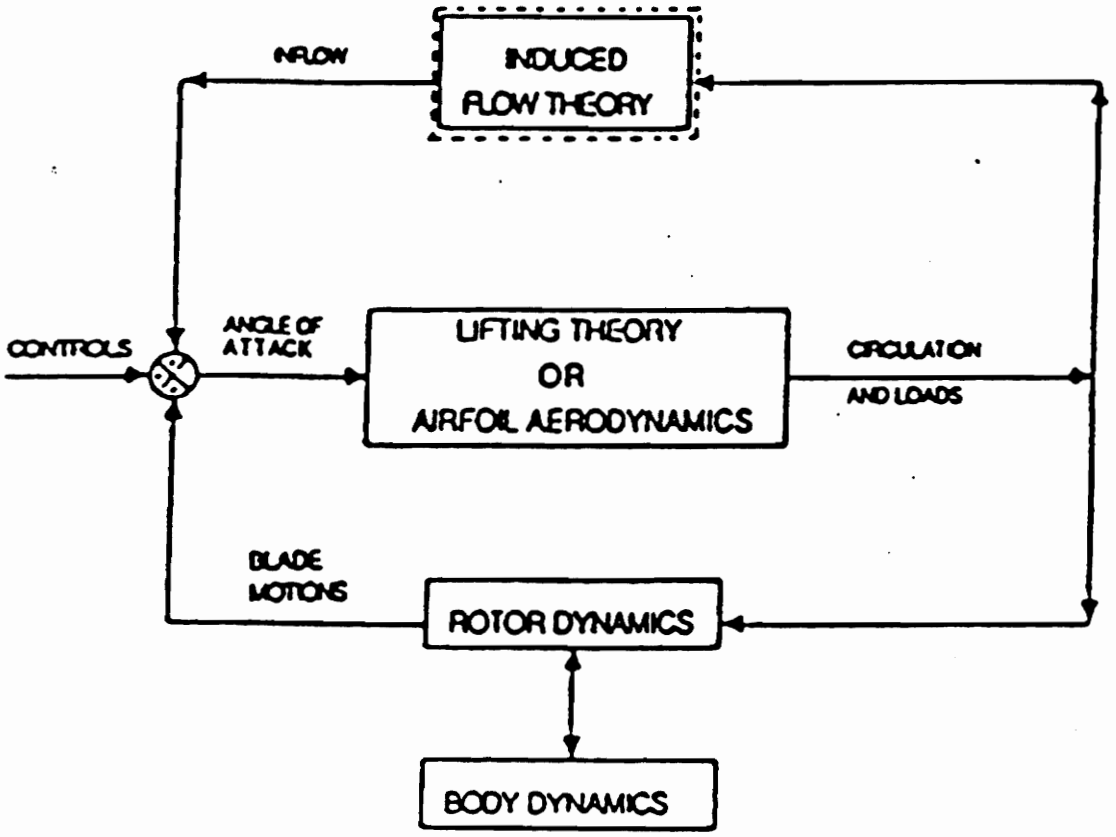

Figure 4. Block diagram of inflow dynamics

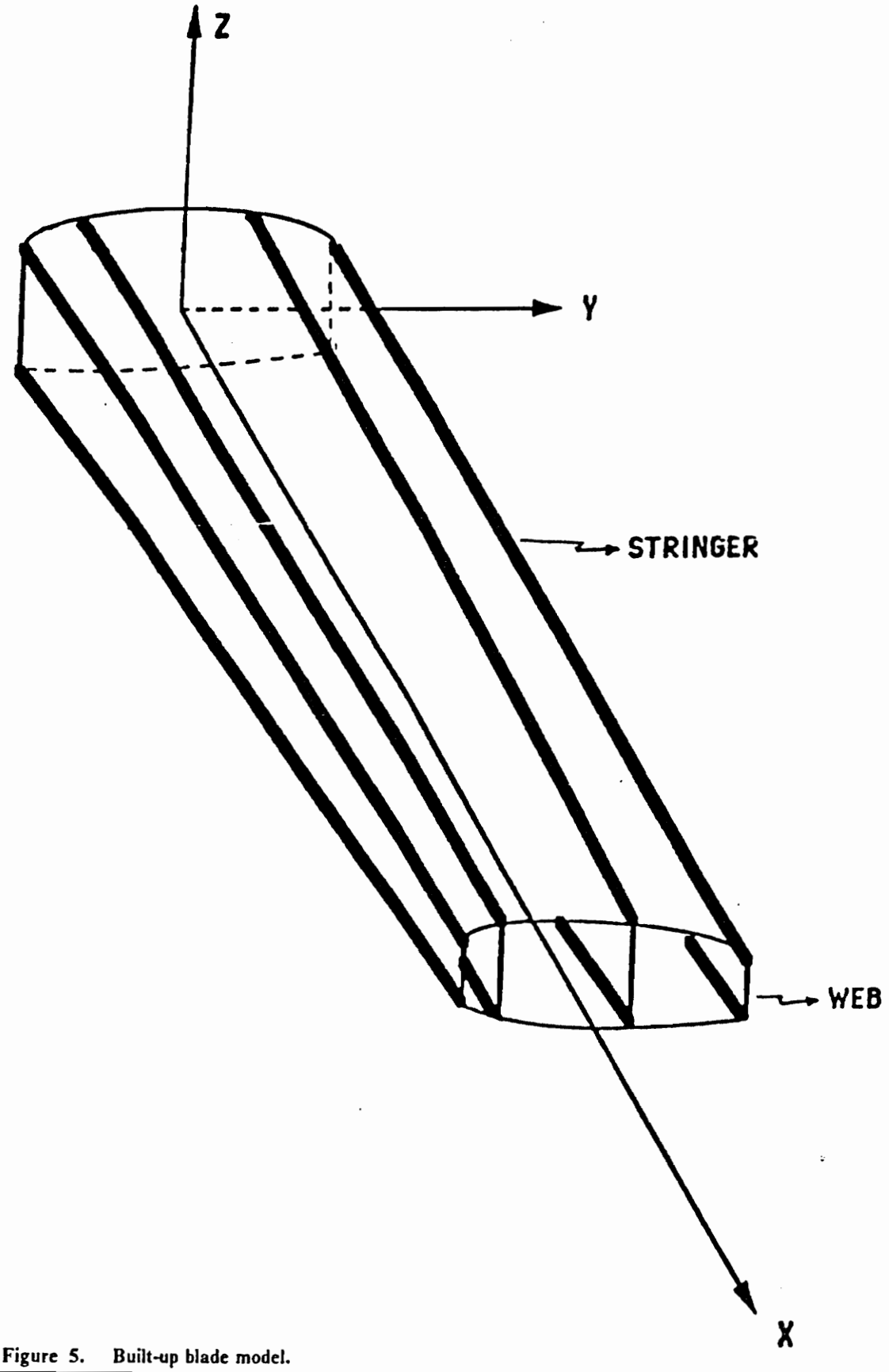

Figure 5. Built-up blade model.

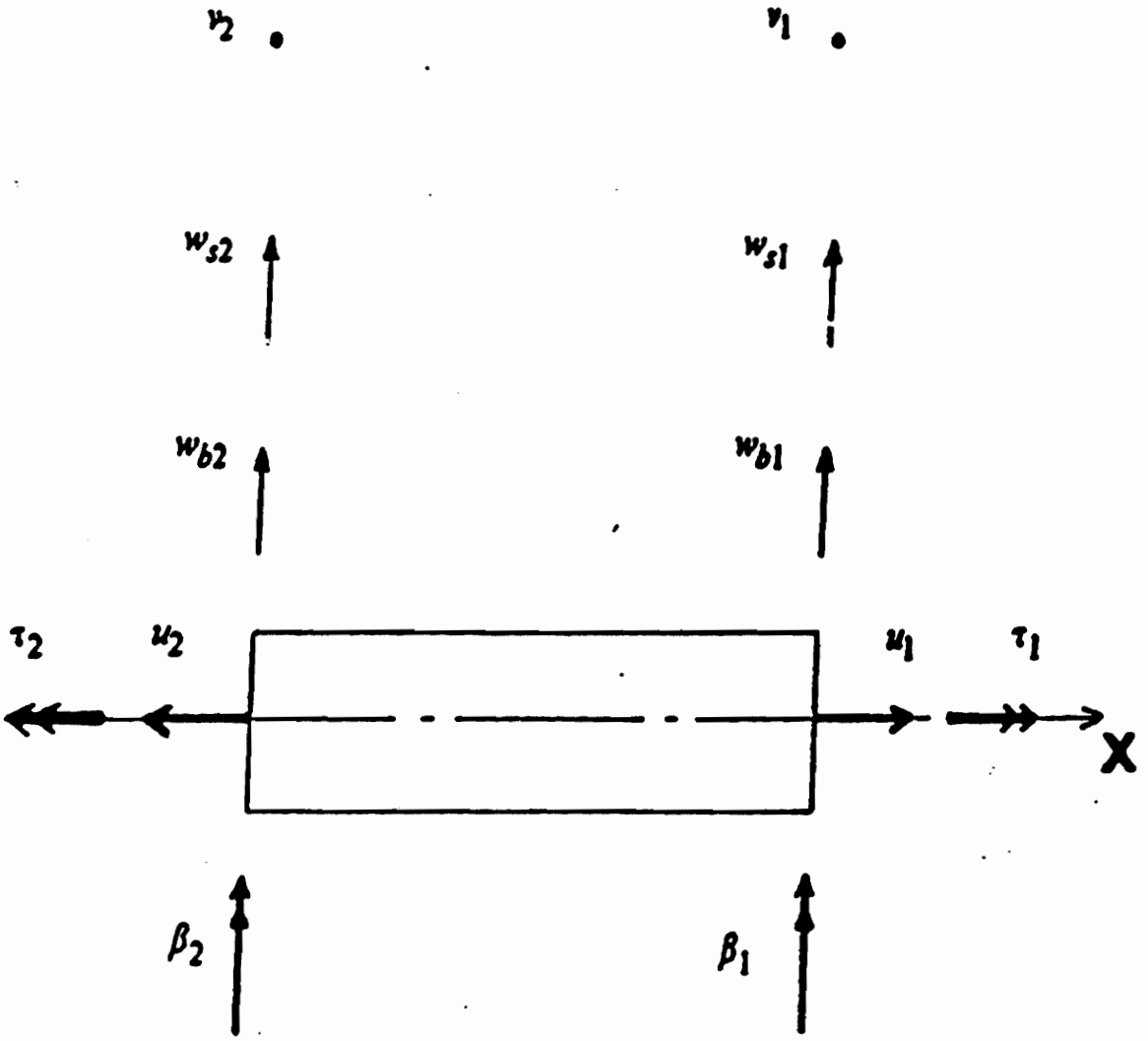

Figure 6. Element degrees of freedom

$$
[B] = \begin{bmatrix}
2/LN'_1 & 2/LN'_1 & 0 & 0 & 0 & 0 & 0 & 0 & 0 & 0 & 0 & 0 \\
0 & 0 & 0 & 0 & 0 & 0 & 0 & 0 & N_1 & N_2 & 0 & 0 \\
0 & 0 & 4/L^2N''_1 & 4/L^2N''_2 & 0 & 0 & 0 & 0 & 0 & 0 & 0 & 0 \\
0 & 0 & 0 & 0 & 0 & 0 & 4/LN'_1 & 4/LN'_2 & 0 & 0 & 0 & 0 \\
0 & 0 & 0 & 0 & 2/LN'_1 & 2/LN'_2 & 0 & 0 & 0 & 0 & 0 & 0 \\
0 & 0 & 0 & 0 & 0 & 0 & 0 & 0 & 0 & 0 & 4/L^2N''_1 & 4/L^2N''_2
\end{bmatrix}
$$

$$
\begin{bmatrix}
2/LN'_3 & 2/LN'_3 & 0 & 0 & 0 & 0 & 0 & 0 & 0 & 0 & 0 & 0 \\
0 & 0 & 0 & 0 & 0 & 0 & 0 & 0 & N_3 & N_4 & 0 & 0 \\
0 & 0 & 4/L^2N''_3 & 4/L^2N''_4 & 0 & 0 & 0 & 0 & 0 & 0 & 0 & 0 \\
0 & 0 & 0 & 0 & 0 & 0 & 4/LN'_3 & 4/LN'_4 & 0 & 0 & 0 & 0 \\
0 & 0 & 0 & 0 & 2/LN'_3 & 2/LN'_4 & 0 & 0 & 0 & 0 & 0 & 0 \\
0 & 0 & 0 & 0 & 0 & 0 & 0 & 0 & 0 & 0 & 4/L^2N''_3 & 4/L^2N''_4
\end{bmatrix}
$$

Figure 7. Strain-Displacement Matrix

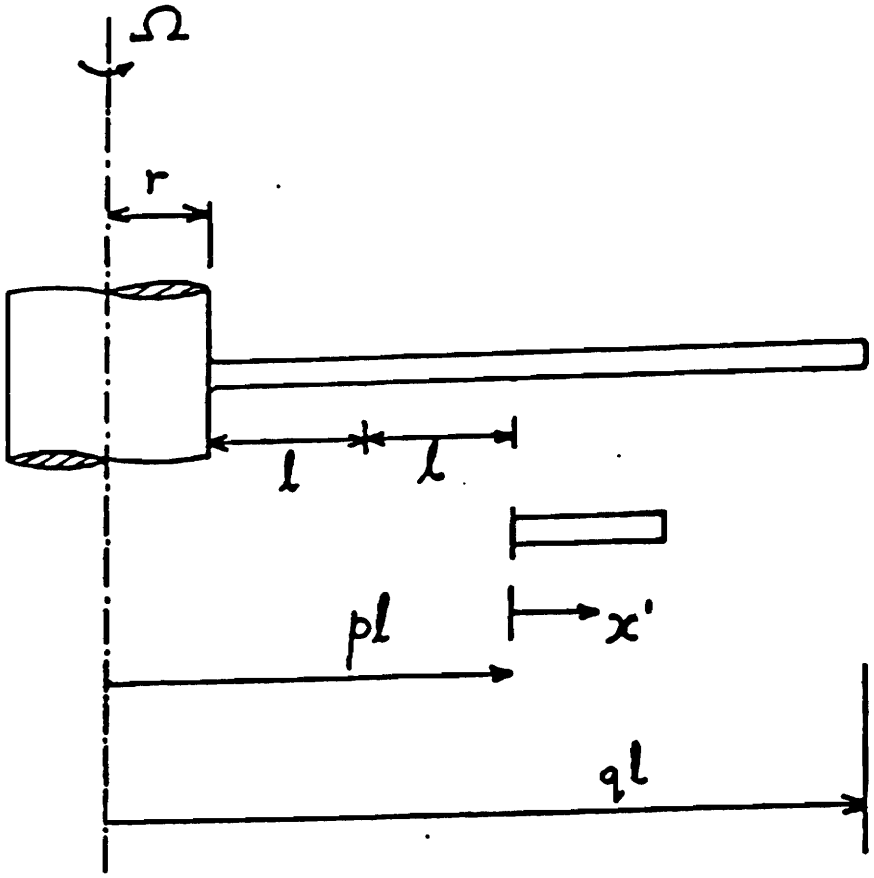

Figure 8. Configuration of a rotating beam.

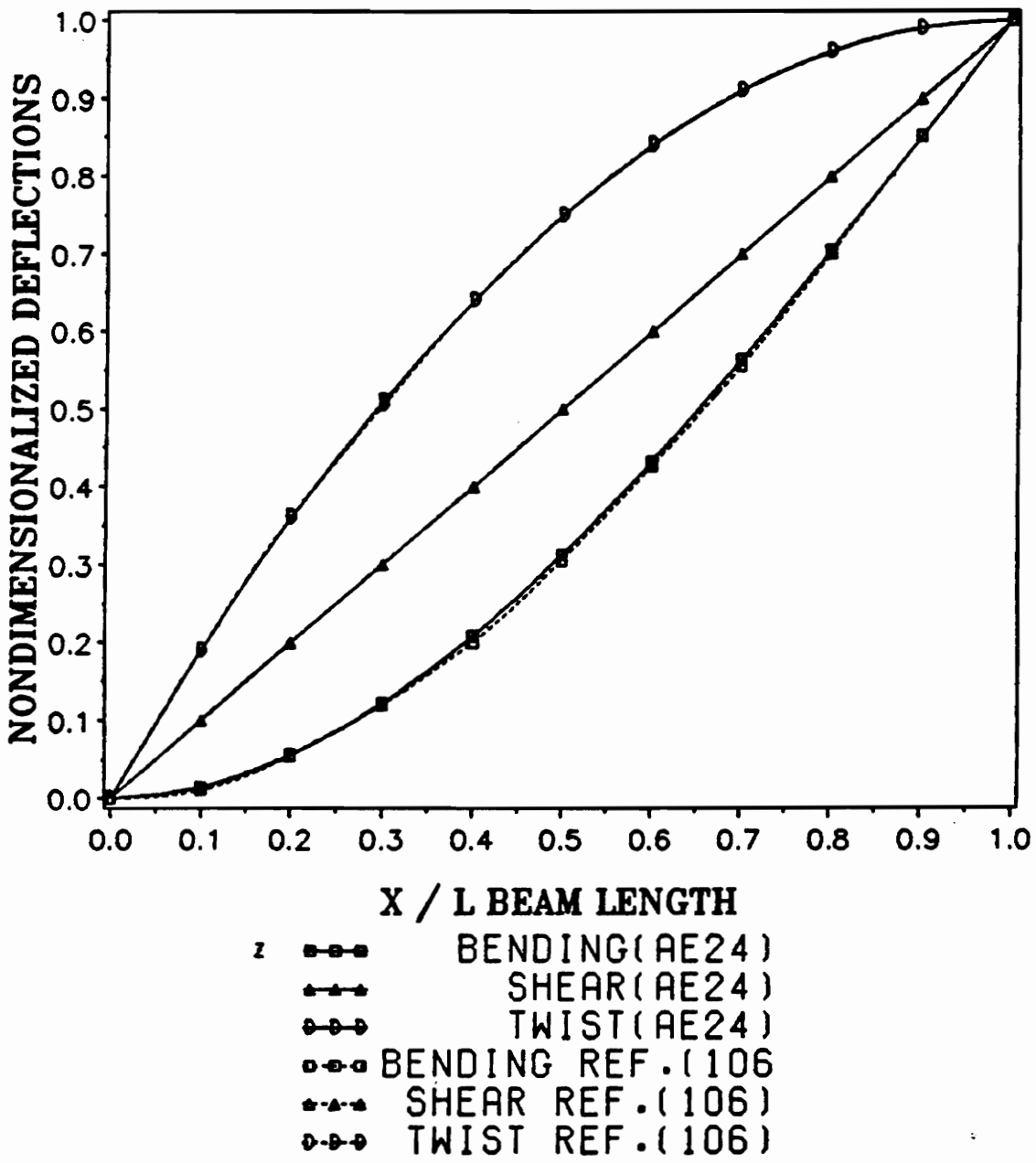

Figure 9. Distribution of deflections due to bending and shear deformations and twisting angle for a 16 ply $[45_4 / -45_4]$, under a tip load **P**.

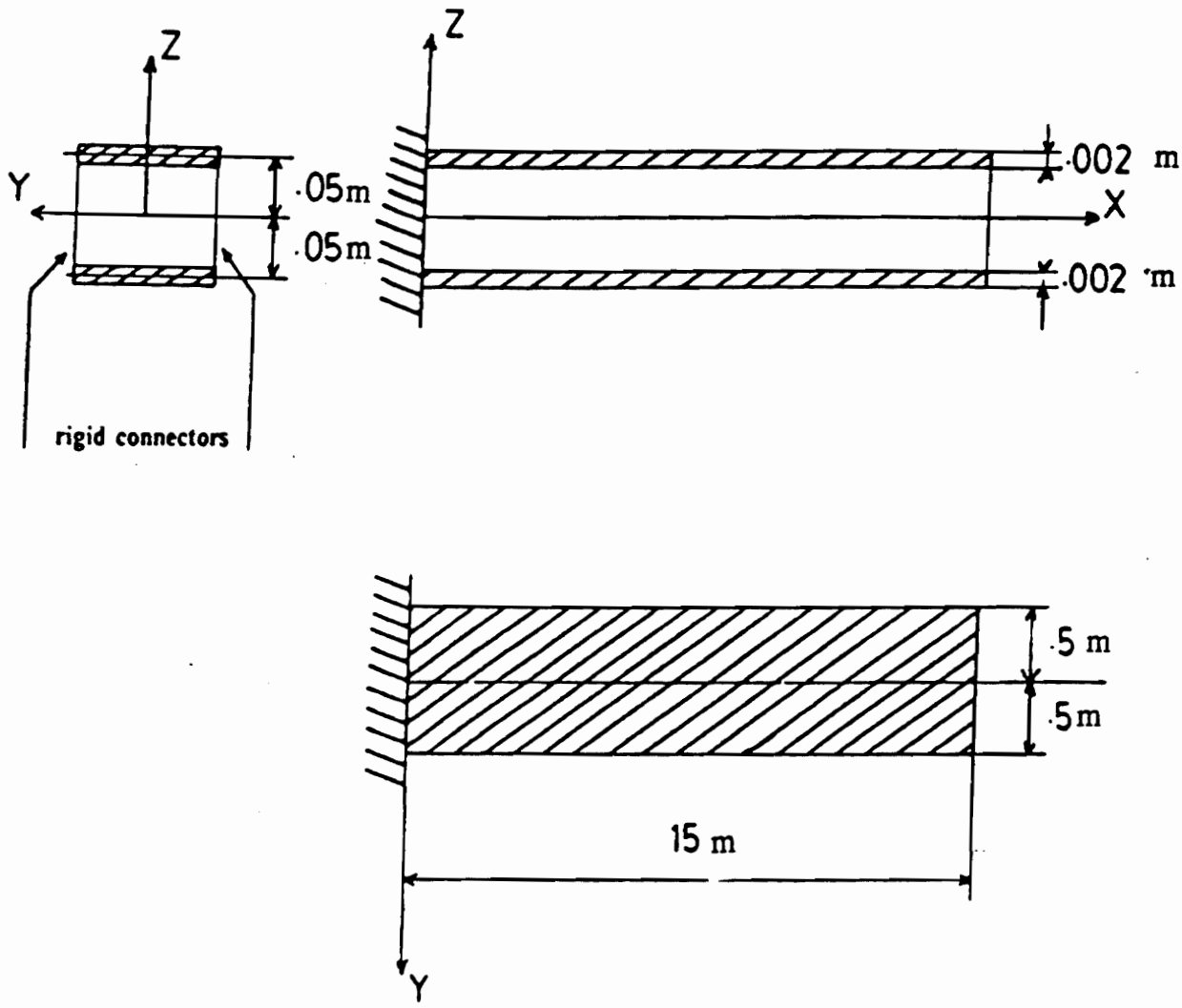

Figure 10. Box Beam Geometry Ref. [14]

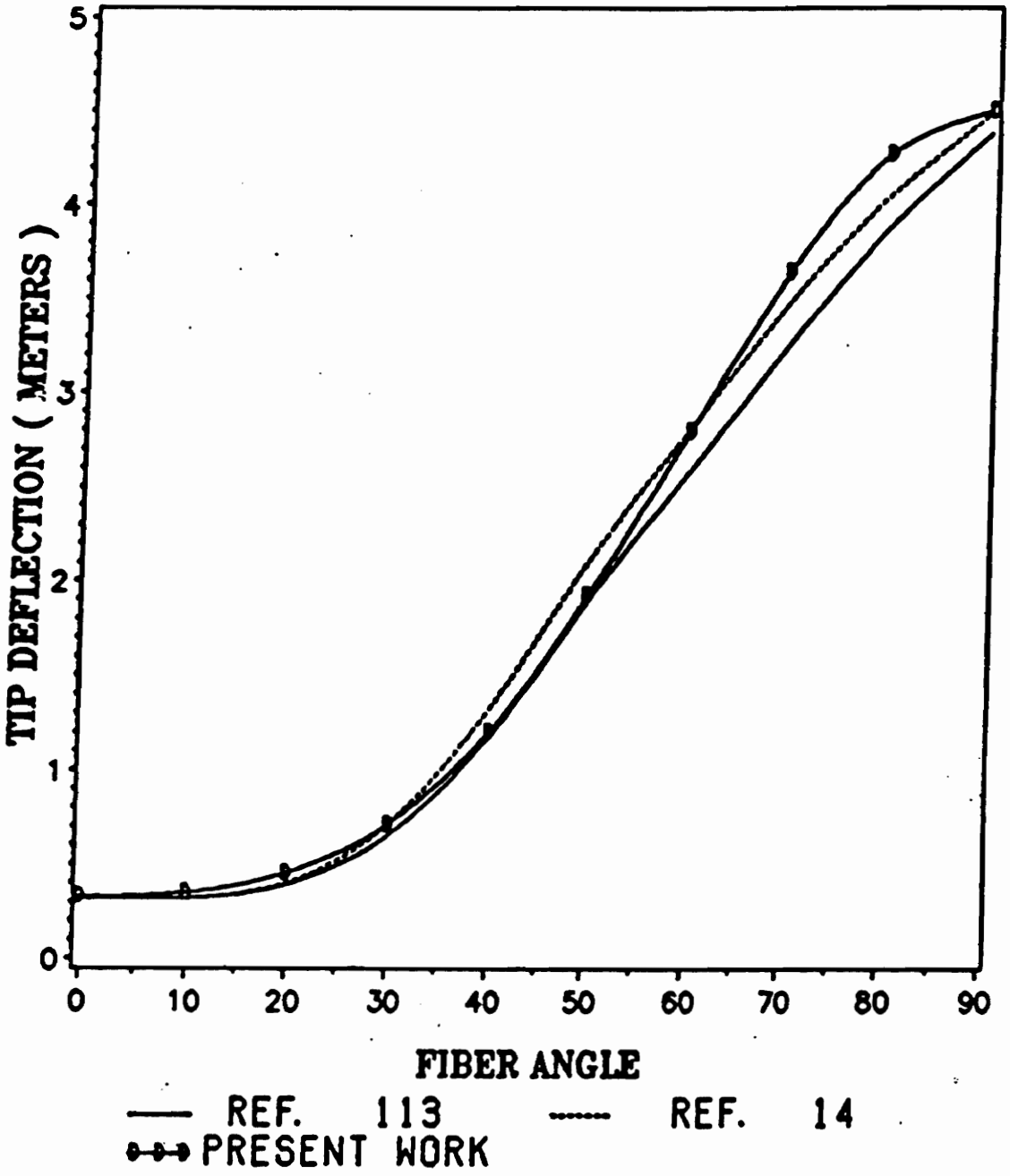

Figure 11. Box Beam Tip Deflection Under a Tip Load

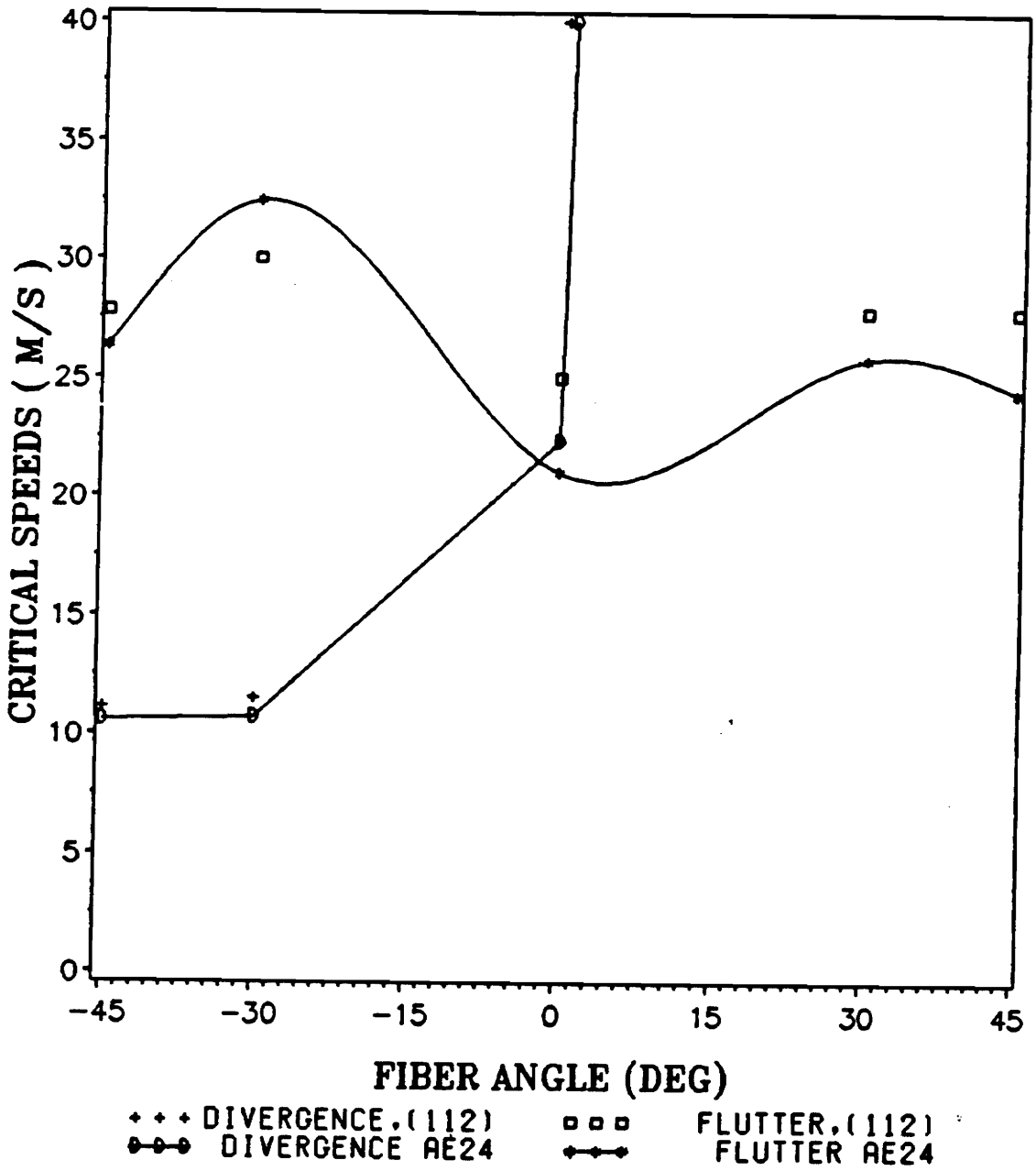

Figure 12. Critical Speed of an Unswept Graphite/Epoxy Plate, (θ_2 / 0),

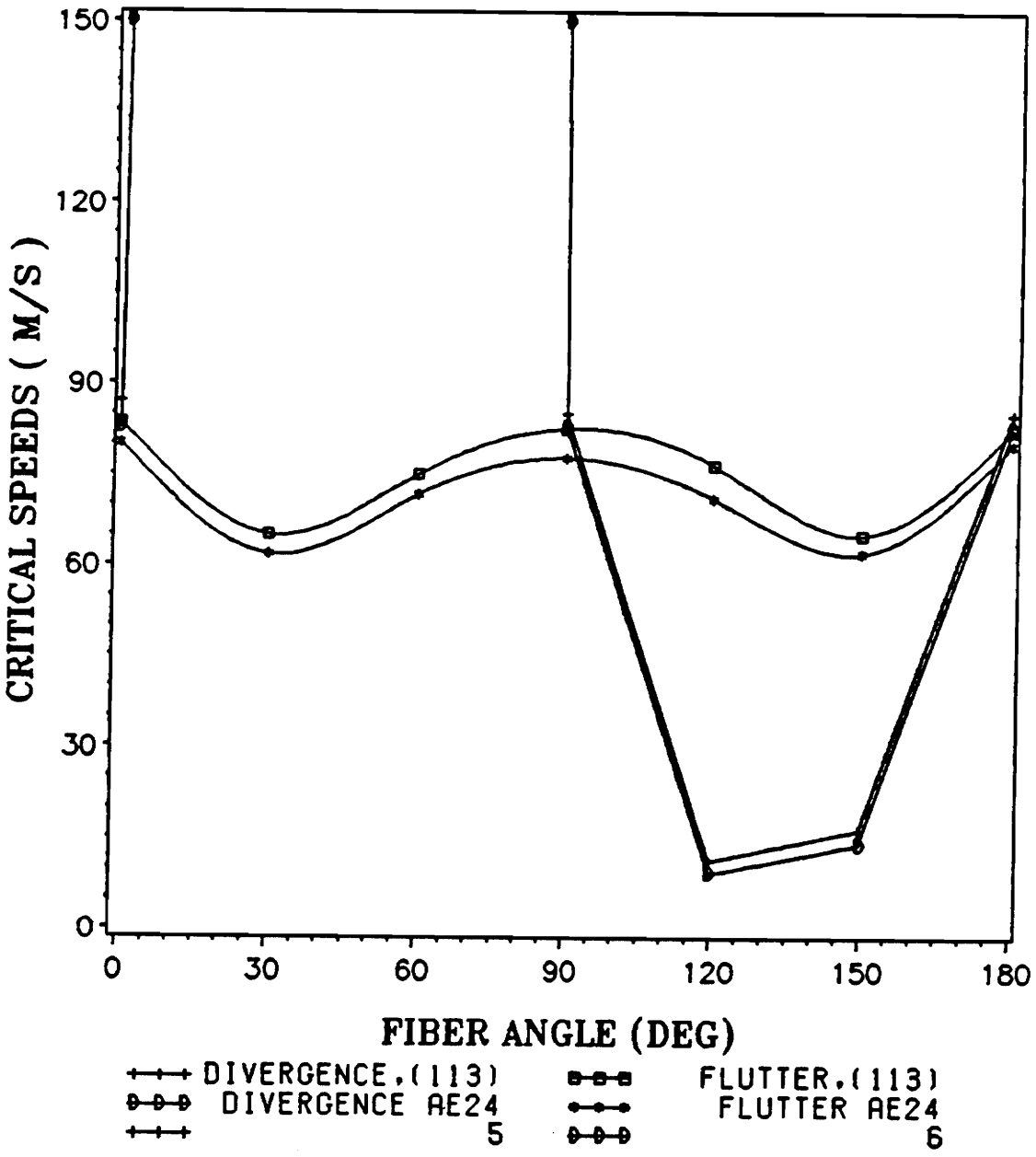

Figure 13. Flutter and Divergence Speeds of an Unswept Box Beam

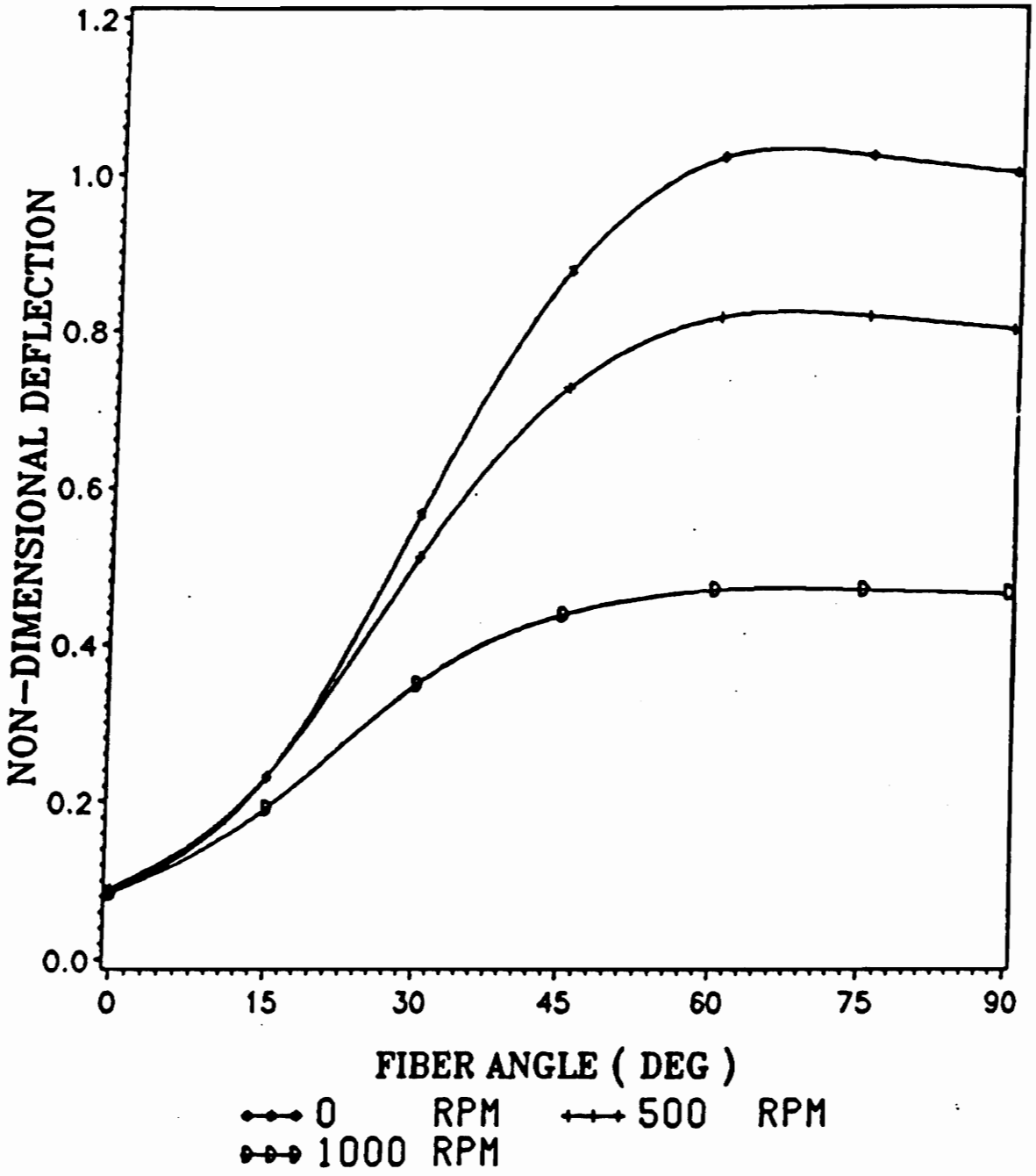

Figure 14. Tip deflection vs θ for a rotating (θ_2 / 0), plate.

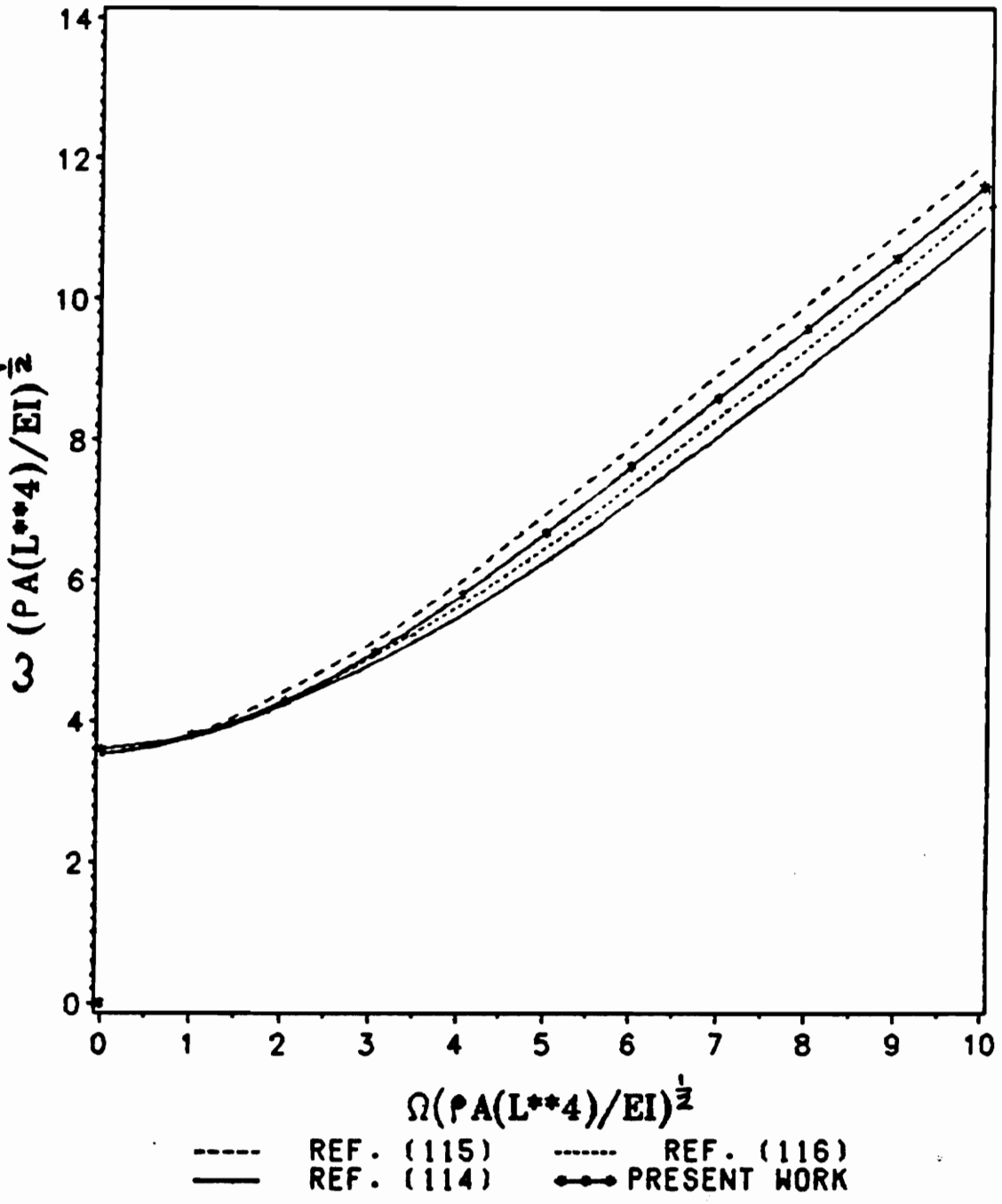

Figure 15. Variation of first natural frequencies of vibration with angular velocity for an isotropic beam, $\bar{R} = 0$.

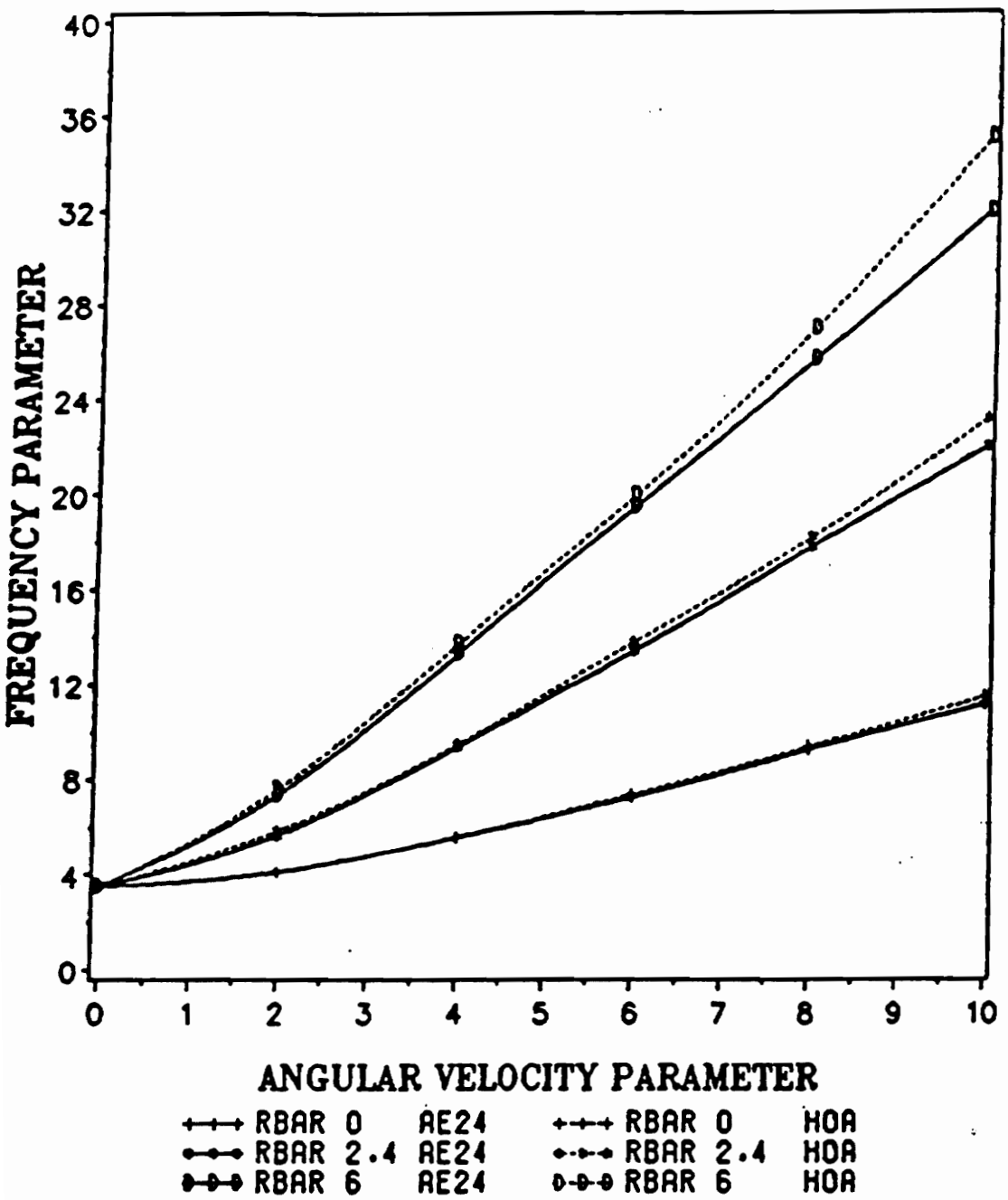

Figure 16. Variation of first natural frequencies of vibration with angular velocity for isotropic beam with different values of R

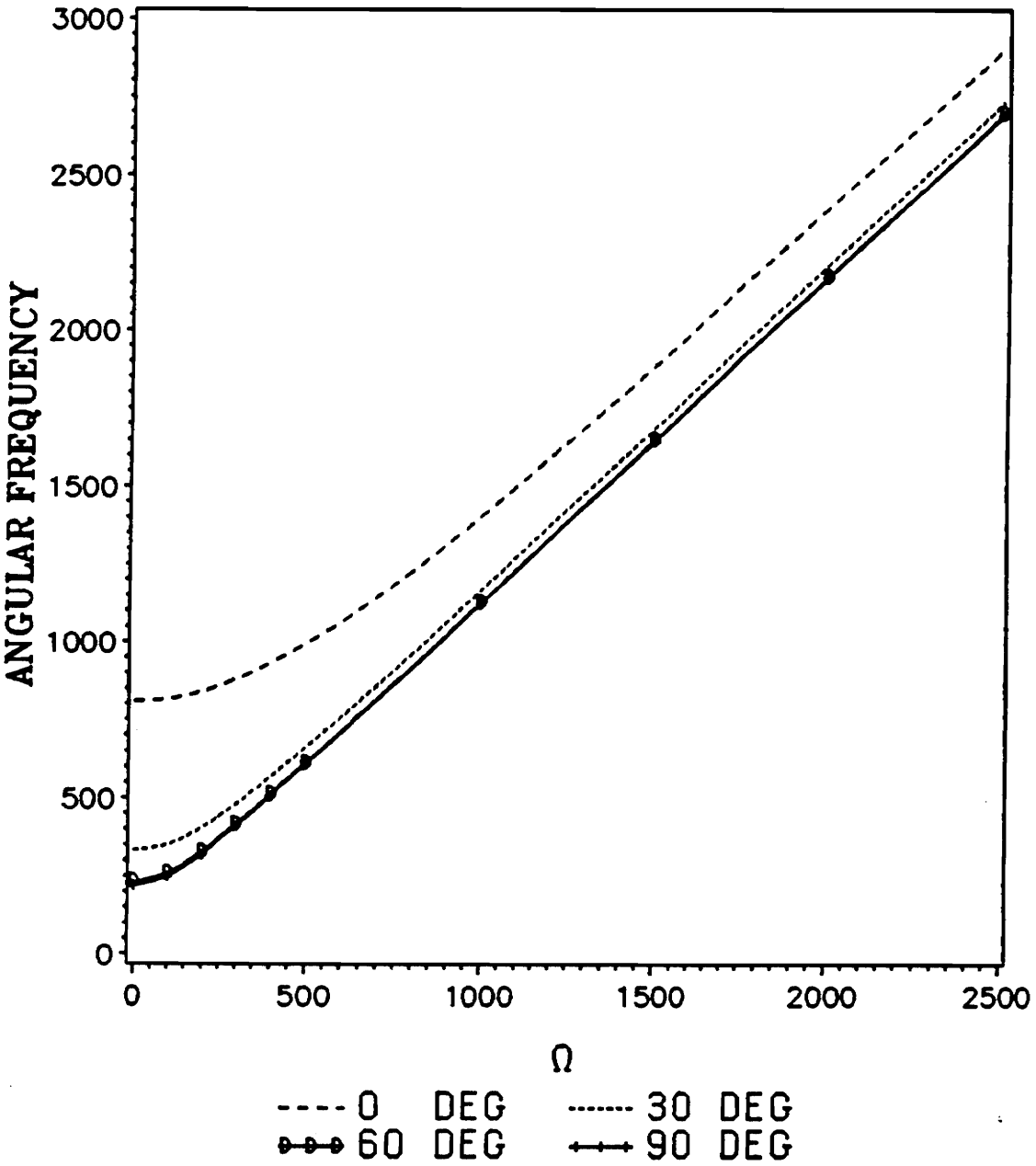

Figure 17. Variation of first natural frequencies of vibration with angular velocity for the Graphite/Epoxy plate $\bar{R} = 0$.

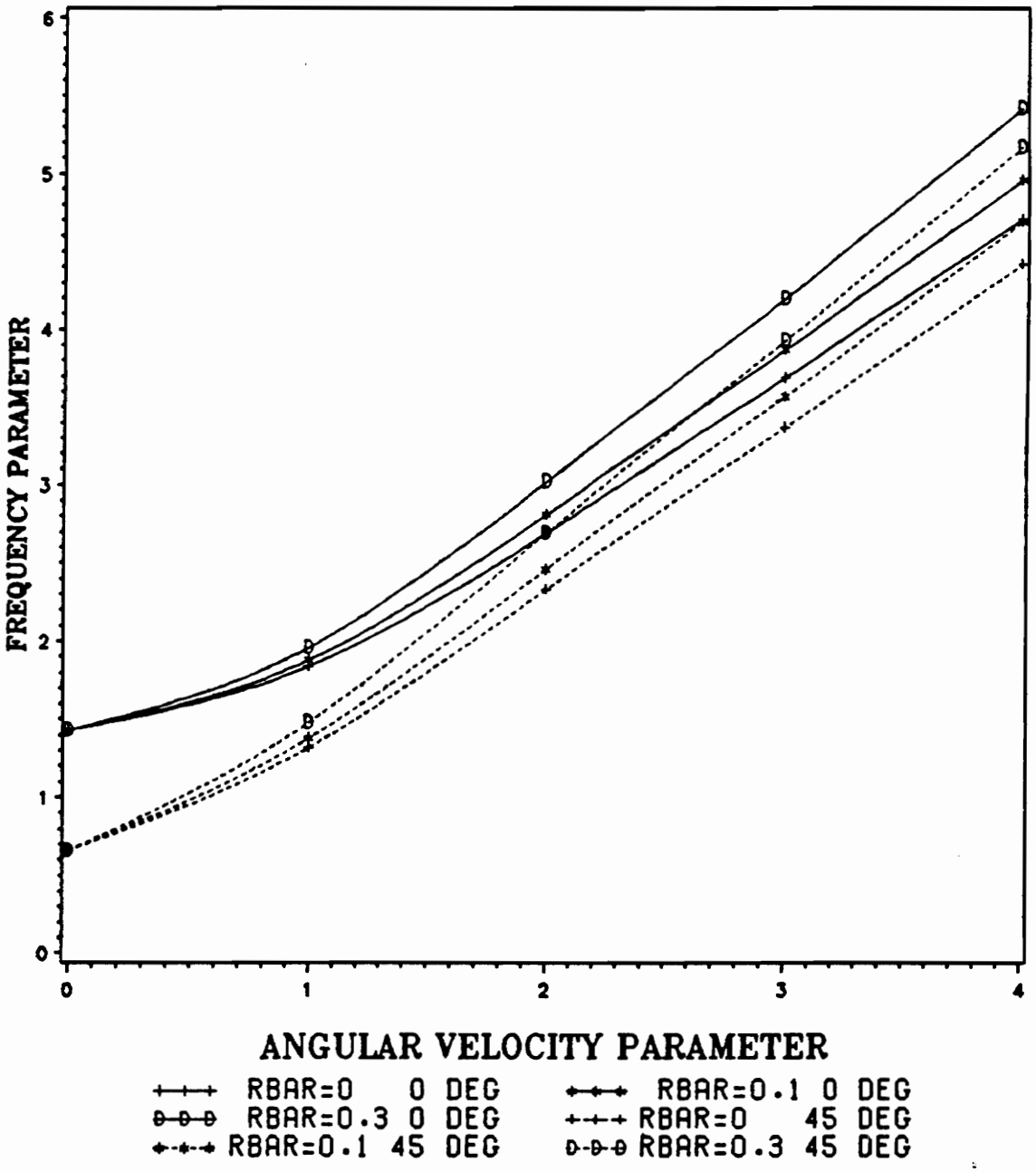

Figure 18. Variation of first natural frequencies of vibration with angular velocity for the Box-Beam with different values of $\bar{R}$

Appendix A. The Incremental Stiffness Matrix

We will be referring to Figure 8 for deriving expression for the centrifugal force [104].

Consider the finite element shown in the figure. The centrifugal force associated with an infinitesimal length dx' of the element located at x' is,

$$dF_{x'} = A^e \gamma \Omega^2 (R + pl + x') dx'$$

where A^e is the area (assumed to be constant) of the element and Ω the rotational speed of the blade.

The force acting on any section at a distance x' from the left end of the element is,

$$F_{x'} = \int_{x'}^{l} A^e \gamma \Omega^2 (R + pl + x')\, dx' + \int_{(p+1)l}^{ql} A \gamma \Omega^2 (R + x)\, dx$$

where A is the area distribution along the span, which for our discussion is assumed to be linear. Note that function A could obtained from the coordinates of the section nodes which are input to AE24.

Expression for the centrifugal force is obtained as,

$$= \gamma \Omega^2 l^2 [c - A^e(\overline{R} + \eta)\eta - \frac{A^e}{2}\eta^2]$$

where $A(x) = A + bx, \quad \eta = \frac{x}{l}, \quad \overline{R} = \frac{R}{l}$

and

$$c = A^e(p + \frac{1}{2} + \overline{R}) + a\overline{R}(q - p - 1) + \frac{1}{2}(a + bp)(q^2 - p^2 - 2p - 1)$$

Substituting in [1.18] yields incremental matrix as a sum of three matrices since the expression for the force is quadratic. The three matrices are the same for each of the terms, the representation of all the degree of freedoms being similar.

$$[KG1] = \begin{bmatrix} \frac{3}{5} & \frac{1}{10}l & -\frac{3}{5} & 0 \\ \frac{1}{10}l & \frac{1}{30}l^2 & -\frac{1}{10}l & -\frac{1}{60}l^2 \\ -\frac{3}{5} & -\frac{1}{10} & \frac{3}{5} & 0 \\ 0 & -\frac{1}{60}l^2 & 0 & \frac{1}{10}l^2 \end{bmatrix}$$

$$[KG2] = \begin{bmatrix} \frac{12}{35} & \frac{3}{42}l & -\frac{12}{35} & -\frac{1}{35}l \\ \frac{1}{14}l & \frac{2}{105}l^2 & -\frac{1}{14}l & -\frac{1}{70}l^2 \\ -\frac{12}{35} & -\frac{1}{14}l & \frac{12}{35} & \frac{1}{35}l \\ -\frac{1}{35}l & -\frac{1}{70}l^2 & \frac{1}{35}l & \frac{3}{35}l^2 \end{bmatrix}$$

$$[KG3] = \begin{bmatrix} \frac{6}{5} & \frac{1}{10}l & -\frac{6}{5} & \frac{1}{10}l \\ \frac{1}{10}l & \frac{2}{15}l^2 & -\frac{1}{10}l & -\frac{1}{30}l^2 \\ -\frac{6}{5} & -\frac{1}{10}l & \frac{6}{5} & -\frac{1}{10}l \\ \frac{1}{10}l & -\frac{1}{30}l^2 & -\frac{1}{10}l & \frac{2}{15}l^2 \end{bmatrix}$$

Appendix B. The Data File

A sample data file is presented at the end of this appendix. The file is organized as follows:

- ***Data Deck 1***

  This deck contains information about blade and hub dimensions and about the rotational speed of the blade. First entry is the angular velocity of the blade in rad/sec., radius of the hub, area of the cross - section of the blade at the root and tip. Linear interpolation is done for the values in between. Next entry is the blade material density and lastly the length of the blade.

- ***Data Deck 2***

  this deck contains the number of elements, the number of lowest vibration modes to be printed for both the natural frequencies and the flutter analysis, and the value of NFLAG1 and NFLAG2. If NFLAG1 = 1, the analysis is linear and non - linear when equals 2. If NFLAG2 = 2 then the program sets

the spanwise reference axis at the midchord and computes the offset between this axis and the center of gravity position. If NFLAG2 = 1, the offsets are supplied by the user (see data deck 7).

- ***Data Deck 3***

  This data deck contains the geometric boundary conditions for all the degrees of freedom. There is a line for each section (number of sections = number of elements + 1), and a 0 or 1 for each degree of freedom of the section. A 0 indicates the corresponding displacement is constrained to zero, a 1 indicates no geometric constraint.

- ***Data Deck 4***

  This data deck contains the sampling point abcissas and the coefficients for the Gaussian quadrature, and should not be modified.

- ***Data Deck 5***

  This data deck contains the Timoshenko shear coefficient and the warping stiffness correction factor (for definition refer [14])

- ***Data Deck 6***

  This data deck contains the air density, and default values for the initial reduced frequency, step size and number of iterations used in the flutter search (see Appendix C).

- ***Data Deck 7***

This data deck contains the information necessary to define the elements. This includes for each element :

On the first line : the total number of skin plies (top + bottom), the number of top plies, the shear modulus of the webs, the length of the elements and the material density.

On the second line :

- The non-dimensional (with respect to the aerodynamic semichord) offset between the aerodynamic center and the midchord, positive towards the trailing edge,

- The non-dimensional (with respect to the aerodynamic semichord) offset between the reference line and the midchord, positive towards the trailing edge. If NFLAG2 = 2, AE is set to zero.

- The non-dimensional (with respect to the structural semichord) offset between the center of gravity and the midchord, positive towards the trailing edge. If NFLAG2 = 2, the input value is ignored and cg is computed internally.

- The value of the lift-curve slope.

- The value of the reference line sweep angle in degrees, positive back.

There is a line for each skin layer, from top to bottom. Each line includes the material properties E_1 , E_2 , ν_{12} , G_{12} , G_{13} , the fiber orientation angle (relative to the spanwise axis, positive counterclockwise), and the two design variables pertaining to this particular layer (refer [14]).

Immediately following the layers data is a line containing the thicknesses of the four longitudinal web.

The last two lines for the element contain the stringers moduli E_i and cross-section areas A_i respectively.

- ***Data Deck 8***

  This data deck contains the geometric data defining all the sections. For each section this includes:

  On the first line : the aerodynamic semichord

  On the second line : The chordwise coordinates of each pair of section nodes

  On the third line : The thickness coordinates of the four top nodes

  On the fourth line : The thickness coordinates of the four bottom nodes

- ***Data Deck 9***

  This data deck contains the 29 design variables.

- ***Data Deck 10***

  This data deck contains information for the subroutine SECPRO computing section properties, and should not be modified.

- ***Data Deck 11***

  This data deck contains the nodal loads used in the static deflection analysis. There is a line for each section, and a value for each degree of freedom of the section.

```
**********************************************************************
** FREQUENCY OF ROTATION OF THE BLADE,RADIUS OF THE HUB,AREA OF CROSS**
** SECTION OF THE BLADE AT THE ROOT,AT THE TIP, DENSITY OF MATERIAL, **
** LENGTH OF THE BLADE.                                        ****
0.0       0.0  0.0625   0.0625   1.449E-4  7.5
**********************************************************************
** NUMBER OF ELTS, NUMBER OF FREQUENCIES TO BE PRINTED,          **
** NFLAG1 (1-LINEAR ANALYSIS, 2-NON-LINEAR ANALYSIS),          *
** NFLAG2 (1-INPUT VALUES FOR AE & CG, 2-COMPUTED VALUES)        **
    4   1  1   2
** GEOMETRIC BOUNDARY CONDITIONS FOR EACH D.O.F. (0:CONSTRAINED, 1:FREE)
 0  1  0  0  0  1  0  1  0  1  0  0
 1  1  1  1  1  1  1  1  1  1  1  1
 1  1  1  1  1  1  1  1  1  1  1  1
 1  1  1  1  1  1  1  1  1  1  1  1
 1  1  1  1  1  1  1  0  1  1  1  1
** GAUSSIAN QUADRATURE COEFFICIENTS                           **
-0.90617984593866400   0.236926885056189000
-0.53846931010568300   0.478628670499366000
 0.00000000000000000   0.568888888888889000
 0.53846931010568300   0.478628670499366000
 0.90617984593866400   0.236926885056189000
** SHEAR COEFFICIENT ALPHA, WARPING STIFFNESS CORRECTION K1T       **
  0.8333  1.570796
** AEROD. DATA: RO AIR, INIT. RED. FREQ., STEP SIZE, # OF ITERATIONS **
1.226       .3     .010   11
**********************************************************************
  FOR     NLAYER, NLAYERTOP, G13WEB, LENGTH, WIDTH, DENSITY,
          AC, AE, CG, CLA, SWEEP
          FOR EACH LAYER:
          LAYER THICKNESS, E1, E2, NU12, G12, G13, THETA, DESIGN VAR.
  EACH    WEB THICKNESSES
          STRINGER MODULI
  ELT     STRINGER AREAS
**********************************************************************
1  1       0.00E+40  1.875  0.5   1.449E-04
  -0.5     0.        0.     6.28319            0.0
   0.125    18.7E06  1.36E06  0.3  0.7479E06  0.624E06  0.  9   29
   0.0    0.0    0.0   0.0
0.0  0.0  0.0  0.0  0.0  0.0  0.0  0.0
0.0  0.0  0.0  0.0  0.0  0.0  0.0  0.0
**                                                  **
1  1       0.00E+40  1.875  0.5   1.449E-04
  -0.5     0.        0.     6.28319            0.0
   0.125    18.7E06  1.36E06  0.3  0.7479E06  0.624E06  0.  9   29
   0.0    0.0    0.0   0.0
0.0  0.0  0.0  0.0  0.0  0.0  0.0  0.0
0.0  0.0  0.0  0.0  0.0  0.0  0.0  0.0
**                                                  **
1  1       0.00E+40  1.875  0.5   1.449E-04
  -0.5     0.        0.     6.28319            0.0
   0.125    18.7E06  1.36E06  0.3  0.7479E06  0.624E06  0.  9   29
   0.0    0.0    0.0   0.0
0.0  0.0  0.0  0.0  0.0  0.0  0.0  0.0
0.0  0.0  0.0  0.0  0.0  0.0  0.0  0.0
```

```
**                                                        **
1  1        0.00E+40  1.875  0.5    1.449E-04
  -0.5      0.        0.      6.28319           0.0
   0.125     18.7E06   1.36E06  0.3  0.7479E06  0.624E06  0.  9    29
   0.0     0.0     0.0    0.0
0.0  0.0  0.0  0.0  0.0  0.0  0.0  0.0
0.0  0.0  0.0  0.0  0.0  0.0  0.0  0.0
**                                                        **
*************************************************************************
 FOR          AIRFOIL SEMICHORD

 EACH          SECTION GEOMETRY    X(1) - - - X(4)      *--*--*--*
                                Y(1) - - - Y(4)
 SECTION                             Y(5) - - - Y(8)      *--*--*--*
*************************************************************************
0.25
        0.0          0.1667        0.333         0.5
        0.125         0.125         0.125         0.125
        0.0          0.0           0.0           0.0
**                                                        **
0.25
        0.0          0.1667        0.333         0.5
        0.125         0.125         0.125         0.125
        0.0          0.0           0.0           0.0
**                                                        **
0.25
        0.0          0.1667        0.333         0.5
        0.125         0.125         0.125         0.125
        0.0          0.0           0.0           0.0
**                                                        **
0.25
        0.0          0.1667        0.333         0.5
        0.125         0.125         0.125         0.125
        0.0          0.0           0.0           0.0
**                                                        **
0.25
        0.0          0.1667        0.333         0.5
        0.125         0.125         0.125         0.125
        0.0          0.0           0.0           0.0
**                                                        **
**********    DESIGN VARIABLES        *****TETA=0.0      *********
0.0075   0.0075   0.0075   0.0075   0.0075    0.0075   0.0075
0.0075   0.00000  0.00375  0.00375  0.00375   0.00375  0.00375
0.00375  0.00375  2.55000  1.63200  1.16586   0.77724  0.62169
0.46614  0.31110  0.15555  0.04800  0.03600   0.02400  0.02400
60.0
**********   VLASOV DATA; NOT TO BE MODIFIED  ******************
NUMBER OF ELEMENTS IN THE SECTION, NUMBER OF NODES
         8          8
ELEMENT #, NODE 1, NODE 2
    1           1       2
    2           2       3
    3           3       4
    4           4       8
    5           8       7
    6           7       6
```

```
    7          6       5
    8          5       1
INITIAL POLE COORDINATES
70.          0.0
**********     NODAL LOADS          ****************************
0.0   0.0   0.0   0.0   0.0   0.0   0.0   0.0   0.0   0.0   0.0   0.0
0.0   0.0   0.0   0.0   0.0   0.0   0.0   0.0   0.0   0.0   0.0   0.0
0.0   0.0   0.0   0.0   0.0   0.0   0.0   0.0   0.0   0.0   0.0   0.0
0.0   0.0   0.0   0.0   0.0   0.0   0.0   0.0   0.0   0.0   0.0   0.0
0.0   0.0   0.0   0.0   0.0   0.0   0.0   0.0   0.0   0.0   0.0   0.0
```

```
*****************************************************************
C  FINITE ELEMENT PROGRAM FOR THE AEROELASTIC ANALYSIS OF              C
C  LAMINATED BEAMS.                                                   C
C  THE BEAM ELEMENT HAS 12 DEGREES OF FREEDOM, AND IT INCLUDES        C
C  THE EFFECT OF UNSYMMETRY, TRANSVERSE SHEAR  AND LATERAL DEFLECTION. C
C*****************************************************************C
      IMPLICIT DOUBLE PRECISION (A-H,O-Z)
      DIMENSION ESTIF(24,24),NBC(10,12),VL(100),G13(10,21),
     1  GSTIF(100,100),F(100),EX(5),H(5),NLAYER(10),AC(10),CLA(10),
     2  DISPL(12),T(10,21),E1(10,21),E2(10,21),V12(10,21),
     3  XL(10),G12(10,21),DEN(10),XMASS(24,24),GMASS(100,100),
     4  BETA(100),EIG(100),ITEM(100),TSPAR(10,4),X(10,8),Z(10,8),
     5  GSTIF1(100,100),INODE(8,2),T1X(24,24),ES(10,8),
     6  AS(10,8),SWEEP(10),BE(10),AE(10),CG(10),AEP(10),CGP(10),
     7  THETA(10,21),V1(10),V2(10),DV1(10),DV2(10),W1(10),W2(10),
     8  DW1(10),DW2(10),TAU1(10),TAU2(10),DTAU1(10),DTAU2(10)
      REAL*8 LEN,KG(24,24)
      INTEGER GDOF(10,12),ZDOF,IUMEL(8),ISPAR(10)
      COMPLEX*16 ALFA(100),EIVE(100,100),OMESQ,LAMBD
      COMMON /WORKSP/  RWKSP
      REAL RWKSP(30000)
      CALL IWKIN(30000)
C
C     NEL     -  NUMBER OF ELEMENTS
C     NON     -  NUMBER OF NODES = NEL + 1
C     NBC     -  GEOMETRIC BOUNDARY CONDITIONS : 0 OR 1
C     ZDOF    -     NUMBER OF ZERO DEGREES OF FREEDOM
C     NMOD    - NUMBER OF MODES TO BE PRINTED
C     ESTIF   - ELT STIFFNESS MATRIX
C     GSTIF   - GLOBAL STIFFNESS MATRIX
C     XMASS   - ELEMENT MASS MATRIX
C     GMASS   - GLOBAL MASS MATRIX
C     T1X     - TRANSFORMATION MATRIX FROM ELT TO GLOBAL COORD. SYSTEM
C     EX      - GAUSSIAN INTEGRATION POINTS
C     H       - GAUSSIAN INTEGRATION COEFFICIENTS
C     XL      - ELEMENT LENGTH
C     DEN     - ELEMENT DENSITY
C     CG      - NONDIMENSIONAL CG OFFSET FROM REF. LINE (WRT STRUCTURAL
C               SEMICHORD, POSITIVE TOWARDS T.E.)
C     NLAYER - TOTAL NUMBER OF LAYERS FOR AN ELEMENT. THE WEBS ARE
C              TREATED AS A LAYER BETWEEN THE TOP AND BOTTOM SKINS
C              HAVING TRANSVERSE SHEAR (G13) PROPERTIES ONLY
C     T       - LAYER THICKNESSES
C     TSPAR   - WEB THICKNESSES
C     ES      - SPAR CAPS MODULI
C     AS      - SPAR CAPS AREAS
C     X       - STRUCTURAL SECTION NODES COORDINATES, CHORDWISE
C     Z       - STRUCTURAL SECTION NODES COORDINATES, THICKNESSWISE
C     BE      - SECTION AERODYNAMIC SEMICHORD
C     SWEEP   - ELEMENT SWEEP ANGLE, POSITIVE BACK
C     CLA     - LIFT CURVE SLOPE
C     AC      - NONDIMENSIONAL AERODYNAMIC CENTER OFFSET FROM THE
C               REFERENCE LINE, POSITIVE TOWARDS T.E.
C               ( AC DIM. = (AC N.D.)*AEROD. SEMICHORD )
C     AE      - NONDIMENSIONAL REFERENCE LINE OFFSET FROM AEROD. MIDCHORD
C               (WRT AERODYNAMIC SEMICHORD, POSITIVE TOWARDS T.E.)
C     OMEGA   - THE ROTATIONAL SPEED OF THE ROTOR BLADE
C     RHUB    - RADIUS OF THE HUB.
C     DENS    - DENSITY OF THE MATERIAL OF THE ROTOR BLADE.
C     LEN     - LENGTH OF THE ROTOR BLADE.
C     ACS     - CROSS - SECTIONAL AREA OF THE ROTOR BLADE.
C
C
      CALL INPUT(AS,NEL,NON,NMOD,NFLAG1,NFLAG2,NBC,EX,H,ALPHA,NLAYER,
     1           T,E1,E2,V12,G12,G13,THETA,XL,DEN,VL,TSPAR,WK1T,
     2           X,Z,ES,NUMEL,NNODE,IUMEL,INODE,XAP,ZAP,SWEEP,
     3           RAIR,RFR,STEP,ITER,BE,AE,CG,ISPAR,CLA,AC,RHUB,OMEGA,
```

```
     4           DENS,A,B,LEN)
      ZDOF = 0
      K=1
      DO 1 I = 1,NON
        DO 1 J = 1,12
          IF (NBC(I,J).EQ.0) THEN
            GDOF(I,J)=0
            ZDOF = ZDOF+1
          ELSE
            GDOF(I,J)=K
            K=K+1
          ENDIF
 1    CONTINUE
C
C   INITIALIZE GLOBAL STIFFNESS, MASS AND THE DISPLACEMENT MATRICES
C
C        - NORD IS THE ORDER OF THE ASSEMBLED MATRIX-
C
      NORD =  12*NON-ZDOF
      DO 3 I = 1,NORD
        DO 3 J = 1,NORD
          GSTIF(I,J) = 0.0
  3     GMASS(I,J) = 0.0
      IF (NFLAG1.EQ.2) GO TO 221
C
C  ***************************************************************************
C  *                                                                         *
C  *                  L I N E A R     PROBLEM                                *
C  *                                                                         *
C  ***************************************************************************
C
C  ASSEMBLE GLOBAL STIFFNESS MATRIX AND MASS MATRIX
C
      DO 17 IK = 1,NEL
        NPLIES = NLAYER(IK)
c       CALL TGLOB(SWEEP,T1X,IK)
        CALL STIFF(NPLIES,IK,NUMEL,NNODE,IUMEL,INODE,ISPAR(IK),NK1T,
     1             EX,H,ALPHA,T,E1,E2,V12,G12,G13,THETA,XL,ESTIF,TSPAR,
     2             X,Z,ES,AS,XAP,ZAP,SWEEP,X2P,AEP(IK))
        IF(NFLAG2.EQ.2) AE(IK)=00.00
c       CALL TRASF(ESTIF,T1X)
C       EXJ=0.0
        CALL INCREM(NEL,IK,KG,XL(IK),RHUB,DENS,OMEGA,A,B,TOTXL)
        CALL KADD(ESTIF,KG)
        CALL ASSEM(ESTIF,IK,GDOF,GSTIF)
        CALL MASS(EX,H,XL(IK),DEN(IK),IK,XMASS,CG(IK),NPLIES,T,TSPAR,X,
     1       Z,AS,NUMEL,NNODE,IUMEL,INODE,XAP,ZAP,X2P,NFLAG1,ISPAR(IK))
C       CALL TRASF(XMASS,T1X)
   17   CALL ASSEM(XMASS,IK,GDOF,GMASS)
      DO 18 I = 1,NORD
        DO 18 J = 1,NORD
 18   GSTIF1(I,J) = GSTIF(I,J)
C
C******** STATIC  ANALYSIS *************************************************
C
C   ASSEMBLE LOAD VECTOR {F}
C
      N = 0
      KJ = 1
      DO 50 I = 1,NON
        DO 54 J = 1,12
          N = N+1
          IF(NBC(I,J).EQ.0) GOTO 54
          F(KJ) = VL(N)
          KJ = KJ+1
 54     CONTINUE
```

```
 50   CONTINUE
C
C   SOLVE THE SYSTEM  [K] {Q} = {F}
C     DO 12 JK=1,18
      CALL DLSARG(NORD,GSTIF,100,F,1,VL)
      WRITE(6,190)
      K = 0
      DO 56 I = 1,NON
        DO 57 J =1,12
          IF (NBC(I,J).EQ.0) THEN
C           DISPL(I,J) = 0.0
            DISPL(J) = 0.0
          ELSE
            K = K+1
C           DISPL(I,J) = VL(K)
            DISPL(J) = VL(K)
          ENDIF
 57     CONTINUE
C
 56   WRITE(6,200) I,(DISPL(J),J=1,12)
C
C******** FREE-VIBRATION  PROBLEM ***************************************
C
      CALL DGVCRG(NORD,GSTIF,100,GMASS,100,ALFA,BETA,EIVE,100)
      DO 60 I = 1,NORD
        DO 60 J = 1,NORD
 60   GSTIF(I,J) =REAL(EIVE(I,J))
      DO 61 I = 1,NORD
        IF (BETA(I).EQ.0) THEN
          EIG(I)=1.E+40
          GOTO 61
        END IF
        OMESQ = ALFA(I)/BETA(I)
        EIG(I) =REAL(OMESQ)
 61   CONTINUE
C   REARRANGE EIGENVALUES IN INCREASING ORDER OF MAGNITUDE
      CALL SORT(NORD,EIG,ITEM)
      WRITE(6,210)
      PI=4.*ATAN(1.)
      DO 64 L = 1,NMOD
        I = ITEM(L)
        EIGVL = EIG(I)
        OMEGA = SQRT(EIGVL)
        WRITE(6,*)
        WRITE(6,*) 'MODE # ',L,' FREQUENCY (RAD/S): ', OMEGA
       WRITE(6,*)
        WRITE(6,190)
        KN = 0
        KM = 0
        DO 64 J = 1,NON
          DO 66 K = 1,12
            KM = KM+1
            IF(NBC(J,K).EQ.0)THEN
              DISPL(K) = 0.0
            ELSE
              KN=KN+1
              IF(L.EQ.1)VL(KN) = GSTIF(KN,I)
              DISPL(K) = GSTIF(KN,I)
            ENDIF
 66       CONTINUE
 64   WRITE(6,200)J,(DISPL(N),N=1,12)
C64   CONTINUE
      CALL AERO(GSTIF1,GMASS,NEL,NORD,GDOF,RAIR,RFR,STEP,ITER,XL,
     $          BE,AE,CG,SWEEP,NMOD,AC ,CLA)
c
c
```

```
C********** FORMAT STATEMENTS ***********************************************
C
 190  FORMAT(5X,15H DISPLACEMENTS:,/)
 200  FORMAT(3X,10H NODE NO. ,I5,/,4H U  ,10X,E12.5,
     1 /,8H DER-U  ,6X,E12.5,/,4H W-B,10X,E12.5,/,8H THETA-B,6X,E12.5,/
     1 ,4H W-S,10X,E12.5,/,8H THETA-S,6X,E12.5,/,4H TAU,10X,E12.5,/,
     1 8H DER.TAU,6X,E12.5,/,4H BET,10X,E12.5,/,8H DER-BET,6X,E12.5,/,
     1 4H V  ,10X,E12.5,/,8H DER-V  ,6X,E12.5,/)
 210  FORMAT(5X,/,47HDYNAMIC ANALYSIS: NATURAL FREQUENCIES AND MODES,/)
 220  FORMAT(5X,8HMODE NO.,I5,3X,28HEIGENVECTORS AT EIGENVALUE =,E15.6
     1,2X,19HFREQUENCY (RAD/S) =,E15.6,/)
C
C*******************************************************************************
C
C
C   SUBROUTINE ASSEM - THIS SUBROUTINE ASSEMBLES THE ELEMENT STIFFNESS
C   AND MASS MATRICES INTO GLOBAL MATRICES
C
      SUBROUTINE ASSEM(XMATR,IK,GDOF,GMATR)
        IMPLICIT DOUBLE PRECISION (A-H,O-Z)
      DIMENSION XMATR(24,24),GMATR(100,100),LM(24)
      INTEGER GDOF(10,12)
      DO 2 K = IK,IK+1
        DO 2 J = 1,12
          N=J
          IF(K.EQ.IK+1)N=J+12
 2    LM(N) = GDOF(K,J)
      DO 4 II = 1,24
        IDOF = LM(II)
        IF(IDOF.EQ.0)GOTO 4
        DO 5 JJ = 1,24
          JDOF = LM(JJ)
          IF(JDOF.EQ.0)GOTO 5
          GMATR(IDOF,JDOF) = GMATR(IDOF,JDOF)+XMATR(II,JJ)
 5      CONTINUE
 4    CONTINUE
      RETURN
      END
C
C*******************************************************************
C
      SUBROUTINE STIFF(NLAYER,IK,NUMEL,NNODE,IUMEL,INODE,ISPAR,MK1T,
     1 EX,H,ALPHA,T,E1,E2,V12,G12,G13,THETA,XL,XKMAT,SPAR,X,Z,ES,AS,
     2 XAP,ZAP,SWEEP,X2C,AE)
       IMPLICIT DOUBLE PRECISION (A-H,O-Z)
C
C  THIS SUBROUTINE  CALCULATES THE LINEAR STIFFNESS MATRIX
C  FOR EACH ELEMENT
C
      DIMENSION A(3,3),B(3,3),D(3,3),BTC(24,6),ES(10,8),AS(10,8),
     1          XKM(24,24),BK(6,24),BT(24,6),XK(24,24),EX(5),H(5),
     2          TX(24),XKMAT(24,24),G13(10,21),G12(10,21),SPAR(10,4),
     3          T(10,21),E1(10,21),E2(10,21),V12(10,21),THETA(10,21),
     4          XL(10),D44(10),ZIT(8),IUMEL(8),COORD(8,2),INODE(8,2),
     5          X(10,8),Z(10,8),XT(8),ZT(8),COEF(8,8),UT(8),CSTIF(6,6),
     7          SWEEP(10),YA(3),YB(3),CDUM(5,5),E1S(10,8),TT1(8),
     8          QA11(8),QA16(8),QA66(8),QD11(8),QD16(8),QD66(8),ZTO(8)

C
C*          NUMBER OF GAUSS POINTS
C*
      L=5
        NTLAY=ISPAR-1
        TT=0.000000000000
        DO 21 I=1,NTLAY
 21     TT=TT+T(IK,I)
        DO 51 I=1,3
```

```
 51     TT1(I)=TT
        TT=0.000000000000
        DO 22 I=NLAYER,ISPAR+1,-1
 22     TT=TT+T(IK,I)
        DO 52 I=5,7
 52     TT1(I)=TT
C
C       THE REFERENCE IS THE SECTION GEOMETRIC CENTROID
C
        DO 452 I=1,8
          QA11(I)=1.
          QA16(I)=0.0000000000000
          QA66(I)=0.0000000000000
          QD11(I)=0.0000000000000
          QD16(I)=0.0000000000000
          QD66(I)=0.0000000000000
 452    E1S(IK,I)=1.0000000000000
C
C    ***** WEB PROPERTIES   ********
C
        TT1(4)=SPAR(IK,4)
        TT1(8)=SPAR(IK,1)
C
      DO 20 IL = 1,24
        DO 20 JL = 1,24
          XK(IL,JL) = 0.00000000000000
          XKM(IL,JL) = 0.0000000000000
 20    XKMAT(IL,JL) = 0.0D0
      DO 30 IL = 1,24
        DO 30 JL = 1,6
 30    BT(IL,JL) = 0.0D0
      DO 40 KI = 1,L
        EXV = EX(KI)
C
C               LINEAR VARIATION OF THE CHORD AND SECTION
C               NODES ALONG THE SPAN OF THE ELEMENT
C
        DO 50 I=1,8
          XT(I)=(X(IK+1,I)-X(IK,I))*EXV/2.+(X(IK+1,I)+X(IK,I))/2.
 50     ZIT(I)=(Z(IK+1,I)-Z(IK,I))*EXV/2.+(Z(IK+1,I)+Z(IK,I))/2.
        WT=ABS(XT(1)-XT(4))
        DO 60 I=1,8
          COORD(I,1)=XT(I)
 60     COORD(I,2)=ZIT(I)
C
        CALL SECPRO(NUMEL,NNODE,IUMEL,INODE,XAP,ZAP,COORD,QA11,QA16,
     $       QA66,QD11,QD16,QD66,TT1,X2C,Z2C,AS,E1S,WT,IK,X5P,Z5P,CDUM)
C       X0=X2C-XT(1)
        X0=WT/2.
C     IF (KI.EQ.1) THEN
C       AE= (X2C-XT(1)-WT/2.)
C     END IF
C
C      ******* CHANGE OF COORD. SYSTEM: CHORDWISE FROM -1 TO +1,
C                                       THICKNESS FROM CENTROID
C
        DO 80 I=1,8
 80     ZT(I)=ZIT(I)-Z2C
        DO 90 I=1,8
 90     UT(I)=(2.*XT(I)-XT(4)-XT(1))/(XT(4)-XT(1))
C
C   **** STRINGER CONTRIBUTION   *****
C
        TAS=0.0D0
        TBS=0.0D0
        TDS=0.0D0
        YTAS=0.0D0
```

```
        YTBS=0.0D0
        YTDS=0.0D0
        DO 100 I=1,8
          TAS=TAS+ES(IK,I)*AS(IK,I)
          TBS=TBS+ES(IK,I)*AS(IK,I)*ZT(I)
          TDS=TDS+ES(IK,I)*AS(IK,I)*ZT(I)**2
          YTAS=YTAS+ES(IK,I)*AS(IK,I)*UT(I)*WT/2.
          YTBS=YTBS+ES(IK,I)*AS(IK,I)*ZT(I)*UT(I)*WT/2.
 100    YTDS=YTDS+ES(IK,I)*AS(IK,I)*(UT(I)*WT/2.)**2
        DO 120 I=1,8
          DO 120 J=1,8
 120    COEF(I,J)=0.0D0
        DO 130 I=1,4
          DO 140 J=1,3
            COEF(I,J)=UT(I)**(4-J)
 140    COEF(I+4,J+4)=UT(I+4)**(4-J)
        COEF(I,4)=1.0D0
 130    COEF(I+4,8)=1.0D0
      CALL DLSLRG(8,COEF,8,ZT,1,ZT)
        CALL LAMINA(IK,NLAYER,ZT,T,E1,E2,V12,G12,THETA,D44,G13,A,B,D,
     $              SPAR,WT,EX,H,UT,YA,YB,YD,XO,ISPAR)
        A(1,1)=A(1,1)+TAS
        B(1,1)=B(1,1)+TBS
        D(1,1)=D(1,1)+TDS
        YA(1)=YA(1)+YTAS
        YB(1)=YB(1)+YTBS
        YD=YD+YTDS
        CALL CMATR(A,B,D,ALPHA,IK,D44,CSTIF,YA,YB,YD,WK1T)
        CALL BKMATR (EXV,XL(IK),BK)
        DO 150 LI = 1,24
          DO 150 LJ = 1,6
 150    BT(LI,LJ)=BK(LJ,LI)
        CALL MULT(BT,CSTIF,24,6,6,BTC)
        CALL MULT(BTC,BK,24,6,24,XK)
        DO 160 I = 1,24
          DO 160 J = 1,24
 160    XKM(I,J)=XKM(I,J)+XK(I,J)*H(KI)*(XL(IK)/2.)
 40   CONTINUE
      CALL TMATR(XL(IK),TX)
      DO 170 I = 1,24
        DO 170 J = 1,24
 170  XKMAT(I,J) = TX(I)*XKM(I,J)*TX(J)
 240  RETURN
      END
C*
C*********************************************************************
C*
C  SUBROUTINE LAMINA - THIS SUBROUTINE CALCULATES THE [A], [B], AND [D]
C  MATRICES FOR EACH ELEMENT
C
      SUBROUTINE LAMINA(IK,NLAYER,YT,T,E1,E2,V12,G12,THETA,D44,
     1                  G13,A,B,D,TSPAR,WT,EX,H,UT,YA,YB,YD,YO,ISPAR)
      IMPLICIT DOUBLE PRECISION (A-H,O-Z)
      DIMENSION A(3,3),B(3,3),D(3,3),QRTRNS(3,3),T(10,21),
     1          E1(10,21),E2(10,21),V12(10,21),THETA(10,21),G12(10,21),
     2          D44(10),G13(10,21),YT(8),EX(5),H(5),TSPAR(10,4),UT(8),
     3          ZF(4),ZF1(4),YA(3),YB(3)
      REAL*8 YD,WT,YO
      INTEGER   NLAYER,ISPAR
C*
C*  INITIALIZE MATRICES
C*
      D44(IK)=0.0D0
      ZK=0.0D0
      ZK1=0.0D0
      YD=0.0D0
      DO 10 I=1,3
```

```
        YA(I)=0.0D0
        YB(I)=0.0D0
        DO 10 J=1,3
          A(I,J)=0.0D0
          B(I,J)=0.0D0
 10   D(I,J)=0.0D0
C*
C*    COMPUTE THE A,B,D MATRICIES
C*
        DO 70 I=1,4
        ZF(I)=YT(1)*UT(I)**3+YT(2)*UT(I)**2+YT(3)*UT(I)+YT(4)
        DO 200 IL=1,ISPAR-1
 200    ZF(I)=ZF(I)-T(IK,IL)/2.
 70     CONTINUE
      ZD1=-YT(5)+YT(6)-YT(7)+YT(8)
      ZE1=YT(5)+YT(6)+YT(7)+YT(8)
      L=5
      DO 30 KI=1,L
        EXV=EX(KI)
        Z0=YT(1)*EXV**3+YT(2)*EXV**2+YT(3)*EXV+YT(4)
        DO 203 IL=1,ISPAR-1
 203    Z0=Z0+T(IK,IL)/2.
        ZK1=Z0
        WC=WT
        DO 40 I=1,ISPAR-1
          CALL QSTIFF(E1(IK,I),E2(IK,I),V12(IK,I),G12(IK,I),THETA(IK,I),
     1                QRTRNS)
          ZK=ZK1-T(IK,I)
          YD=YD+QRTRNS(1,1)*(ZK1-ZK)*H(KI)*(WT*(EXV+1)/2.-Y0)**2*WT/2.
          D44(IK)=D44(IK) + G13(IK,I)*(ZK1-ZK)*H(KI)*WT/2.
        DO 60 J=1,3
         YA(J)=YA(J)+QRTRNS(1,J)*(ZK1-ZK)*H(KI)*(WT*(EXV+1)/2-Y0)*WT/2.
           YB(J)=YB(J) + (1./2.)*QRTRNS(1,J)*(ZK1*ZK1-ZK*ZK)*H(KI)
     $           *(WT*(EXV+1)/2.-Y0)*WT/2.
          DO 60 K=1,3
            A(J,K)=A(J,K) + QRTRNS(J,K)*(ZK1-ZK)*H(KI)*WT/2.
            B(J,K)=B(J,K) + (1./2.)*QRTRNS(J,K)*(ZK1*ZK1-ZK*ZK)*H(KI)
     $      *WT/2.
 60       D(J,K)=D(J,K) + (1./3.)*QRTRNS(J,K)*(ZK1**3-ZK**3)*H(KI)*WT/2.
          ZK1=ZK
          WC=WT
 40     CONTINUE
 30   CONTINUE
      DO 20 I=1,4
      ZF1(I)=YT(5)*UT(I)**3+YT(6)*UT(I)**2+YT(7)*UT(I)+YT(8)
      DO 210 IL=ISPAR+1,NLAYER
 210  ZF1(I)=ZF1(I)+T(IK,IL)/2.
 20   CONTINUE
      DO 80 KI=1,L
C     KI=5
        EXV=EX(KI)
        Z0=YT(5)*EXV**3+YT(6)*EXV**2+YT(7)*EXV+YT(8)
        DO 90 I=ISPAR+1,NLAYER
 90     Z0=Z0+T(IK,I)/2.
        ZK1=Z0
        DO 110 I=ISPAR+1,NLAYER
C     I=NLAYER
          CALL QSTIFF(E1(IK,I),E2(IK,I),V12(IK,I),G12(IK,I),THETA(IK,I),
     1                QRTRNS)
          ZK=ZK1-T(IK,I)
          YD=YD+QRTRNS(1,1)*(ZK1-ZK)*H(KI)*(WT*(EXV+1)/2.-Y0)**2*WT/2.
          D44(IK)=D44(IK) + G13(IK,I)*(ZK1-ZK)*H(KI)*WT/2.
          DO 120 J=1,3
           YA(J)=YA(J)+QRTRNS(1,J)*(ZK1-ZK)*H(KI)*(WT*(EXV+1)/2.-Y0)*
     $      WT/2.
           YB(J)=YB(J) + (1./2.)*QRTRNS(1,J)*(ZK1*ZK1-ZK*ZK)*H(KI)
```

```
     $            *(WT*(EXV+1)/2.-YO)*WT/2.
C     STOP
            DO 120 K=1,3
C     A(J,K)=0.0
              A(J,K)=A(J,K) + QRTRNS(J,K)*(ZK1-ZK)*H(KI)*WT/2.
              B(J,K)=B(J,K) + (1./2.)*QRTRNS(J,K)*(ZK1*ZK1-ZK*ZK)*H(KI)
     $        *WT/2.
 120       D(J,K)=D(J,K) + (1./3.)*QRTRNS(J,K)*(ZK1**3-ZK**3)*H(KI)*WT/2.
           ZK1=ZK
           WC=WT
 110     CONTINUE
 80    CONTINUE
C          CALL QSTIFF(E1(IK,ISPAR),E2(IK,ISPAR),V12(IK,ISPAR),
C     1                 G12(IK,ISPAR),THETA(IK,ISPAR),QRTRNS)
       DO 141 JK=1,4
 141      D44(IK)=D44(IK) + G13(IK,ISPAR)*(ZF(JK)-ZF1(JK))*TSPAR(IK,JK)
       DO 142 I=1,3
         DO 142 J=1,I
           A(I,J)=A(J,I)
           B(I,J)=B(J,I)
 142   D(I,J)=D(J,I)
       RETURN
       END
C*
C*****************************************************************
C*
C*    SUBROUTINE CMATR-THIS SUBROUTINES CALCULATES THE [C] MATRIX WHICH
C*    IS DEFINED AS:
C*                       {N}=[C] {E}
C*
        SUBROUTINE CMATR(A,B,D,ALPHA,IK,D44,CSTIF,YA,YB,YD,WK1T)
         IMPLICIT DOUBLE PRECISION (A-H,O-Z)
        DIMENSION CSTIF(6,6),A(3,3),B(3,3),D(3,3),F(2,6),FX(6,2),
     1 FXY(6,6),CT(6,6),D44(10),YA(3),YB(3)
C*
        DO 3 I = 1,6
        DO 4 J = 1,6
        CSTIF(I,J) = 0.0D0
        CT(I,J) = 0.0D0
     4  CONTINUE
     3  CONTINUE
        FRA1 = B(2,2)/D(2,2)
        FRA2 = B(2,2)/A(2,2)
        DEN1 = ((B(2,2)**2)/D(2,2))-A(2,2)
        DEN2 = ((B(2,2)**2)/A(2,2))-D(2,2)
        F(1,1) = (A(1,2)-B(1,2)*FRA1)/DEN1
        F(1,2) = (A(2,3)-B(2,3)*FRA1)/DEN1
        F(1,3) = (B(1,2)-D(1,2)*FRA1)/DEN1
        F(1,4) = (B(2,3)-D(2,3)*FRA1)/DEN1
        F(1,5) = 0.0D0
        F(1,6) = (YA(2)+YB(2)*FRA1)/DEN1
        F(2,1) = (B(1,2)-A(1,2)*FRA2)/DEN2
        F(2,2) = (B(2,3)-A(2,3)*FRA2)/DEN2
        F(2,3) = (D(1,2)-B(1,2)*FRA2)/DEN2
        F(2,4) = (D(2,3)-B(2,3)*FRA2)/DEN2
        F(2,5) = 0.0D0
        F(2,6) = (YB(2)+YA(2)*FRA2)/DEN2
        FX(1,1) = A(1,2)
        FX(1,2) = B(1,2)
        FX(2,1) = A(2,3)
        FX(2,2) = B(2,3)
        FX(3,1) = B(1,2)
        FX(3,2) = D(1,2)
        FX(4,1) = B(2,3)
        FX(4,2) = D(2,3)
        FX(5,1) = 0.0D0
        FX(5,2) = 0.0D0
```

```
      FX(6,1) = YA(2)
      FX(6,2) = YB(2)
      CALL MULT(FX,F,6,2,6,FXY)
      CT(1,1) = A(1,1)
      CT(1,2) = A(1,3)
      CT(1,3) = B(1,1)
      CT(1,4) = B(1,3)
      CT(2,1) = A(1,3)
      CT(2,2) = A(3,3)
      CT(2,3) = B(1,3)
      CT(2,4) = B(3,3)
      CT(3,1) = B(1,1)
      CT(3,2) = B(1,3)
      CT(3,3) = D(1,1)
      CT(3,4) = D(1,3)
      CT(4,1) = B(1,3)
      CT(4,2) = B(3,3)
      CT(4,3) = D(1,3)
      CT(4,4) = D(3,3)
      CT(5,5) = ALPHA*D44(IK)
      CT(1,6) = YA(1)
      CT(2,6) = YA(3)
      CT(3,6) = YB(1)
      CT(4,6) = YB(3)
      CT(6,6) = YD
      CT(6,1) = YA(1)
      CT(6,2) = YA(3)
      CT(6,3) = YB(1)
      CT(6,4) = YB(3)
C
C     ***** FOLLOWING FOR WARPING CORRECTION   *****
C
      CT(4,4)=CT(4,4)*(WK1T/1.570796)**2
C
C
      CALL ADD(CT,FXY,6,6,CSTIF)
C
C
      RETURN
      END
C*
C*********************************************************************
C*
C*   SUBROUTINE BKMATR- THIS SUBROUTINES CALCULATES THE MATRIX [BK],
C*   WHERE [BK] IS DEFINED AS:
C*                        {E}=[BK] {Q}
C*
      SUBROUTINE BKMATR(EX,XL,BK)
       IMPLICIT DOUBLE PRECISION (A-H,O-Z)
      DIMENSION BK(6,24)
C*
      DO 1 I = 1,6
      DO 2 J = 1,24
      BK(I,J)=0.0D0
    2 CONTINUE
    1 CONTINUE
      XN1 = 0.25*(2.-3.*EX+EX**3)
      XN2 = 0.25*(EX**3-EX**2-EX+1.)
      XN3 = 0.25*(2.+3.*EX-EX**3)
      XN4 = 0.25*(EX**3+EX**2-EX-1.)
      BK(1,1)=2.0*(-0.75+0.75*(EX**2))/XL
      BK(1,2)=2.0*(-0.25-0.5*EX+0.75*(EX**2))/XL
      BK(1,13)=2.0*(0.75-0.75*(EX**2))/XL
      BK(1,14)=2.0*(-0.25+0.5*EX+0.75*(EX**2))/XL
      BK(2,9)=XN1
      BK(2,10)=XN2
      BK(2,21)=XN3
```

```
        BK(2,22)=XN4
        BK(3,3)=4.0*(1.5*EX)/(XL**2)
        BK(3,4)=4.0*(-0.5+1.5*EX)/(XL**2)
        BK(3,15)=4.0*(-1.5*EX)/(XL**2)
        BK(3,16)=4.0*(0.5+1.5*EX)/(XL**2)
        BK(4,7)=4.0*(-0.75+0.75*(EX**2))/XL
        BK(4,8)=4.0*(-0.25-0.5*EX+0.75*(EX**2))/XL
        BK(4,19)=4.0*(0.75-0.75*(EX**2))/XL
        BK(4,20)=4.0*(-0.25+0.5*EX+0.75*(EX**2))/XL
        BK(5,5)=2.0*(-0.75+0.75*(EX**2))/XL
        BK(5,6)=2.0*(-0.25-0.5*EX+0.75*(EX**2))/XL
        BK(5,17)=2.0*(0.75-0.75*(EX**2))/XL
        BK(5,18)=2.0*(-0.25+0.5*EX+0.75*(EX**2))/XL
        BK(6,11)=4.0*(1.5*EX)/(XL**2)
        BK(6,12)=4.0*(-0.5+1.5*EX)/(XL**2)
        BK(6,23)=4.0*(-1.5*EX)/(XL**2)
        BK(6,24)=4.0*(0.5+1.5*EX)/(XL**2)
        RETURN
        END
C
C*********************************************************************
C
C   SUBROUTINE TMATR -  THIS SUBROUTINE CREATES THE TRANSFORMATION
C                       VECTOR (TX) TO TRANSFORM THE STIFFNESS MATRIX
C                       FROM NONDIMENSIONAL COORDINATE SYSTEM TO
C                       X-COORDINATE SYSTEM.
C
      SUBROUTINE TMATR(XL,TX)
        IMPLICIT DOUBLE PRECISION (A-H,O-Z)
      DIMENSION TX(24)
      DO 12 I = 1,24
 12   TX(I) = 0.0D0
      DO 13 I = 1,23,2
 13   TX(I) = 1.0D0
      DO 14 I = 2,24,2
 14   TX(I) = XL/2.
      RETURN
      END
C
C*********************************************************************
C
      SUBROUTINE MASS(EX,H,XL,DEN,IK,XMASS,CG,NLAYER,T,TSPAR,
     $ X,Z,AS,NUMEL,NNODE,IUMEL,INODE,XAP,ZAP,X2P,NFLAG1,ISPAR)
        IMPLICIT DOUBLE PRECISION (A-H,O-Z)
C
C   THIS SUBROUTINE CREATES THE MASS MATRIX FOR EACH ELEMENT
C
        DIMENSION XMASS(24,24),EX(5),H(5),XN(4),
     1            XMA(4,4),TX(24),XMC(4,4),COORD(8,2),XMB(4,4),T(10,21),
     2            SWEEP(10),TSPAR(10,4),ROS(10,8),AS(10,8),
     3            QA11(8),QA16(8),QA66(8),QD11(8),QD16(8),QD66(8),TT1(8),
     4            IUMEL(8),INODE(8,2),X(10,8),Z(10,8),C(5,5)
        DO 7 I = 1,24
        DO 7 J = 1,24
 7      XMASS(I,J) = 0.000
       DO 1 I=1,8
         ROS(IK,I)=DEN
         QA11(I)=DEN
         QA16(I)=0.0
         QA66(I)=DEN
         QD11(I)=DEN
         QD16(I)=0.0
 1     QD66(I)=DEN
       TT=0.0
       DO 11 I=1,ISPAR-1
 11    TT=TT+T(IK,I)
       DO 12 I=1,3
```

```
 12    TT1(I)=TT
       TT=0.0
       DO 13 I=ISPAR+1,NLAYER
 13    TT=TT+T(IK,I)
       DO 14 I=5,7
 14    TT1(I)=TT
       TT1(4)=0.0
       TT1(8)=0.0
        L = 5
        DO 4 JK = 1,4
        DO 4 KJ = 1,4
        XMA(JK,KJ) = 0.0
        XMB(JK,KJ) = 0.0
        XMC(JK,KJ) = 0.0
4       CONTINUE
        DO 2 KI= 1,L
          EXV=EX(KI)
        XN(1) = 0.25*(2.0-3.0*EXV+EXV**3)
        XN(2) = 0.25*(EXV**3-EXV**2-EXV+1.)
        XN(3) = 0.25*(2.0+3.0*EXV-EXV**3)
        XN(4) = 0.25*(EXV**3+EXV**2-EXV-1.)
         DO 50 I=1,8
           COORD(I,1)=(X(IK+1,I)-X(IK,I))*EXV/2.+(X(IK+1,I)+X(IK,I))/2.
 50      COORD(I,2)=(Z(IK+1,I)-Z(IK,I))*EXV/2.+(Z(IK+1,I)+Z(IK,I))/2.
       WT=ABS(COORD(1,1)-COORD(4,1))
         CALL SECPRO(NUMEL,NNODE,IUMEL,INODE,XAP,ZAP,COORD,QA11,QA16,
      $             QA66,QD11,QD16,QD66,TT1,XG,ZG,AS,ROS,WT,IK,X1P,Y1P,C)
       R=XG-COORD(1,1)-WT/2.
       IF(NFLAG1.EQ.1) R=CG*WT/2.
        DO 3 K = 1,4
        DO 3 J = 1,4
        XMA(K,J) = XMA(K,J)+XN(K)*XN(J)*H(KI)*(XL/2.)*C(1,1)
        E=XN(K)*XN(J)*H(KI)*(XL/2.)*C(1,1)
        XMB(K,J) = XMB(K,J)-E*0.2775557561562891 35E-16
        XMC(K,J) = XMC(K,J)+XN(K)*XN(J)*H(KI)*(XL/2.)*(C(2,2)+C(3,3))
3       CONTINUE
 2      CONTINUE
        XMASS(3,5) = XMA(1,1)
        XMASS(3,6) = XMA(1,2)
        XMASS(3,17) = XMA(1,3)
        XMASS(3,18) = XMA(1,4)
        XMASS(4,5) = XMA(2,1)
        XMASS(4,6) = XMA(2,2)
        XMASS(4,17) = XMA(2,3)
        XMASS(4,18) = XMA(2,4)
        XMASS(5,15) = XMA(3,1)
        XMASS(6,15) = XMA(3,2)
        XMASS(15,17) = XMA(3,3)
        XMASS(15,18) = XMA(3,4)
        XMASS(5,16) = XMA(4,1)
        XMASS(6,16) = XMA(4,2)
        XMASS(16,17) = XMA(4,3)
        XMASS(16,18) = XMA(4,4)
        XMASS(5,5) = XMA(1,1)
        XMASS(5,6) = XMA(1,2)
        XMASS(5,17) = XMA(1,3)
        XMASS(5,18) = XMA(1,4)
        XMASS(6,6) = XMA(2,2)
        XMASS(6,17) = XMA(2,3)
        XMASS(6,18) = XMA(2,4)
        XMASS(17,17) = XMA(3,3)
        XMASS(17,18) = XMA(3,4)
        XMASS(18,18) = XMA(4,4)
        XMASS(3,3) = XMA(1,1)
        XMASS(3,4) = XMA(1,2)
        XMASS(3,15) = XMA(1,3)
        XMASS(3,16) = XMA(1,4)
```

```
      XMASS(4,4) = XMA(2,2)
      XMASS(4,15) = XMA(2,3)
      XMASS(4,16) = XMA(2,4)
      XMASS(15,15) = XMA(3,3)
      XMASS(15,16) = XMA(3,4)
      XMASS(16,16) = XMA(4,4)
      XMASS(1,1) = XMA(1,1)
      XMASS(1,2) = XMA(1,2)
      XMASS(1,13) = XMA(1,3)
      XMASS(1,14) = XMA(1,4)
      XMASS(2,2) = XMA(2,2)
      XMASS(2,13) = XMA(2,3)
      XMASS(2,14) = XMA(2,4)
      XMASS(13,13) = XMA(3,3)
      XMASS(13,14) = XMA(3,4)
      XMASS(14,14) = XMA(4,4)
      XMASS(11,11) = XMA(1,1)
      XMASS(11,12) = XMA(1,2)
      XMASS(11,23) = XMA(1,3)
      XMASS(11,24) = XMA(1,4)
      XMASS(12,12) = XMA(2,2)
      XMASS(12,23) = XMA(2,3)
      XMASS(12,24) = XMA(2,4)
      XMASS(23,23) = XMA(3,3)
      XMASS(23,24) = XMA(3,4)
      XMASS(24,24) = XMA(4,4)
C
C       *******  FOLLOWING FOR CG OFFSET COUPLING *******
C
      XMASS(3,7)=XMB(1,1)
      XMASS(3,8)=XMB(1,2)
      XMASS(3,19)=XMB(1,3)
      XMASS(3,20)=XMB(1,4)
      XMASS(4,7)=XMB(2,1)
      XMASS(4,8)=XMB(2,2)
      XMASS(4,19)=XMB(2,3)
      XMASS(4,20)=XMB(2,4)
      XMASS(5,7)=XMB(1,1)
      XMASS(5,8)=XMB(1,2)
      XMASS(5,19)=XMB(1,3)
      XMASS(5,20)=XMB(1,4)
      XMASS(6,7)=XMB(2,1)
      XMASS(6,8)=XMB(2,2)
      XMASS(6,19)=XMB(2,3)
      XMASS(6,20)=XMB(2,4)
      XMASS(7,15)=XMB(1,3)
      XMASS(7,16)=XMB(1,4)
      XMASS(7,17)=XMB(1,3)
      XMASS(7,18)=XMB(1,4)
      XMASS(8,15)=XMB(2,3)
      XMASS(8,16)=XMB(2,4)
      XMASS(8,17)=XMB(2,3)
      XMASS(8,18)=XMB(2,4)
      XMASS(15,19)=XMB(3,3)
      XMASS(15,20)=XMB(3,4)
      XMASS(16,19)=XMB(3,4)
      XMASS(16,20)=XMB(4,4)
      XMASS(17,19)=XMB(3,3)
      XMASS(17,20)=XMB(3,4)
      XMASS(18,19)=XMB(3,4)
      XMASS(18,20)=XMB(4,4)
C
      XMASS(7,7) = XMC(1,1)
      XMASS(7,8) = XMC(1,2)
      XMASS(7,19) = XMC(1,3)
      XMASS(7,20) = XMC(1,4)
      XMASS(8,8) = XMC(2,2)
```

```
        XMASS(8,19) = XMC(2,3)
        XMASS(8,20) = XMC(2,4)
        XMASS(19,19) = XMC(3,3)
        XMASS(19,20) = XMC(3,4)
        XMASS(20,20) = XMC(4,4)
        DO 6 I = 1,24
        DO 6 J = 1,24
        XMASS(J,I) = XMASS(I,J)
6       CONTINUE
C
C    ****  COORD TRANSF.   *******
C
       CALL TMATR(XL,TX)
        DO 10 I = 1,24
        DO 10 J = 1,24
 10     XMASS(I,J) = TX(I)*XMASS(I,J)*TX(J)
        RETURN
        END
C
C*********************************************************************
C
C    SUBROUTINE TGLOB -  THIS SUBROUTINE CREATES THE TRANSFORMATION
C                        MATRIX  T1X TO TRANSFORM THE STIFFNESS MATRIX
C                        FROM LOCAL COORDINATE SYSTEM TO GLOBAL
C                        COORDINATE SYSTEM
C
       SUBROUTINE TGLOB(DV,DW,TAU,T1X)
       IMPLICIT DOUBLE PRECISION (A-H,O-Z)
       DIMENSION T1X(24,24),T2X(12,12)
       REAL*8 DV,DW,TAU,A,B,C
       A=DV**2
       B=DW**2
       C=TAU**2
       DO 10 I=1,12
         DO 10 J=1,12
 10      T2X(I,J)=0.0
         DO 20 I=1,24
           DO 20 J=1,24
 20    T1X(I,J)=0.0
C
C
       T2X(1,1)=1.0-A/2.0-B/2.0
       D1=T2X(1,1)
       T2X(1,3)=DW
       D3=T2X(1,3)
       T2X(1,11)=DV
       D2=T2X(1,11)
       T2X(3,1)=DV*TAU-DW
       D7=T2X(3,1)
       T2X(3,3)=1.0-B/2.0-C/2.0
       D9=T2X(3,3)
       T2X(3,11)=-TAU-DV*DW/2.0
       D8=T2X(3,11)
       T2X(4,2)=-DV-DW*TAU
       D4=T2X(4,2)
       T2X(4,4)=1.0-A/2.0-C/2.0
       D5=T2X(4,4)
       T2X(11,3)=TAU-DV*DW/2.0
       D6=T2X(11,3)
C
C
       T2X(1,5)=D3
       T2X(2,2)=D1
       T2X(2,4)=D2
       T2X(2,6)=D2
       T2X(2,12)=D3
       T2X(4,7)=D4
```

```
      T2X(4,12)=D6
      T2X(5,5)=D9
      T2X(6,6)=D5
      T2X(7,7)=D1
      T2X(7,9)=D3
      T2X(8,8)=D1
      T2X(8,10)=D2
      T2X(9,7)=D7
      T2X(9,9)=D9
      T2X(10,8)=D4
      T2X(10,10)=D5
      T2X(11,1)=D4
      T2X(11,5)=D6
      T2X(11,11)=D5
      T2X(12,2)=D7
      T2X(12,4)=D8
      T2X(12,6)=D8
      T2X(12,12)=D9
C
      DO 30 I=1,12
        DO 30 J=1,12
      T1X(I,J)=T2X(I,J)
 30   T1X(I+12,J+12)=T2X(I,J)
      RETURN
      END
C
C
      SUBROUTINE TRASF(XMAT,T1X)
      IMPLICIT DOUBLE PRECISION (A-H,O-Z)
      DIMENSION XMAT(24,24),T1X(24,24),XGMAT(24,24)
C
C  *******    TRANSF. FROM ELEMENT TO GLOBAL COORD. SYSTEM   ******
C
      DO 10 I=1,24
       DO 10 J=1,24
         XGMAT(I,J)=0.0
            DO 10 K=1,24
  10           XGMAT(I,J)=XGMAT(I,J)+XMAT(I,K)*T1X(K,J)
      DO 20 I=1,24
       DO 20 J=1,24
           XMAT(I,J)=0.0
              DO 20 K=1,24
  20            XMAT(I,J)=XMAT(I,J)+T1X(K,I)*XGMAT(K,J)
C
      RETURN
      END
C
C*********************************************************************
C
      SUBROUTINE QSTIFF(E1,E2,V12,G12,THETA,QRTRNS)
        IMPLICIT DOUBLE PRECISION (A-H,O-Z)
C*
C*    INPUT:  E1,E2,V12,G12,THETA     ENGINEERING CONSTANTS
C*    OUTPUT: QR(3,3)     --- REDUCED STIFFNESS MATRIX USING INPUT
C*            QRTRNS(3,3) --- TRANSFORMED REDUCED STIFFNESS AT THETA
C*
      DIMENSION  QR(3,3), QRTRNS(3,3)
C*
C* INITIALIZE MATRICES
C*
      DO 1110 I=1,3
        DO 1110 J=1,3
          QR(I,J)=0.0
 1110 QRTRNS(I,J)=0.0
C*
      S11 = 1./E1
      S12 = -V12/E1
```

```
      S22 = 1./E2
      S66 = 1./G12
C*
C*
C*****************  REDUCED STIFFNESS MATRIX  ***************************
C*
C*
      QDENOM = S11*S22 - S12*S12
      QR(1,1) = S22/QDENOM
      QR(1,2) = -(S12/QDENOM)
      QR(2,1) = QR(1,2)
      QR(2,2) = S11/QDENOM
      QR(3,3) = 1./S66
C*
      THETAR = THETA * 3.14159265 / 180.
      SIN1 = SIN(THETAR)
      SIN2 = SIN1 * SIN1
      SIN3 = SIN1 * SIN2
      SIN4 = SIN1 * SIN3
      COS1 = COS(THETAR)
      COS2 = COS1 * COS1
      COS3 = COS1 * COS2
      COS4 = COS1 * COS3
C*
C***********  TRANSFORMED REDUCED STIFFNESS MATRIX  ***********************
C*
      QRTRNS(1,1) = QR(1,1)*COS4 + 2.*(QR(1,2) + 2.*QR(3,3))*SIN2*COS2 +
     1              QR(2,2)*SIN4
      QRTRNS(1,2) = (QR(1,1) + QR(2,2) - 4.*QR(3,3))*SIN2*COS2 +
     1              QR(1,2)*(SIN4 + COS4)
      QRTRNS(2,2) = QR(1,1)*SIN4 + 2.*(QR(1,2) + 2.*QR(3,3))*SIN2*COS2 +
     1              QR(2,2)*COS4
      QRTRNS(1,3) = (QR(1,1) - QR(1,2) - 2.*QR(3,3))*SIN1*COS3 +
     1              (QR(1,2) - QR(2,2) + 2.*QR(3,3))*SIN3*COS1
      QRTRNS(2,3) = (QR(1,1) - QR(1,2) - 2.*QR(3,3))*SIN3*COS1 +
     1              (QR(1,2) - QR(2,2) + 2.*QR(3,3))*SIN1*COS3
      QRTRNS(3,3) = (QR(1,1) + QR(2,2) - 2.*QR(1,2) - 2.*QR(3,3))*
     1              SIN2*COS2 + QR(3,3)*(SIN4 + COS4)
      QRTRNS(2,1) = QRTRNS(1,2)
      QRTRNS(3,1) = QRTRNS(1,3)
      QRTRNS(3,2) = QRTRNS(2,3)
      RETURN
      END
C
C*******************************************************************************
C
       SUBROUTINE MULT(X,Y,M,K,N,XM)
        IMPLICIT DOUBLE PRECISION (A-H,O-Z)
C
C   THIS SUBROUTINE CALCULATES THE PRODUCT OF TWO MATRICES.
C
       DIMENSION X(M,K),Y(K,N),XM(M,N)
       DO 2 I = 1,M
       DO 2 J = 1,N
       XM(I,J) = 0.0D0
       DO 2 L = 1,K
       XM(I,J) = X(I,L)*Y(L,J)+XM(I,J)
 2     CONTINUE
       RETURN
       END
C
C*******************************************************************************
C
       SUBROUTINE ADD(X,Y,M,N,XY)
        IMPLICIT DOUBLE PRECISION (A-H,O-Z)
C
```

```
C   THIS SUBROUTINE PERFORMS MATRIX ADDITION
C
      DIMENSION X(M,N),Y(M,N),XY(M,N)
      DO 1 I = 1,M
      DO 1 J = 1,M
      XY(I,J) = X(I,J)+Y(I,J)
1     CONTINUE
      RETURN
      END
C
      SUBROUTINE SORT(NORD,EIG,ITEM)
       IMPLICIT DOUBLE PRECISION (A-H,O-Z)
C
C     THIS SUBROUTINE REARRANGES THE EIGENVALUES IN INCREASING ORDER OF
C     MAGNITUDE
C
      DIMENSION EIG(100),ITEM(100)
      XMIN = 0.0
      DO 62 I = 1,NORD
      XMAX = 1.0E+60
      DO 63 J = 1,NORD
      TEIG = EIG(J)
      IF(TEIG.LE.XMIN)GOTO 63
      IF(TEIG.GT.XMAX)GOTO 63
      ITEM(I)=J
      XMAX = TEIG
63    CONTINUE
      XMIN = XMAX
62    CONTINUE
      RETURN
      END
C
C
      SUBROUTINE AERO(K,M,NEL,NORD,GDOF,RAIR,RFR,STEP,IT,L
     $,BE,AE,CG,SW,NMOD,AC,CLA)
      IMPLICIT DOUBLE PRECISION (A-H,O-Z)
      REAL*8  L(10),K(100,100),M(100,100),T1X(24,24),
     1     AE(10),BE(10),RFR,RW(200),SW(10),STEP,RAIR,
     2     CG(10),PI,RA(100,100),BETA(100),
     3     FREQ(100),DAMP(100),AC(10),CLA(10),REFR(100)
      COMPLEX*16 A(100,100),F(100,100),B(100,100),CK(100,100),W(100),
     1        ALFA(100),EIGB(100)
      INTEGER NEL,NORD,GDOF(10,12),ITEM(100)
      PI=4.*ATAN(1.)
      IF (ABS(BE(NEL+1)-BE(NEL)).LT.(BE(NEL)/1000)) BE(NEL+1)=BE(NEL)
      IDIV=1
      CALL CASSEM(RAIR,A,NEL,NORD,3,L,AE,BE,RFR,SW,IDIV,GDOF,AC,CLA)
      DO 711 I=1,NORD
        DO 711 J=1,NORD
          RA(I,J) =REAL(A(I,J))
 711  CK(I,J)=K(I,J)
C     CALL DGVLRG(NORD,K,100,RA,100,ALFA,BETA)
C     SUP=REAL(BETA(1)/ALFA(1))
C     DO 41 I=2,NORD
C       EV=BETA(I)/ALFA(I)
C       SP=REAL(BETA(I)/ALFA(I))
C41   IF(SP.GT.SUP) SUP=SP
C     IF(SUP.LE.0.) THEN
C       WRITE(7,81)
C     ELSE
C         WRITE(7,51)  1/SQRT(SUP)
C       END IF
C51     FORMAT(/,' DIVERGENCE SPEED: ',F10.2)
C81   FORMAT(/,'  ***  NO DIVERGENCE  ***',/)
      IDIV=0
C
```

```
C     ************** DIVERGENCE FROM THE V-G METHOD  **********
C
      RFR=0.000001
        CALL CASSEM(RAIR,A,NEL,NORD,3,L,AE,BE,RFR,SW,IDIV,GDOF,AC,CLA)
        DO 87 I=1,NORD
          DO 87 J=1,NORD
 87     B(I,J)=M(I,J)+A(I,J)
        CALL DGVLCG(NORD,CK,100,B,100,ALFA,EIGB)
        DO 103 I=1,NORD
          RZ=REAL(EIGB(I)/ALFA(I))
          CZ=REAL((0.,-1.)*EIGB(I)/ALFA(I))
          IF (RZ.LE.0.) THEN
              FREQ(I)=-55.
              DAMP(I)=-55.
              GOTO 103
          ELSE
            FREQ(I)=1/SQRT(RZ)
            DAMP(I)=CZ/RZ
          END IF
 103      CONTINUE
CC  REARRANGE FREQUENCIES IN INCREASING ORDER OF MAGNITUDE
       CALL SORT(NORD,FREQ,ITEM)
       I = ITEM(1)
       FREQS = FREQ(I)
       DAMPS = DAMP(I)
       SPEED=FREQS*BE(1)/RFR
      WRITE(7,151) SPEED
151     FORMAT(/,' DIVERGENCE SPEED (V-G): ',F10.2,/)
      WRITE(7,*)
      IFL=0
 111  WRITE(7,*)
      WRITE(7,*)'DO YOU WANT AN AUTOMATIC SEARCH (0/1, 2 TO QUIT)'
      READ(7,*) ISER
      IF (ISER.EQ.2) RETURN
      IF (ISER.EQ.1) THEN
        IF (IFL.EQ.1) THEN
          WRITE(7,*)' SAME MODE (0/1)'
          READ (7,*) ISMM
          IF (ISMM.EQ.1) THEN
            RFR=RFR+STEP
            STEP=STEP/10.
            IT=11
            IFL=0
            GOTO 113
          ELSE
            IFL=0
            GOTO 114
          END IF
        END IF
 114     WRITE(7,*)' ENTER INITIAL REDUCED FREQUENCY, STEP SIZE, NUMBER'
          WRITE(7,*)' OF ITERATIONS AND MODE NUMBER'
          READ (7,*) RFR, STEP, IT,NMSC
      ELSE
        IFL=0
      WRITE(7,*)' ENTER INITIAL REDUCED FREQUENCY, STEP SIZE AND NUMBER'
      WRITE(7,*)' OF ITERATIONS'
        READ (7,*) RFR, STEP, IT
      END IF
 113  DO 60 KI=1,IT
        IF (ISER.NE.1) WRITE(7,50) RFR
        CALL CASSEM(RAIR,A,NEL,NORD,3,L,AE,BE,RFR,SW,IDIV,GDOF,AC,CLA)
        DO 80 I=1,NORD
          DO 80 J=1,NORD
 80     B(I,J)=M(I,J)+A(I,J)
        CALL DGVLCG(NORD,CK,100,B,100,ALFA,EIGB)
        DO 100 I=1,NORD
          RZ=REAL(EIGB(I)/ALFA(I))
```

```
          CZ=REAL((0.,-1.)*EIGB(I)/ALFA(I))
          IF (RZ.LE.0.) THEN
              FREQ(I)=-55.
              DAMP(I)=-55.
              GOTO 100
          ELSE
            FREQ(I)=1/SQRT(RZ)
            DAMP(I)=CZ/RZ
          END IF
 100      CONTINUE
CC  REARRANGE FREQUENCIES IN INCREASING ORDER OF MAGNITUDE
       CALL SORT(NORD,FREQ,ITEM)
      IF (ISER.EQ.1) THEN
        I=ITEM(NMSC)
        IF (DAMP(I).GT.0.0) THEN
          IFL=1
          FREQS = FREQ(I)
          DAMPS = DAMP(I)
          SPEED=FREQS*BE(1)/RFR
          WRITE(7,50) RFR
          WRITE(7,110) NMSC,SPEED,DAMPS,FREQS
          GOTO 111
        ELSE
          GOTO 60
        END IF
      ELSE
        DO 64 L1 = 1,NMOD
          I = ITEM(L1)
          FREQS = FREQ(I)
          DAMPS = DAMP(I)
          SPEED=FREQS*BE(1)/RFR
 64     WRITE(7,110) L1,SPEED,DAMPS,FREQS
        WRITE(7,*)
      END IF
 60   RFR=RFR-STEP
      IF ((ISER.EQ.1).AND.(IFL.EQ.0)) THEN
        RFR=RFR+STEP
        I = ITEM(NMSC)
        FREQS = FREQ(I)
        DAMPS = DAMP(I)
        SPEED=FREQS*BE(1)/RFR
        WRITE(7,50) RFR
        WRITE(7,110) NMSC,SPEED,DAMPS,FREQS
      END IF
      GOTO 111
 20   FORMAT(/,'NODE         V          DV/DX          TWIST',/)
 50   FORMAT (/,'  MODE        SPEED          DAMPING       FREQUENCY
     &K=',F8.6,/)
C70   FORMAT(/,'                          REDUCED FREQUENCY RFR=',E10.4,/)
 110  FORMAT(2X,I3,6X,E10.4,4X,E10.4,4X,E10.4)
      END
C
      SUBROUTINE GAUSS(QA,QB,QD,QE,QF,QG,QH,L,BF,BI,BR,RFK)
        IMPLICIT DOUBLE PRECISION (A-H,O-Z)
      DIMENSION H(5),X(5)
      REAL*8 L,U,CO(8,5),BO(4,5),BF,BI,RFK
      COMPLEX*16 QA(12,12,3),QB(12,12,5),QD(12,12,5),
     1QE(12,12,3),QF(12,12,3),QG(12,12,3),QH(12,12,3),
     2Q(4,8,8),QI(12,24,7),C,CK(2,5)
      DATA H(1),H(2),H(3),H(4),H(5),X(1),X(2),X(3),X(4),X(5)/
     1.5688888889,.4786286705,.4786286705,.2369268851,
     2.2369268851,0.,.5384693101,-.5384693101,.9061798459,-.9061798459/
      DO 10 K=1,5
        U=X(K)
        CO(1,K)=(2-3*U+U**3)/4
        CO(2,K)=(U**3-U**2-U+1)*L/8
        CO(3,K)=(2+3*U-U**3)/4
```

```
      CO(4,K)=(U**3+U**2-U-1)*L/8
      CO(5,K)=3*(U**2-1)/(2*L)
      CO(6,K)=(3*U**2-2*U-1)/4
      CO(7,K)=-CO(5,K)
      CO(8,K)=(3*U**2+2*U-1)/4
      BO(1,K)=(BF-BI)*U/2+(BF+BI)/2
      BO(2,K)=BO(1,K)**2
      BO(3,K)=BO(1,K)**3
      BO(4,K)=BO(1,K)**4
      CK(1,K)=1.
      RF=RFK*BO(1,K)/BR
      C=1.+10.61*RFK*BO(1,K)*(0.,1.)/BR
      C=C*(1.+1.774*RFK*BO(1,K)*(0.,1.)/BR)
      C=C/(1.+13.51*RFK*BO(1,K)*(0.,1.)/BR)
 10   CK(2,K)=C/(1.+2.745*RFK*BO(1,K)*(0.,1.)/BR)
      DO 20 I=1,4
        DO 20 J=1,8
          DO 20 M=1,4
          Q(I,J,M)=0.0
          Q(I,J,M+4)=0.0
          DO 20 K=1,5
      Q(I,J,M)=Q(I,J,M)+L*H(K)*CO(I,K)*CO(J,K)*BO(M,K)*CK(1,K)/2
 20   Q(I,J,M+4)=Q(I,J,M+4)+L*H(K)*CO(I,K)*CO(J,K)*BO(M,K)*CK(2,K)/2
      DO 21 I=1,12
        DO 21 J=1,24
          DO 21 M=1,7
 21   QI(I,J,M)=0.0
      DO 110 M=1,7
        DO 110 I=1,3
          DO 110 J=1,3
            DO 110 K=1,4
              DO 110 IA=1,2
                DO 110 JA=1,2
                  DO 110 KA=1,2
110     QI(IA+2*(I-1)+6*(KA-1),JA+2*(J-1)+(K-1)*6,M)=Q(IA+(KA-1)*2,
     XJA+(K-1)*2,M)
        DO 30 I=1,12
          DO 30 J=1,12
            QA(I,J,1)=QI(I,J,1)
            QA(I,J,2)=QI(I,J,2)
            QA(I,J,3)=QI(I,J,5)
            DO 100 M=1,5
              QB(I,J,M)=0.
100         QD(I,J,M)=0.0
            QE(I,J,1)=QI(I,J+12,1)
            QE(I,J,2)=QI(I,J+12,2)
            QE(I,J,3)=QI(I,J+12,5)
            DO 30 M=1,3
            QF(I,J,M)=0.
            QG(I,J,M)=0.
30      QH(I,J,M)=0.
        DO 40 I=1,12
          DO 40 M=1,3
            QA(I,5,M)=0.
            QA(I,6,M)=0.
            QA(I,11,M)=0.
            QA(I,12,M)=0.
            QE(I,5,M)=0.
            QE(I,6,M)=0.
            QE(I,11,M)=0.
40          QE(I,12,M)=0.
        DO 50 J=1,12
          DO 50 M=1,3
            QA(5,J,M)=0.
            QA(6,J,M)=0.
            QA(11,J,M)=0.
            QA(12,J,M)=0.
```

```
            QE(5,J,M)=0.
            QE(6,J,M)=0.
            QE(11,J,M)=0.
 50       QE(12,J,M)=0.
        DO 60 I=1,10
          DO 60 K=1,2
            DO 60 KA=1,2
              DO 160 M=1,3
              QB(I,4+K+(KA-1)*6,M)=QI(I,4+K+(KA-1)*6,M)
              QB(5,4+K+(KA-1)*6,M)=0.0
 160          QB(6,4+K+(KA-1)*6,M)=0.0
              DO 170 M=4,5
              QB(I,4+K+(KA-1)*6,M)=QI(I,4+K+(KA-1)*6,M+1)
              QB(5,4+K+(KA-1)*6,M)=0.0
 170          QB(6,4+K+(KA-1)*6,M)=0.0
        QF(I,4+K+(KA-1)*6,1)=QI(I,4+K+(KA+1)*6,2)
        QF(I,4+K+(KA-1)*6,2)=QI(I,4+K+(KA+1)*6,3)
        QF(I,4+K+(KA-1)*6,3)=QI(I,4+K+(KA+1)*6,6)
        DO 60 M=1,3
              QF(5,4+K+(KA-1)*6,M)=0.0
 60           QF(6,4+K+(KA-1)*6,M)=0.0
        DO 70 K=1,2
          DO 70 KA=1,2
            DO 71 J=1,10
              QG(4+K+(KA-1)*6,J,1)=QI(4+K+(KA-1)*6,J+12,2)
              QG(4+K+(KA-1)*6,J,2)=QI(4+K+(KA-1)*6,J+12,3)
 71           QG(4+K+(KA-1)*6,J,3)=QI(4+K+(KA-1)*6,J+12,6)
            DO 72 M=1,3
              QG(4+K+(KA-1)*6,5,M)=0.0
 72           QG(4+K+(KA-1)*6,6,M)=0.0
 70     CONTINUE
        DO 120 I=5,6
          DO 120 J=5,6
            DO 120 K=1,2
              DO 120 KA=1,2
              DO 180 M=1,3
 180          QD(I+(K-1)*6,J+(KA-1)*6,M)=QI(I+(K-1)*6,J+(KA-1)*6,M+1)
              DO 190 M=4,5
 190          QD(I+(K-1)*6,J+(KA-1)*6,M)=QI(I+(K-1)*6,J+(KA-1)*6,M+2)
        QH(I+(K-1)*6,J+(KA-1)*6,1)=QI(I+(K-1)*6,J+(KA+1)*6,3)
        QH(I+(K-1)*6,J+(KA-1)*6,2)=QI(I+(K-1)*6,J+(KA+1)*6,4)
 120    QH(I+(K-1)*6,J+(KA-1)*6,3)=QI(I+(K-1)*6,J+(KA+1)*6,7)
      RETURN
      END
C
      SUBROUTINE CASSEM(RAIR,T,NE,NORD,IM,L,AE,BE,RFR,SW,IDIV,GDOF,AC,
     &                  CLA)
      IMPLICIT DOUBLE PRECISION (A-H,O-Z)
      COMPLEX*16 T(100,100),ELA(24,24),ELEA(12,12)
      REAL*8 AE(10),BE(10),L(10),RFR,TIX(24,24),AC(10),CLA(10),
     1 RAIR,SW(10)
      INTEGER GDOF(10,12),LM(24)
      DO 10 I=1,NORD
        DO 10 J=1,NORD
 10   T(I,J)=0.0
       DO 17 IK = 1,NE
         CALL ELAE(ELEA,AE(IK),BE(IK),BE(IK+1),BE(1),L(IK),RFR,RAIR,
     1   SW(IK),IDIV,AC(IK),CLA(IK))
         DO 20 I=1,24
            DO 20 J=1,24
 20           ELA(I,J)=0.0
         DO 30 I=1,6
            DO 30 J=1,6
              ELA(I+2,J+2)=ELA(I+2,J+2)+ELEA(I,J)
              ELA(I+2,J+14)=ELA(I+2,J+14)+ELEA(I,J+6)
              ELA(I+14,J+2)=ELA(I+14,J+2)+ELEA(I+6,J)
```

```
  30          ELA(I+14,J+14)=ELA(I+14,J+14)+ELEA(I+6,J+6)
C        CALL TGLOB(SW,T1X,IK)
C       CALL CTRASF(ELA,T1X)
        DO 2 K = IK,IK+1
        DO 2 J = 1,12
        N=J
        IF(K.EQ.IK+1)N=J+12
        LM(N) = GDOF(K,J)
 2      CONTINUE
        DO 4 II = 1,24
        IDOF = LM(II)
        IF(IDOF.EQ.0)GOTO 4
        DO 5 JJ = 1,24
        JDOF = LM(JJ)
        IF(JDOF.EQ.0)GOTO 5
        T(IDOF,JDOF) = T(IDOF,JDOF)+ELA(II,JJ)
 5      CONTINUE
 4      CONTINUE
 17     CONTINUE
       RETURN
       END
C
       SUBROUTINE DESIGN (NEL,NLAYER,T,THETA,IDV1,IDV2,
      &DEVAR,ISPAR)
         IMPLICIT DOUBLE PRECISION (A-H,O-Z)
C
C      ********   THE DESIGN VARIABLES AFFECT THE THICKNESS AND MATERIAL
C      ORIENTATION OF EACH LAYER AND THE THICKNESS OF THE FRONT AND REAR
C      SPARS. THE FINAL VALUES ARE THE SUM OF THE INITIAL VALUE AND THE
C      DESIGN VARIABLE VALUE  ****************************************
C
       DIMENSION T(10,21),THETA(10,21),DEVAR(30)
       INTEGER IDV1(10,21),IDV2(10,21),NLAYER(10),ISPAR(10)
       DO 10 IK=1,NEL
         DO 20 ILA=1,NLAYER(IK)
           IF (ILA.EQ.ISPAR(IK)) GOTO 20
           T(IK,ILA)=T(IK,ILA)+DEVAR(IDV1(IK,ILA))
           THETA(IK,ILA)=THETA(IK,ILA)+DEVAR(IDV2(IK,ILA))
 20      CONTINUE
 10    CONTINUE
       RETURN
       END
C
C
       SUBROUTINE CTRASF(XMAT,T1X)
       IMPLICIT DOUBLE PRECISION (A-H,O-Z)
       COMPLEX*16 XMAT(12,12),X1MAT(14,14),XGMAT(14,14)
       DIMENSION T1X(14,14)
C
C  *******    TRANSF. FROM ELEMENT TO GLOBAL COORD. SYSTEM   ******
C
       DO 10 I=1,14
         DO 10 J=1,14
 10    XGMAT(I,J)=0.0
       DO 20 I=1,6
         DO 20 J=1,6
           XGMAT(I,J)=XMAT(I,J)
 20    XGMAT(I,J+7)=XMAT(I,J+6)
       DO 30 I=7,12
         DO 30 J=1,6
         XGMAT(I+1,J)=XMAT(I,J)
 30    XGMAT(I+1,J+7)=XMAT(I,J+6)
       DO 40 I=1,14
         DO 40 J=1,14
           X1MAT(I,J)=0.0
           DO 50 K=1,14
 50    X1MAT(I,J)=X1MAT(I,J)+XGMAT(I,K)*T1X(K,J)
```

```
 40   CONTINUE
      DO 60 I=1,14
        DO 60 J=1,14
          XGMAT(I,J)=0.0
          DO 70 K=1,14
 70       XGMAT(I,J)=XGMAT(I,J)+T1X(K,I)*X1MAT(K,J)
 60   CONTINUE
      DO 80 I=1,6
        DO 80 J=1,6
          XMAT(I,J)=XGMAT(I,J)
 80   XMAT(I,J+6)=XGMAT(I,J+7)
      DO 90 I=7,12
        DO 90 J=1,6
        XMAT(I,J)=XGMAT(I+1,J)
 90   XMAT(I,J+6)=XGMAT(I+1,J+7)
      RETURN
      END
C
      SUBROUTINE SECT (ZA,ZW,ZSW,ZSX,ZSY,ZIXY,ZIXX,ZIYY,ZIWX,ZIWY,ZIWW,
     &ZHS,ZHC,ZHQ,ZHPHI,ZJG,ZRP2,ZZKY,ZZKX,ZZKW,IEBRAN,ISBRAN,IC,ISO,
     &XNODE,YNODE,CA11,CA16,CA66,CD11,CD16,CD66,TT2,GAM,ZTA,CK15,
     &ANG1,ZWC,ZW1,Z5,Z6,ZS,ZCJJ,NUMEL,IJUNCT,XP,YP,ZCT,XCO,YCO)
        IMPLICIT DOUBLE PRECISION (A-H,O-Z)
      DIMENSION IEBRAN(8),ISBRAN(8),XNODE(8,2),YNODE(8,2),ZWC(8),
     &ZW1(8),Z5(8),Z6(8),ZS(8),ZCJJ(8),ANG1(8),ZCT(8),R(8)
      DIMENSION TT2(8),CA11(8),CA16(8),CA66(8),CD11(8),CD16(8),
     &          CD66(8)
CC    SUBROUTINE TO EVALUATE SECTION PROPERTIES
CC
      ZC1=0.0
      ZC2=0.0
      ZA=0.0000000
      ZSX=0.0000000
      ZSY=0.0000000
      ZSW=0.0000000
      ZIXY=0.0000000
      ZIXX=0.0000000
      ZIYY=0.0000000
      ZIWX=0.0000000
      ZIWY=0.0000000
      ZIWW=0.0000000
      ZJG=0.0000000
      ZHS=0.0000000
      ZHC=0.0000000
      ZHQ=0.0000000
      ZHPHI=0.0000000
      ZRP2=0.0000000
      ZZKY=0.0000000
      ZZKX=0.0000000
      ZZKW=0.0000000
CC
CC  **********  FOLLOWING FOR CLOSED SECTION ANALYSIS   *********
CC
      CHC=0.0
      CHS=0.0
      CHQ=0.0
      CK15=0.0
      CJG=0.0
      CSW=0.0
      CIWX=0.0
      CIWY=0.0
      CHQ1=0.0
      C1WW=0.0
      C2WW=0.0
      C11W=0.0
CC
      PI=ARCOS(-1.)
```

```
      PI2=2.*PI
      PIF=PI/2.
      DO 100 L1=1,NUMEL
CC
      TT1=TT2(L1)
      QA11=CA11(L1)
      QA16=CA16(L1)
      QA66=CA66(L1)
      QD11=CD11(L1)
      QD16=CD16(L1)
      QD66=CD66(L1)
      X1=XNODE(L1,1)
      Y1=YNODE(L1,1)
      X2=XNODE(L1,2)
      Y2=YNODE(L1,2)
      ZCJJ(L1)=((X1-X2)*(X1-X2)+(Y1-Y2)*(Y1-Y2))**.5/2.
CC
      CALL VNGDI (X2,Y2,X1,Y1,ANG1(L1))
CC
      CALL VECTA (X1,Y1,X2,Y2,Z5,Z6,XP,YP,L1)
      ZS(L1)=2.*ZCJJ(L1)*TT1
CC
CC  **********  FOLLOWING FOR CLOSED SECTION ANALYSIS   *********
CC
      IF (L1.NE.1) C11W=C11W+R(L1-1)*(ZC2-ZC1)
      ZC1=ZC2
      ZC2=ZC1+2.*ZCJJ(L1)
CC
      ZYS=ZCJJ(L1)*(X1+X2)*TT1
      ZXS=ZCJJ(L1)*(Y1+Y2)*TT1
      ZXYS=ZCJJ(L1)*(2.*X1*Y1+2.*X2*Y2+X1*Y2+X2*Y1)/3.*TT1
      ZYYS=2.*ZCJJ(L1)*(X1*X1+X2*X2+X1*X2)/3.*TT1
      ZXXS=2.*ZCJJ(L1)*(Y1*Y1+Y2*Y2+Y1*Y2)/3.*TT1
      ZA=ZA+QA11*ZS(L1)
      ZSX=ZSX+QA11*ZXS
      ZSY=ZSY+QA11*ZYS
CC
CC  **********  FOLLOWING FOR CLOSED SECTION ANALYSIS   *********
CC
      CK15=CK15+QA16*ZS(L1)
      CJG=CJG+QA66*ZS(L1)
      CHC=CHC+QA16*ZXS
      CHS=CHS+QA16*ZYS
      CSW=CSW+QA11*(ZC2**2-ZC1**2)*TT1/2.
      CHQ1=CHQ1+QA16*(ZC2**2-ZC1**2)*TT1/2.
      CIWX=CIWX+QA11*TT1*(Y1*(ZC2**2-ZC1**2)/2.+(Y2-Y1)*(2.*ZC2**3
     &-3.*ZC1*ZC2**2+ZC1**3)/(6.*(ZC2-ZC1)))
      CIWY=CIWY+QA11*TT1*(X1*(ZC2**2-ZC1**2)/2.+(X2-X1)*(2.*ZC2**3
     &-3.*ZC1*ZC2**2+ZC1**3)/(6.*(ZC2-ZC1)))
      CALL CALCR(X1,Y1,X2,Y2,XP,YP,R(L1))
      C1WW=C1WW+QA11*TT1*(C11W*(ZC2**2-ZC1**2)/2.
     &+R(L1)*(2.*ZC2**3-3.*ZC1*ZC2**2+ZC1**3)/6.)
      C2WW=C2WW+QA11*TT1*(ZC2**3-ZC1**3)/3.
CC
      ZIXY=ZIXY+QA11*ZXYS-
     &QD11*SIN(ANG1(L1))*COS(ANG1(L1))*ZS(L1)*TT1*TT1
      ZIXX=ZIXX+QA11*ZXXS+
     &QD11*COS(ANG1(L1))*COS(ANG1(L1))*ZS(L1)*TT1*TT1
      ZIYY=ZIYY+QA11*ZYYS+
     &QD11*SIN(ANG1(L1))*SIN(ANG1(L1))*ZS(L1)*TT1*TT1
      ZHS=ZHS+2.*QD16*SIN(ANG1(L1))*ZS(L1)*TT1*TT1
      ZHC=ZHC+2.*QD16*COS(ANG1(L1))*ZS(L1)*TT1*TT1
      ZJG=ZJG+4.*QD66*ZS(L1)*TT1*TT1
CC    ZC1=ZC2
 100  CONTINUE
      RETURN
```

```
      END
CC
      SUBROUTINE VECTA (X1,Y1,X2,Y2,Z5,Z6,XP,YP,N1)
        IMPLICIT DOUBLE PRECISION (A-H,O-Z)
      DIMENSION Z5(8),Z6(8)
CC    CHECK FOR COINCIDENCE
      IF ((ABS(XP-X1).LT.0.00001).AND.(ABS(YP-Y1).LT.0.00001)) GOTO 120
 100  IF ((ABS(XP-X2).LT.0.00001).AND.(ABS(YP-Y2).LT.0.00001)) GOTO 120
 110  CALL VNGDI (X1,Y1,XP,YP,ANG0)
      CALL VNGDI (X2,Y2,XP,YP,ANG00)
      DANG=ABS(ANG0-ANG00)
CC    CHECK FOR COLLINEARITY
      IF (DANG.LT.0.005) GOTO 120
      IF (DANG.GT.3.13659265.AND.DANG.LT.3.14659265) GOTO 120
      Z5(N1) =(X1-XP)*((Y1+Y2)/2.-YP)-(Y1-YP)*((X1+X2)/2.-XP)
      Z6(N1)=(X1-XP)*((-Y1+Y2)/2.)-(Y1-YP)*((-X1+X2)/2.)
      GOTO 130
 120  Z5(N1) =0.00000000
      Z6(N1)=0.00000000
 130  CONTINUE
      RETURN
      END
CC
CC
      SUBROUTINE VNGDI (X,Y,XC,YC,ANG)
        IMPLICIT DOUBLE PRECISION (A-H,O-Z)
 1    FORMAT(1X,'WARNING MESSAGE: SINGULARITY,ARC POINT COINCIDES WITH',
     &' CENTER OF CURVATURE')
      PI=ARCOS(-1.)
      XX=X-XC
      YY=Y-YC
      IF (ABS(XX).LT.0.0001) GOTO 10
      ANG=ATAN(YY/XX)
      IF (ABS(ANG).LT.0.0001) GOTO 30
      IF (ANG.LT.0.) GOTO 20
 40   IF (XX.LT.0.) GOTO 41
 42   ANG=ANG
      GOTO 50
 41   ANG=ANG+PI
      GOTO 50
 30   IF (XX.LT.0.) GOTO 31
 32   ANG=0.
      GOTO 50
 31   ANG=PI
      GOTO 50
 20   IF (XX.LT.0.) GOTO 21
      ANG=ANG+2.*PI
      GOTO 50
 21   ANG=ANG+PI
      GOTO 50
 10   IF (ABS(YY).LT.0.0001) GOTO 13
      IF (YY.LT.0.) GOTO 11
 12   ANG=PI/2.
      GOTO 50
 11   ANG=PI*1.5
      GOTO 50
 13   WRITE(6,1)
 50   RETURN
      END
CC
      SUBROUTINE CALCR(X1,Y1,X2,Y2,XP,YP,R)
        IMPLICIT DOUBLE PRECISION (A-H,O-Z)
      A=X2-X1
      B=Y2-Y1
      C=B*(XP-X1)-A*(YP-Y1)
      DELTA=A**2+B**2
      DX=-B*C/DELTA
```

```
      DY=A*C/DELTA
      R=SQRT(DX**2+DY**2)
CC
CC    *****  TO DETERMINE THE SIGN OF R  *****
CC
      SIG=0.0
      IF (X1.EQ.X2) GOTO 10
      IF (DY.NE.0.0) SIG=A*DY/(ABS(A)*ABS(DY))
      GOTO 20
 10   IF (DX.NE.0.0) SIG=-B*DX/(ABS(B)*ABS(DX))
 20   R=R*SIG
 30   RETURN
      END
C
C
C
      SUBROUTINE INCREM(NEL,IK,KG,XL,RHUB,DENS,OMEGA,A,B,TOTXL)
      IMPLICIT DOUBLE PRECISION(A-H,O-Z)
      REAL*8 OMEGA,LEN,RHUB,DENS,XL
      REAL*8 KG(24,24),KGW1(24,24),KGW2(24,24),KGW3(24,24),
     1KGV1(24,24),KGV2(24,24),KGV3(24,24)
C
C     ASSUME EACH ELEMENT IS OF THE SAME LENGTH.
C
      PREF=DENS*(OMEGA**2)*XL
      RBAR=RHUB/XL
      ELCOV=IK-1
      ANEL=NEL
C
      AREA=A+B*(TOTXL+XL/2.0)
C
      PKG1=-(RBAR+ELCOV)*AREA
      PKG2=-0.5*AREA
      PKG3=AREA*(ELCOV+0.5+RBAR)+A*RBAR*(ANEL-ELCOV-1.0)+
     1     0.5*(A+B*RHUB)*((ANEL**2)-(ELCOV**2)-2.0*ELCOV-1.0)
     2     +XL*B/3.0*((ANEL**3)-((ELCOV+1.0)**3))
C
C
      DO 10 I=1,24
          DO 10 J=1,24
             KG(I,J)=0.0
             KGW1(I,J)=0.0
             KGW2(I,J)=0.0
             KGW3(I,J)=0.0
             KGV1(I,J)=0.0
             KGV2(I,J)=0.0
             KGV3(I,J)=0.0
 10   CONTINUE
C
C
      KGW1(3,3)=0.6
      KGW1(3,4)=0.1*XL
      KGW1(3,15)=-0.6
      KGW1(3,16)=0.0
      KGW1(4,3)=0.1*XL
      KGW1(4,4)=0.0333*(XL**2)
      KGW1(4,15)=-0.1*XL
      KGW1(4,16)=-0.0167*(XL**2)
      KGW1(15,3)=-0.6
      KGW1(15,4)=-0.1*XL
      KGW1(15,15)=0.6
      KGW1(15,16)=0.0
      KGW1(16,3)=0.0
      KGW1(16,4)=-0.0167*(XL**2)
      KGW1(16,15)=0.0
```

```
      KGW1(16,16)=0.1*(XL**2)
C
C
      KGW2(3,3)=0.343
      KGW2(3,4)=0.0714*XL
      KGW2(3,15)=-0.343
      KGW2(3,16)=-0.0286*XL
      KGW2(4,3)=0.0714*XL
      KGW2(4,4)=0.019*(XL**2)
      KGW2(4,15)=-0.0714*XL
      KGW2(4,16)=-0.0143*(XL**2)
      KGW2(15,3)=-0.343
      KGW2(15,4)=-0.0714*XL
      KGW2(15,15)=0.343
      KGW2(15,16)=0.0286*XL
      KGW2(16,3)=-0.0286*XL
      KGW2(16,4)=-0.0143*(XL**2)
      KGW2(16,15)=0.0286*XL
      KGW2(16,16)=0.0857*(XL**2)
C
C
      KGW3(3,3)=1.2
      KGW3(3,4)=0.1*XL
      KGW3(3,15)=-1.2
      KGW3(3,16)=0.1*XL
      KGW3(4,3)=0.1*XL
      KGW3(4,4)=0.13*(XL**2)
      KGW3(4,15)=-0.1*XL
      KGW3(4,16)=-0.03*(XL**2)
      KGW3(15,3)=-1.2
      KGW3(15,4)=-0.1*XL
      KGW3(15,15)=1.2
      KGW3(15,16)=-0.1*XL
      KGW3(16,3)=0.1*XL
      KGW3(16,4)=-0.03*(XL**2)
      KGW3(16,15)=-0.1*XL
      KGW3(16,16)=0.13*(XL**2)
C
C
      KGV1(11,11)=0.6
      KGV1(11,12)=0.1*XL
      KGV1(11,23)=-0.6
      KGV1(11,24)=0.0
      KGV1(12,11)=0.1*XL
      KGV1(12,12)=0.0333*(XL**2)
      KGV1(12,23)=-0.1*XL
      KGV1(12,24)=-0.0167*(XL**2)
      KGV1(23,11)=-0.6
      KGV1(23,12)=-0.1*XL
      KGV1(23,23)=0.6
      KGV1(23,24)=0.0
      KGV1(24,11)=0.0
      KGV1(24,12)=-0.0167*(XL**2)
      KGV1(24,23)=0.0
      KGV1(24,24)=0.1*(XL**2)
C
C
      KGV2(11,11)=0.343
      KGV2(11,12)=0.0714*XL
      KGV2(11,23)=-0.343
      KGV2(11,24)=-0.0286*XL
      KGV2(12,11)=0.0714*XL
      KGV2(12,12)=0.019*(XL**2)
      KGV2(12,23)=-0.0714*XL
      KGV2(12,24)=-0.0143*(XL**2)
      KGV2(23,11)=-0.343
      KGV2(23,12)=-0.0714*XL
```

```
      KGV2(23,23)=0.343
      KGV2(23,24)=0.0286*XL
      KGV2(24,11)=-0.0286*XL
      KGV2(24,12)=-0.0143*(XL**2)
      KGV2(24,23)=0.0286*XL
      KGV2(24,24)=0.0857*(XL**2)
C
C
      KGV3(11,11)=1.2
      KGV3(11,12)=0.1*XL
      KGV3(11,23)=-1.2
      KGV3(11,24)=0.1*XL
      KGV3(12,11)=0.1*XL
      KGV3(12,12)=0.13*(XL**2)
      KGV3(12,23)=-0.1*XL
      KGV3(12,24)=-0.03*(XL**2)
      KGV3(23,11)=-1.2
      KGV3(23,12)=-0.1*XL
      KGV3(23,23)=1.2
      KGV3(23,24)=-0.1*XL
      KGV3(24,11)=0.1*XL
      KGV3(24,12)=-0.03*(XL**2)
      KGV3(24,23)=-0.1*XL
      KGV3(24,24)=0.13*(XL**2)
C
C
      DO 20 I=1,24
         DO 20 J=1,24
           KGW1(I,J)=KGW1(I,J)*PKG1
           KGW2(I,J)=KGW2(I,J)*PKG2
           KGW3(I,J)=KGW3(I,J)*PKG3
           KGV1(I,J)=KGV1(I,J)*PKG1
           KGV2(I,J)=KGV2(I,J)*PKG2
           KGV3(I,J)=KGV3(I,J)*PKG3
      KG(I,J)=KG(I,J)+KGW1(I,J)+KGW2(I,J)+KGW3(I,J)+KGV1(I,J)+KGV2(I,J)
     1   +KGV3(I,J)
  20  CONTINUE
C
      DO 30 I=1,24
         DO 30 J=1,24
            KG(I,J)=KG(I,J)*PREF
  30  CONTINUE
      TOTXL=TOTXL+XL
      RETURN
      END
C
C
C
      SUBROUTINE KADD(ESTIF,KG)
      IMPLICIT DOUBLE PRECISION(A-H,O-Z)
      REAL*8 ESTIF(24,24),KG(24,24)
      DO 10 I=1,24
          DO 10 J=1,24
  10  ESTIF(I,J)=ESTIF(I,J)+KG(I,J)
      RETURN
      END
C
C
C
      SUBROUTINE INPUT(AS,NEL,NON,NMOD,NFLAG1,NFLAG2,NBC,EX,H,ALPHA,
     1                 NLAYER,T,E1,E2,V12,G12,G13,THETA,XL,DEN,F,TSPAR,
     2                 MK1T,X,Z,ES,INUMEL,NNODE,IUMEL,INODE,XAP,YAP,
     3                 SWEEP,RAIR,RFR,STEP,ITER,BE,AE,CG,ISPAR,CLA,AC,
     4                 RHUB,OMEGA,DENS,A,B,LEN)
C    4                 RHUB,DENS,A,B,LEN)
      IMPLICIT DOUBLE PRECISION(A-H,O-Z)
C
```

```
C   THIS SUBROUTINE READS THE INPUT VALUES USING FREE FORMAT
C
      DIMENSION NBC(10,12),EX(5),H(5),NLAYER(10),F(100),
     1 T(10,21),E1(10,21),E2(10,21),V12(10,21),G12(10,21),
     2 THETA(10,21),XL(10),W(10),DEN(10),G13(10,21),
     3 IDV1(10,21),IDV2(10,21),ISPAR(10),DEVAR(30),
     4 X(10,8),Z(10,8),ES(10,8),AS(10,8),SWEEP(10),
     5 IUMEL(8),INODE(8,2),TSPAR(10,4),
     6 BE(10),AE(10),CG(10),AC(10),CLA(10)
       REAL*8 LEN
      DO 313 I=1,4
 313  READ(8,*)
      READ(8,*)OMEGA,RHUB,AROOT,ATIP,DENS,LEN
      A=AROOT
      B=(ATIP-AROOT)/LEN
      DO 314 I=1,4
 314  READ(8,*)
      READ(8,*)NEL,NMOD,NFLAG1,NFLAG2
      NON=NEL+1
      NTDF = 12*NON
      READ(8,*)
      READ(8,*)((NBC(I,J),J=1,12),I=1,NON)
      READ(8,*)
      READ(8,*)(EX(I),H(I),I=1,5)
      READ(8,*)
      READ(8,*)ALPHA,WK1T
      READ(8,*)
      READ(8,*) RAIR,RFR,STEP,ITER
      READ(8,*)
      READ(8,*)
      READ(8,*)
      READ(8,*)
      READ(8,*)
      READ(8,*)
      READ(8,*)
      READ(8,*)
      READ(8,*)
      DO 10 I=1,NEL
        READ(8,*) NLAYER(I),NTOP,G13W,XL(I),DEN(I)
        READ(8,*)AC(I),AE(I),CG(I),CLA(I),SWEEP(I)
        NLAYER(I)=NLAYER(I)+1
        ISPAR(I)=NTOP+1
        G13(I,ISPAR(I))=G13W
        SWEEP(I)=SWEEP(I) * 3.14159265 / 180.
        DO 11 J=1,ISPAR(I)-1
        READ(8,*)T(I,J),E1(I,J),E2(I,J),V12(I,J),G12(I,J),G13(I,J),
     1  THETA(I,J),IDV1(I,J),IDV2(I,J)
 11     CONTINUE
        DO 12 J=ISPAR(I)+1,NLAYER(I)
        READ(8,*)T(I,J),E1(I,J),E2(I,J),V12(I,J),G12(I,J),G13(I,J),
     1  THETA(I,J),IDV1(I,J),IDV2(I,J)
 12     CONTINUE
        READ(8,*) (TSPAR(I,J),J=1,4)
        READ(8,*) (ES(I,J),J=1,8)
        READ(8,*) (AS(I,J),J=1,8)
 10     READ(8,*)
      READ(8,*)
      READ(8,*)
      READ(8,*)
      READ(8,*)
      READ(8,*)
      READ(8,*)
      READ(8,*)
      DO 30 I = 1,NON
        READ(8,*) BE(I)
        READ(8,*) (X(I,J),J=1,4)
        DO 20 J=1,4
```

```
 20     X(I,J+4)=X(I,J)
        READ(8,*) (Z(I,J),J=1,4)
        READ(8,*) (Z(I,J+4),J=1,4)
 30    READ(8,*)
       READ(8,*)
C
C      *********  READ DESIGN VARIABLES   ************************
C
       READ(8,*)((DEVAR((I-1)*7+J),J=1,7),I=1,4)
       READ(8,*) DEVAR(29)
       DEVAR(30) = 0.0
       CALL DESIGN(NEL,NLAYER,T,THETA,IDV1,IDV2,DEVAR,ISPAR)
       READ(8,*)
C      *********  READ VLASOV DATA ***********************************
       READ(8,*)
       READ(8,*) INUMEL,NNODE
       READ(8,*)
       DO 60 I=1,INUMEL
       READ(8,*) IUMEL(I),INODE(I,1),INODE(I,2)
 60    CONTINUE
       READ(8,*)
       READ(8,*) XAP,YAP
C
C      *********  READ NODAL LOADS ***********************************
C
       READ(8,*)
       READ(8,*)((F((I-1)*12+J),J=1,12),I=1,NON)
       DO 80 I=1,NEL
 80    SWE=SWEEP(I)*180.0/3.1415926
       RETURN
       END
C*
       SUBROUTINE SECPRO(NUML,NNOD,IUMEL,JNODE,XAP,YAP,ENODE,PA11,PA16,
      $           PA66,PD11,PD16,PD66,T11,X1C,Y1C,AS,ES,NT,IK,X1P,Y1P,C)
       IMPLICIT DOUBLE PRECISION(A-H,O-Z)
C  ***********************************************************************
C  *                                                                     *
C  *                     CODE: VLASOV2                                   *
C  *                                                                     *
C  *          ********* BASED ON ISOKON2 ************                   *
C  *                                                                     *
C  *             CALCULATION OF SECTION PROPERTIES                       *
C  *                                                                     *
C  *                                                                     *
C  *    .SECOND FINAL VERSION AS OF JULY 1985. PATRICK K. LO.            *
C  * THIS IS THE ORIGINAL (BACKUP) VERSION                               *
C  ***********************************************************************
C
C      GEOMETRY INFORMATION 04 DISK DATA FILE
C      MATERIAL INFORMATION 05 DISK DATA FILE
C
       CHARACTER*60 TITLE
       DIMENSION IUMEL(8),INODE(8,2),IUMPT(8),DNODE(8,2),
      &XNODE(8,2),YNODE(8,2),IEBRAN(8),ISBRAN(8),ZWC(8),ZW1(8),
      &Z5(8),Z6(8),ZS(8),ZCJJ(8),ANG1(8),C(5,5),ES(10,8),AS(10,8),
      &JNODE(8,2),ENODE(8,2),ZCT(8)
       DIMENSION T11(8),PA11(8),PA16(8),PA66(8),PD11(8),PD16(8),
      &          PD66(8)
       DIMENSION TT1(8),QA11(8),QA16(8),QA66(8),QD11(8),QD16(8),
      &          QD66(8)
       DATA ZA,ZSX,ZSY,ZSW,ZIXY,ZIXX,ZIYY,ZIWX,ZIWY,ZIWW,ZHS,ZHC,ZHQ,
      &ZJG/14*0.000000/
       DATA ZWC,ZW1/8*0.000000,8*0.000000/
       DATA ZW/0.000000/
       NUMEL=NUML
       NNODE=NNOD
       DO 719 I=1,8
```

```
      DO 719 J=1,2
        INODE(I,J)=JNODE(I,J)
719   DNODE(I,J)=ENODE(I,J)
      DO 619 I=1,8
        QA11(I)=PA11(I)
        QA16(I)=PA16(I)
        QA66(I)=PA66(I)
        QD11(I)=PD11(I)
        QD16(I)=PD16(I)
        QD66(I)=PD66(I)
619   TT1(I)=T11(I)
      ZA=0.0
      ZSX=0.0
      ZSY=0.0
      ZSW=0.0
      ZIXY=0.0
      ZIYY=0.0
      ZIWX=0.0
      ZIWY=0.0
      ZIWW=0.0
      ZHS=0.0
      ZHC=0.0
      ZHQ=0.0
      ZJG=0.0
      ZW=0.0
      ZBY=0.0
      ZBX=0.0
      ZBXX=0.0
      ZBXY=0.0
      ZBYY=0.0
      SAS=0.0
1     FORMAT(1X,A60)
2     FORMAT(12X,I2,11X,I2)
3     FORMAT(/,1X,I5,11X,I5,5X,I5)
4     FORMAT(1X,I5,11X,I5,5X,I5)
5     FORMAT(//,1X,I5,11X,F15.9,5X,F15.9)
6     FORMAT(1X,I5,11X,F15.9,5X,F15.9)
7     FORMAT(//,1X,F15.9,1X,F15.9)
8     FORMAT(/,1X,'PRINCIPAL POLE',/,1X,F15.9,1X,F15.9)
  10     FORMAT(F16.4,F15.4,F5.3,F15.4)
11    FORMAT(I2)
12    FORMAT(I2,3X,F10.6,F10.4)
20    FORMAT(1X,'--PLY--',5X,'----THETA : DEG/RAD ----',5X,
     &'-THICKNESS-',8X,'---INTERFACES---')
21    FORMAT(3X,I2,5X,F10.4,4X,F10.6,7X,F9.6,9X,F7.5,4X,F7.5)
22    FORMAT(1X,'Q(1,1)=',E12.5,3X,'Q(1,2)=',E12.5,3X,'Q(1,6)= ',
     &'0.00000E+00',/,1X,22X,'Q(2,2)=',E12.5,3X,'Q(2,6)= 0.00000E+00',
     &/,1X,44X,'Q(6,6)=',E12.5)
23    FORMAT(1X,'--PLY--',3X,'-----QBAR 11-----',2X,'-----QBAR 13-----',
     &3X,'-----QBAR 66-----')
24    FORMAT(2X,I3,8X,E12.5,7X,E12.5,8X,E12.5)
25    FORMAT(1X,'ABD COEFFICIENTS',/,1X,5X,'A11',10X,E12.5,/,1X,5X,
     &'D11',10X,E12.5,/,1X,5X,'D16',10X,E12.5,/,1X,5X,'D66',10X,E12.5)
30    FORMAT(1X,'CONNECTIVITY')
31    FORMAT(/,1X,'COORDINATES')
32    FORMAT(1X,5X,'O')
33    FORMAT(1X,16X,F15.9,5X,F15.9)
40    FORMAT(/,1X,'CROSS-SECTION AREA A',19X,E14.7)
41    FORMAT(1X,'SECOND MOMENT IXX',22X,E14.7)
42    FORMAT(1X,'SECOND MOMENT IYY',22X,E14.7)
43    FORMAT(1X,'SECOND SECTORIAL MOMENT IWW',12X,E14.7)
44    FORMAT(/,1X,'INTEGRAL HS',28X,E14.7,/,1X,'INTEGRAL HC',
     &28X,E14.7,/,1X,'INTEGRAL HQ',28X,E14.7)
45    FORMAT(1X,'INTEGRAL H-PHI',25X,E14.7)
46    FORMAT(1X,'TORSIONAL STIFFNESS',20X,E14.7)
50    FORMAT(/,1X,'COORDINATES OF CENTROID IN THE ARBITRARY CARTESIAN',
     &/,1X,'  --RELATIVE TO ORIGIN--',18X,E10.4,5X,F10.5)
```

```
 51   FORMAT(1X,'INCLINATION OF PRINCIPAL AXIS',/,1X,
     &'  --RELATIVE TO ORIGINAL CARTESIAN AXIS--',16X,F10.5)
 52   FORMAT(1X,'COORDINATES OF PRINCIPAL POLE',/,1X,
     &'  --RELATIVE TO THE CENTROID--',12X,E10.4,5X,F10.5)
 53   FORMAT(1X,'RADIUS OF GYRATION : RAISED TO POWER OF TWO',/,1X,
     &'  --WITH RESPECT TO PRINCIPAL POLE--',21X,F10.7)
 54   FORMAT(1X,'RADIUS OF GYRATION : RAISED TO POWER OF TWO',/,1X,
     &'  --BY PARALLEL AXIS THEOREM --',26X,F10.7)
 55   FORMAT(/,1X,'CURVATURE KY',45X,F10.7,/,1X,'CURVATURE KX',
     &45X,F10.7,/,1X,'CURVATURE KW',45X,F10.7)
 60   FORMAT(1X,'---NUMEL---',I2,'---NNODE---',I2)
 61   FORMAT(/,1X,'CONNECTIVITY')
 62   FORMAT(1X,I5,'.',10X,I5,5X,I5)
 63   FORMAT(/,1X,'JUNCTION MATRIX')
 64   FORMAT(/,1X,'COORDINATES')
 65   FORMAT(1X,I5,'.',10X,F15.9,5X,F15.9)
 91   FORMAT(1X,'*DATA BLOCK*')
 98   FORMAT(1X,'* WARNING : ZIWW HAS LESS THAN 5 SIGNIFICANT FIGURES')
 99   FORMAT(/,1X,'*****     *****     *****     *****     *****     ',
     &'*****     *****     *****',/)
      IJUNCT=0
      IF (NUMEL.EQ.0) GOTO 170
      DO 160 K1=1,NUMEL
      DO 160 K2=1,NUMEL
      IF (INODE(K1,1).NE.INODE(K2,2)) GOTO 160
      IJUNCT=IJUNCT+1
      ISBRAN(IJUNCT)=K1
      IEBRAN(IJUNCT)=K2
 160  CONTINUE
 170  TEMP=0.0000000
      ANG1PD=0.0
CC
CC    TO FIND THE CENTROID
CC
      DO 200 L1=1,NUMEL
      X1=DNODE(INODE(L1,1),1)
      XNODE(L1,1)=DNODE(INODE(L1,1),1)
      Y1=DNODE(INODE(L1,1),2)
      YNODE(L1,1)=DNODE(INODE(L1,1),2)
      X2=DNODE(INODE(L1,2),1)
      XNODE(L1,2)=DNODE(INODE(L1,2),1)
      Y2=DNODE(INODE(L1,2),2)
      YNODE(L1,2)=DNODE(INODE(L1,2),2)
 200  CONTINUE
CC
      CALL SECT (ZA,ZW,ZSW,ZSX,ZSY,ZIXY,ZIXX,ZIYY,ZIWX,ZIWY,ZIWW,
     &ZHS,ZHC,ZHQ,ZHPHI,ZJG,ZRP2,ZZKY,ZZKX,ZZKW,IEBRAN,ISBRAN,IC,ISO,
     &XNODE,YNODE,QA11,QA16,QA66,QD11,QD16,QD66,TT1,GAM,ZTA,CK15,
     &ANG1,ZWC,ZW1,Z5,Z6,ZS,ZCJJ,NUMEL,IJUNCT,XAP,YAP,ZCT,XC0,YC0)
CC
CC  ***** STIFFENERS IN CENTROID POSITION  ********
CC
      DO 260 I=1,8
        ZBY=ZBY+DNODE(I,1)*ES(IK,I)*AS(IK,I)
        ZBX=ZBX+DNODE(I,2)*ES(IK,I)*AS(IK,I)
        ZBYY=ZBYY+DNODE(I,1)**2*ES(IK,I)*AS(IK,I)
        ZBXY=ZBXY+DNODE(I,1)*DNODE(I,2)*ES(IK,I)*AS(IK,I)
        ZBXX=ZBXX+DNODE(I,2)**2*ES(IK,I)*AS(IK,I)
 260  SAS=SAS+ES(IK,I)*AS(IK,I)
      ZSY1=ZSY+ZBY
      ZSX1=ZSX+ZBX
      ZA1=ZA+SAS
      ZIYY1=ZIYY+ZBYY
      ZIXY1=ZIXY+ZBXY
      ZIXX1=ZIXX+ZBXX
CC  ******                                    ********
CC
```

```
CC     POSITION OF CENTROID IN ORIGINAL CARTESIAN
CC
       XC=ZSY/ZA
       YC=ZSX/ZA
       X1C=ZSY1/ZA1
       Y1C=ZSX1/ZA1
       ZIIXY=(ZIYY-ZSY*ZSY/ZA)-(ZIXX-ZSX*ZSX/ZA)
       Z11XY=(ZIYY1-ZSY1*ZSY1/ZA1)-(ZIXX1-ZSX1*ZSX1/ZA1)
       IF (ABS(ZIIXY).LT.0.000001) GOTO 350
       ANGP=.5*ATAN(2.*(ZIXY-ZSX*ZSY/ZA)/ZIIXY)
       ANGP1=.5*ATAN(2.*(ZIXY1-ZSX1*ZSY1/ZA1)/Z11XY)
       ANGPD=ANGP*180./ARCOS(-1.)
       ANG1PD=ANG1PD+ANGPD
       GOTO 360
 350   ANGP=ARCOS(-1.)/4.
       ANGP1=ARCOS(-1.)/4.
       ANGPD=ANGP*180./ARCOS(-1.)
 360   ZIIXX=(ZIXX-ZSX*ZSX/ZA)*COS(ANGP)*COS(ANGP)+(ZIYY-ZSY*ZSY/ZA)*
      &SIN(ANGP)*SIN(ANGP)-2.*(ZIXY-ZSX*ZSY/ZA)*COS(ANGP)*SIN(ANGP)
       ZIIYY=(ZIXX-ZSX*ZSX/ZA)*SIN(ANGP)*SIN(ANGP)+(ZIYY-ZSY*ZSY/ZA)*
      &COS(ANGP)*COS(ANGP)+2.*(ZIXY-ZSX*ZSY/ZA)*COS(ANGP)*SIN(ANGP)
       ZIIXY=(ZIXX-ZIYY-ZSX*ZSX/ZA+ZSY*ZSY/ZA)*SIN(ANGP)*COS(ANGP)+
      &(ZIXY-ZSX*ZSY/ZA)*(COS(ANGP)*COS(ANGP)-SIN(ANGP)*SIN(ANGP))
       Z11XX=(ZIXX1-ZSX1*ZSX1/ZA1)*COS(ANGP1)*COS(ANGP1)+
      &(ZIYY1-ZSY1*ZSY1/ZA1)*
      &SIN(ANGP1)*SIN(ANGP1)-2.*(ZIXY1-ZSX1*ZSY1/ZA1)
      &*COS(ANGP1)*SIN(ANGP1)
       Z11YY=(ZIXX1-ZSX1*ZSX1/ZA1)*SIN(ANGP1)*SIN(ANGP1)
      &+(ZIYY1-ZSY1*ZSY1/ZA1)*
      &COS(ANGP1)*COS(ANGP1)+2.*(ZIXY1-ZSX1*ZSY1/ZA1)
      &*COS(ANGP1)*SIN(ANGP1)
       Z11XY=(ZIXX1-ZIYY1-ZSX1*ZSX1/ZA1+ZSY1*ZSY1/ZA1)
      &*SIN(ANGP1)*COS(ANGP1)+
      &(ZIXY1-ZSX1*ZSY1/ZA1)*(COS(ANGP1)*COS(ANGP1)
      &-SIN(ANGP1)*SIN(ANGP1))
 500   DO 13 I = 1,5
         DO 13 J = 1,5
 13    C(I,J) = 0.0
        C(1,1) = ZA1
        C(1,5) = CK15
        C(2,2) = Z11XX
        C(2,5) = ZHC
        C(3,3) = Z11YY
        C(3,5) = -ZHS
C       C(4,4) = ZIIWW
        C(4,4) = ZIWW
        C(4,5) = ZHQ
        C(5,5) = ZJG
CC
CC     *****  THE FOLLOWING TERMS ARE ZERO IN THE FINAL COORD SYSTEM  **
CC
        C(1,2) = -ZSX
        C(1,3) = -ZSY
        C(1,4) = +ZSW
        C(2,3) = ZIIXY
C       C(2,4) = ZIIWX
        C(2,4) = ZIWX
C       C(3,4) = ZIIWY
        C(3,4) = ZIWY
CC
       DO 14 I=1,5
         DO 14 J=1,I
 14    C(I,J)=C(J,I)
       RETURN
       END
C
       SUBROUTINE ELAE(A,AE,BI,BF,BR,L,RFR,RO,SW,IDIV,AC,CLA)
```

```
      IMPLICIT DOUBLE PRECISION(A-H,O-Z)
      REAL*8 SW,PI,AE,BI,BF,BR,L,RO,RFR,RFK
      COMPLEX*16 QA(12,12,3),QB(12,12,5),QD(12,12,5),
     1QE(12,12,3),QF(12,12,3),QG(12,12,3),QH(12,12,3)
      COMPLEX*16 A(12,12),Y,Z
      PI=4.*ATAN(1.)
      RFK=RFR/COS(SW)
      CALL GAUSS(QA,QB,QD,QE,QF,QG,QH,L,BF,BI,BR,RFK)
      DO 50 I=1,12
        DO 50 J=1,12
50    A(I,J)=0.0
      IF (IDIV.EQ.1) THEN
        DO 30 IA=1,6
          DO 30 JA=1,6
            DO 30 K=1,2
              DO 30 M=1,2
                I=IA+(K-1)*6
                J=JA+(M-1)*6
                Z=(AE+.5)*(QD(I,J,1)-TAN(SW)*QG(I,J,1))
                Z=Z-(AE**2)*TAN(SW)*QH(I,J,1)+QB(I,J,1)
                Z=Z-TAN(SW)*(QE(I,J,1)-(.5-AE)*QF(I,J,1))
30      A(I,J)=2*PI*RO*((COS(SW))**2)*Z
        GOTO 40
      END IF
      DO 10 IA=1,6
        DO 10 JA=1,6
            DO 10 K=1,2
              DO 10 M=1,2
                I=IA+(K-1)*6
                J=JA+(M-1)*6
      Z=PI*QA(I,J,2)-(0.,1.)*BR*CLA*QA(I,J,3)/RFK
      Z=Z+PI*AE*QB(I,J,3)+CLA*(BR**2)*QB(I,J,4)/(RFK**2)
      Z=Z+(0.,1.)*BR*((CLA/(2*PI)+AC-AE)*CLA/PI*QB(I,J,5)
     &+QB(I,J,2))*PI/RFK
      Z=Z+PI*AE*QB(J,I,3)-(AE-AC)*CLA*BR*(0.,1.)*QB(J,I,5)/RFK
      Z=Z+PI*((AE**2)+.125)*QD(I,J,3)
     &+CLA*(AE-AC)*(BR**2)*QD(I,J,4)/(RFK**2)
      Z=Z-(0.,2.)*PI*(CLA/(2*PI)+AC-AE)*BR*(.5*QD(I,J,2)
     &-(AE-AC)*CLA/(2*PI)*QD(I,J,5))/RFK
      Y=(0.,-1.)*PI*QE(I,J,2)-CLA*BR*QE(I,J,3)/RFK
      Y=Y-(0.,1.)*AE*PI*QF(I,J,2)+CLA*(CLA/(2*PI)+AC-AE)*
     &BR*QF(I,J,3)/RFK
      Y=Y-(0.,1.)*PI*AE*QG(I,J,2)-(AE-AC)*CLA*BR*QG(I,J,3)/RFK
      Y=Y-(.125+(AE**2))*(0.,1.)*PI*QH(I,J,2)-PI*AE*BR*QH(I,J,1)/RFK
      Y=Y-PI*(CLA/(2*PI)+AC-AE)*BR*(QH(I,J,1)-(AE-AC)*CLA/PI*QH(I,J,3))
     &/RFK
      Z=Z+TAN(SW)*BR*Y/RFK
10      A(I,J)=RO*Z
40    CONTINUE
      RETURN
      END
```

Vita

The author was born in Giridih (Bihar), India on the 3rd August, 1967. He got a B. Tech. degree in Aeonautical Engineering from the Indian Institute of Technology, Kharagpur in June 1988. He joined Virginia Polytechnic Institute and State University in August 1988 to pursue studies towards a Master of Science degree in Aerospace Engineering.